

**The impact of mucolytics on *Chlamydia* infection and the induced immune response**

**Ph.D. thesis**

**Dávid Kókai Pharm.D.**



**Supervisor: Katalin Burián M.D., Med. habil., Ph.D.,**

**Doctoral School of Interdisciplinary Medicine**

**Albert Szent-Györgyi Medical School**

**Department of Medical Microbiology**

**Szeged**

**2022**

## Table of contents

1.	Introduction.....	11
1.1.	General description of the Chlamydiae phylum.....	11
1.2.	General description of the Chlamydiae membrane and their development cycle .....	11
1.3.	<i>Chlamydia pneumoniae</i> infection.....	13
1.4.	The immune response against <i>C. pneumoniae</i> .....	13
1.5.	Characteristics of mucolytics.....	16
2.	Aims and objectives.....	20
3.	Material and Methods .....	21
3.1.	Propagation of <i>C. pneumoniae</i> .....	21
3.2.	<i>In vitro</i> effect of NAC and Ax.....	21
3.3.	Mice and infection conditions .....	22
3.4.	Cultivation of <i>C. pneumoniae</i> from the lungs of mice .....	23
3.5.	RNA extraction from the cells.....	23
3.6.	RNA extraction from the lungs of mice .....	23
3.7.	cDNA synthesis .....	23
3.8.	Quantitative PCR (qPCR) of the <i>Ido1</i> , <i>Ido2</i> , <i>Il12</i> , <i>Il17a</i> , <i>Il17f</i> , <i>Il23</i> , <i>Ifng</i> , <i>Sftpa</i> , <i>Sftpb</i> , <i>Sftpc</i> , <i>Sftpd</i> , <i>Actb</i> .....	24
3.9.	Enzyme-linked immunosorbent assay (ELISA).....	26
3.10.	Western blotting analysis of ERK pathway .....	26
3.11.	Apoptosis assay and flow cytometry .....	27
3.12.	<i>In vitro</i> effects of SP-A and SP-D on <i>C. pneumoniae</i> proliferation and attachment . .....	27
3.13.	Statistical analysis.....	28
4.	Results.....	29
4.1.	NAC increases the <i>in vitro</i> replication of <i>C. pneumoniae</i> .....	29
4.2.	NAC increases the binding of <i>C. pneumoniae</i> to the host cell .....	30
4.3.	Exposure to NAC not only increases the chlamydial lung burden but also prolongs the infection in mice .....	32
4.4.	Ax does not increase the number of infective <i>C. pneumoniae</i> .....	34
4.5.	Ax treatment at elevated concentration suppressed <i>C. pneumoniae</i> proliferation in mouse lungs .....	36
4.6.	Ax treatment altered the gene expression and protein level of IFN- $\gamma$ in the lungs of <i>C. pneumoniae</i> -infected mice .....	37
4.7.	SP treatment increased the attachment of <i>C. pneumoniae</i> to macrophages and decreased bacterial proliferation.....	40

4.8.	Ax treatment did not induce apoptosis via the Caspase-dependent pathway but decreased ERK 1/2 activation in <i>C. pneumoniae</i> -infected cells.....	42
5.	Discussion .....	45
6.	Conclusion .....	50
7.	Summary .....	51
8.	Összefoglalás .....	53
9.	Acknowledgement .....	55
10.	Reference.....	56
11.	Annexes.....	70

## Publications

### Publications related to the subject of the Thesis:

1. N-acetyl-cysteine increases the replication of *Chlamydia pneumoniae* and prolongs the clearance of the pathogen from mice.

**David Kokai**, Timea Mosolygo, Dezso Peter Virok, Valeria Endresz, Katalin Burian  
JOURNAL OF MEDICAL MICROBIOLOGY 67: 5 pp. 702-708. , 7 p (2018).  
doi: 10.1099/jmm.0.000716

**Q2 IF<sub>2018</sub>: 1.926**

2. Ambroxol Treatment Suppresses the Proliferation of *Chlamydia pneumoniae* in Murine Lungs

**Dávid Kókai**, Dóra Paróczai, Dezso Peter Virok, Valéria Endrész, Renáta Gáspár, Tamás Csont, Renáta Bozó and Katalin Burián  
MICROORGANISMS 9: 4 p. 880 , 14 p. (2021)  
<https://doi.org/microorganisms9040880>

**Q2 IF<sub>2020</sub>: 4.128**

**Cumulative impact factor: 6.054**

### Publications not related to the subject of the thesis:

1. Indoleamine 2,3-dioxygenase activity in *Chlamydia muridarum* and *Chlamydia pneumoniae* infected mouse lung tissues

Dezső Virok, Tímea Raffai, **David Kokai**, Dóra Paróczai, Anita Bogdanov, Gábor Veres, László Vécsei, Szilard Poliska, László Tiszlavicz, Ferenc Somogyvári, Valéria Endrész, Katalin Burián

FRONTIERS IN CELLULAR AND INFECTION MICROBIOLOGY 9

Paper: 192, 12 p. (2019)

doi: 10.3389/fcimb.2019.00192

**D1 IF<sub>2019</sub>: 4.123**

3. Aerodynamic properties and in silico deposition of isoniazid loaded chitosan/thiolated chitosan and hyaluronic acid hybrid nanoplex DPIs as a potential TB treatment

Mahwash Mukhtar, Edina Pallagi, Ildikó Csóka, Edit Benke, Árpád Farkas, Mahira Zeeshan, Katalin Burián, **Dávid Kókai**, Rita Ambrus

INTERNATIONAL JOURNAL OF BIOLOGICAL MACROMOLECULES 165 pp. 3007-3019. , 13 p. (2020)

<https://doi.org/10.1016/j.ijbiomac.2020.10.192>

**Q1 IF<sub>2020</sub>: 6.953**

2. Chlamydia pneumoniae Influence on Cytokine Production in Steroid-Resistant and Steroid-Sensitive Asthmatics

Paróczai, Dóra; Mosolygó, Tímea; **Kókai, Dávid**; Endrész, Valéria; Virók, Dezső Péter; Somfay, Attila; Burián, Katalin

PATHOGENS 9: 2 Paper: 112, 13 p. (2020)

doi: 10.3390/pathogens9020112

**Q2 IF<sub>2020</sub>: 3.492**

4. Beneficial Immunomodulatory Effects of Fluticasone Propionate in *Chlamydia pneumoniae*-Infected Mice

Dóra Paróczai, Anita Sejben, **Dávid Kókai**, Dezső P. Virok, Valéria Endrész and Katalin Burián

PATHOGENS 10: 3 Paper: 338, 13 p. (2021)

<https://doi.org/10.3390/pathogens10030338>

**Q2 IF<sub>2020</sub>: 3.492**

5. Freeze-dried vs spray-dried nanoplex DPIs based on chitosan and its derivatives conjugated with hyaluronic acid for tuberculosis: *In vitro* aerodynamic and in silico deposition profiles

Mahwash Mukhtara, Zsolt Szakonyi, Árpád Farkas, Katalin Burian, **Dávid Kókai**, Rita Ambrus

EUROPEAN POLYMER JOURNAL 160 Paper: 110775, 14 p. (2021)

<https://doi.org/10.1016/j.eurpolymj.2021.110775>

**Q1 IF<sub>2020</sub>: 4.598**

6. Indoleamine 2,3-dioxygenase cannot inhibit Chlamydia trachomatis growth in HL-60 human neutrophil granulocytes

Dezso Peter Virok, Ferenc Tömösi, Anita Varga-Bogdanov, Szilard Poliska, Bella Bruszel, Zsuzsanna Cseh, **David Kokai**, Dóra Paróczai, Valeria Endresz, Tamas Janaky, Katalin Burián

FRONTIERS IN IMMUNOLOGY 12 Paper: 717311, 14 p. (2021)

**Q1 IF<sub>2020</sub>:7.561**

7. Physico-Chemical, In Vitro and Ex Vivo Characterization of Meloxicam Potassium-Cyclodextrin Nanospheres

Patrícia Varga , Rita Ambrus , Piroska Szabó-Révész , **Dávid Kókai** , Katalin Burián , Zsolt Bella , Ferenc Fenyvesi , Csilla Bartos

PHARMACEUTICS 13: 11 Paper: 1883, 14 p. (2021)

<https://doi.org/10.3390/pharmaceutics13111883>

**Q1 IF<sub>2020</sub>:6.321**

**Cumulative impact factor:36.54**

### Abstracts related to the subject of the thesis:

1. Katalin, Burián; Bettina, Magyari; Tímea, Mosolygó; Valéria, Endrész; Dezső, Virók; **Dávid, Kókai**  
Effects of mucolitics in in vitro and in vivo *Chlamydophila pneumoniae* infection  
Acta Microbiologica Et Immunologica Hungarica 64: Suppl.1. pp. 115-116., 2 p. (2017)
2. Katalin, Burian; **David, Kokai**; Tímea, Mosolygó; Dezso, Virok; Valeria, Endresz  
N-acetyl-cysteine increases the replication of *Chlamydia pneumoniae* and prolongs the clearance of the pathogen from mice  
In: 28th European Congress of Clinical Microbiology and Infectious Diseases (28th ECCMID)(2018)
3. **David Kokai**; Dora Paróczai; Dezso Virok; Valeria Endresz; Katalin Burian  
Antimicrobial Effect Of The Commonly Used Mucolytic Agent, Ambroxol  
In: A Magyar Mikrobiológiai Társaság 2018. évi Nagygyűlése és a XIII. Fermentációs Kollokvium :(2018) 70 p. p. 33
4. **Dávid, Kókai**; Dóra, Paróczai; Dezső, Virók; Valéria, Endrész; Katalin, Burián  
Antimicrobial effect of the commonly used mucolytic agent, ambroxol  
Acta Microbiologica Et Immunologica Hungarica 66: Suppl. 1 pp. 52-52, 1 p. (2019)
5. **Kókai, Dávid**; Paróczai, Dóra; Burián, Katalin  
Egy mukolitikum in vitro és in vivo anti-chlamydiális hatással  
Medicina Thoracalis (BUDAPEST) 73: 1 pp. 15-16, 2 p. (2020)
6. **David, Kokai**; Dora, Paróczai; Dezso, Virok; Valeria, Endresz; Katalin, Burian  
Ambroxol Possesses An Antichlamydial Effect *In Vitro* And *In Vivo* (2020)  
18th German Chlamydia Workshop 2020 2020-02-05 Lübeck, Germany

### Abstracts not related to the subject of the thesis:

1. **Dávid, Kókai;** Dóra, Paróczai; Dezső, Virók; Valéria, Endrész; Dezső, Csupor; Katalin, Burián  
Growth modulating effect of Hedera helix extract on bacteria  
Acta Microbiologica Et Immunologica Hungarica 66: Suppl. 1pp. 156-157. 2 p.(2019)
2. **Kókai, Dávid;** Paróczai, Dóra; Virók, Dezső Péter; Endrész, Valéria; Somogyvári, Ferenc;  
Bozó, Renáta; Burián, Katalin  
Viscum Album Tumorellenes Hatásának Vizsgálata (2020)  
A Magyar Mikrobiológiai Társaság 2020. évi Nagygyűlése és a XIV. Fermentációs Kollokvium  
2020-10-14 Kecskemét, Magyarország
3. **Dávid, Kókai;** Dóra, Paróczai; Dezső, Péter Virók; Valéria, Endrész; Ferenc, Somogyvári;  
Renáta, Bozó; Katalin, Burián  
Antitumor Effect of Viscum Album  
Acta Microbiologica Et Immunologica Hungarica 68: Supplement 1 p. 24 (2021)
4. **Dávid, Kókai;** Dóra, Paróczai; Zain, Baaity; Dezső, P. Virók; Valéria, Endrész; Rita, Ambrus;  
Renáta, Bozó; Katalin, Burián  
Investigation of antiviral properties of hyaluronic acid (2021)  
23rd Annual Conference of the European Society for Clinical Virology

### Abbreviations

AB	Aberrant bodies
ATP	Adenosine triphosphate
Ax	Ambroxol
BAD	BCL2 associated agonist of cell death
Bcl-2	B-cell lymphoma 2
BSA	Bovine serum albumin
<i>C. pneumoniae</i>	<i>Chlamydia pneumoniae</i>
<i>C. psittaci</i>	<i>Chlamydia psittaci</i>
<i>C. trachomatis</i>	<i>Chlamydia trachomatis</i>
CAP	Community acquired pneumonia
Caspase	Cysteine-aspartic proteases
COMC	Chlamydial outer membrane complex
Cpn	<i>Chlamydia pneumoniae</i>
c-RAF	RAF proto-oncogene serine/threonine-protein kinase
DC	Dendritic cell
EB	Elementary body
ERK	Extracellular signal-regulated kinase
FITC	Fluorescein isothiocyanate
IFU	Inclusion forming unit
IDO	Indoleamine 2, 3-dioxygenase
IFN- $\gamma$	Interferon-gamma
IL	Interleukin
LPS	Lipopolysaccharide

MEK-1	Dual specificity mitogen-activated protein kinase 1
MIP-2	Macrophage inflammatory protein 2
MOI	Multiplicity of infection
MOMP	Major outer membrane protein
MSK-1	Mitogen and stress activated protein kinase 1
NAC	N-acetyl-cysteine
NK	Natural killer
OmcB	Outer membrane complex protein B
OTC	Over-the-counter
<i>p.i.</i>	post infection
PCD	Programmed cell death
qPCR	quantitative Polymerase chain reaction
RB	Reticular body
SDS	Sodium dodecyl sulphate
SP	Surfactant protein

## 1. Introduction

### 1.1. General description of the Chlamydiae phylum

Chlamydiae are obligate Gram-negative intracellular pathogens with a biphasic development cycle. From amoebae to humans can be infected with these organisms. The *Chlamydiaceae* family is the best-studied group in the Chlamydiae phylum, and it comprises 11 species, that are pathogenic to animals including humans<sup>1</sup>. There are three human pathogens in the *Chlamydiaceae* family which are *Chlamydia trachomatis* (*C. trachomatis*), *Chlamydia psittaci* (*C. psittaci*) and *Chlamydia pneumoniae* (*C. pneumoniae*)<sup>2</sup>.

### 1.2. General description of the Chlamydiae membrane and their development cycle

The chlamydial outer membrane complex (COMC) consists of several proteins<sup>3</sup> out of which the major outer membrane protein (MOMP) is the most abundant. In the COMC several cysteine-rich proteins<sup>3</sup> can be detected e.g. the outer membrane complex protein B (OmcB), which is a crucial, highly conserved cysteine-rich protein<sup>3</sup>. Based on DiANNA version 1.1. disulphide bridge prediction software there are many possible disulphide bridges in the molecule<sup>4,5</sup>. The structure of the OmcB has been predicted by AlphaFold Monomer v2.0 and the proteins were visualised by UCSF Chimera (**Figure 1**)<sup>6-8</sup>.

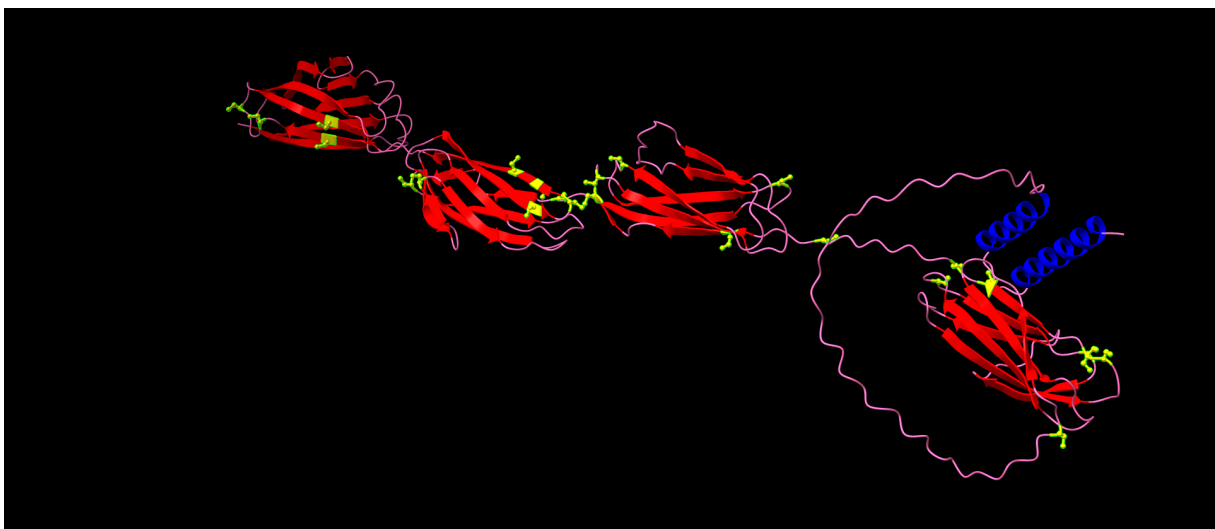


Figure 1: Structure of OmcB

There are two forms in the development cycle of the pathogens in the *Chlamydiaceae* family which are the elementary bodies (EB) and the reticular bodies (RB). These forms are morphologically and functionally different from each other<sup>1</sup>.

The EBs are spore-like forms, which can survive in the extracellular environment. EBs were previously described as metabolically intact; however, in recent years their metabolic and biosynthetic activities have been described as well<sup>9,10</sup>. OmcB is a crucial protein in the EBs COMC, as it is responsible for the attachment to the host cell and the internalization process afterwards<sup>11,12</sup>. In order to form an appropriate attachment to the cell membrane, the OmcB disulphide bridges must be in a reduced state<sup>11,13</sup>. After the EBs enter the cells, they differentiate to RBs (**Figure 2**), and they begin to replicate<sup>14</sup>.

The replication of the RBs takes place in a vacuole named inclusion, and their replication process becomes asynchronous over the time<sup>14</sup>. The RBs are the metabolically active form of the development cycle. To cover the high ATP demand for nutrient acquisition and replication, several proteins involved in ATP generation are expressed highly<sup>9,15</sup>. After 8-10 division cycles the RBs are differentiated to EBs, and the EBs exit the cell via extrusion or budding in order to begin a new infection cycle<sup>14,16</sup> (**Figure 2**).

Some factors (e.g. penicillin, interferon-gamma (IFN- $\gamma$ ), iron deficiency, amino acid starvation) can induce a persistent state of the Chlamydiales<sup>17-19</sup>. In this case, RBs differentiate to aberrant bodies (ABs), which have been described as enlarged, not replicating pleomorphic RBs<sup>20</sup>. After the removal of the inhibiting factors, ABs can differentiate back to RBs, and the replications cycle can continue<sup>14,20</sup> (**Figure 2**).

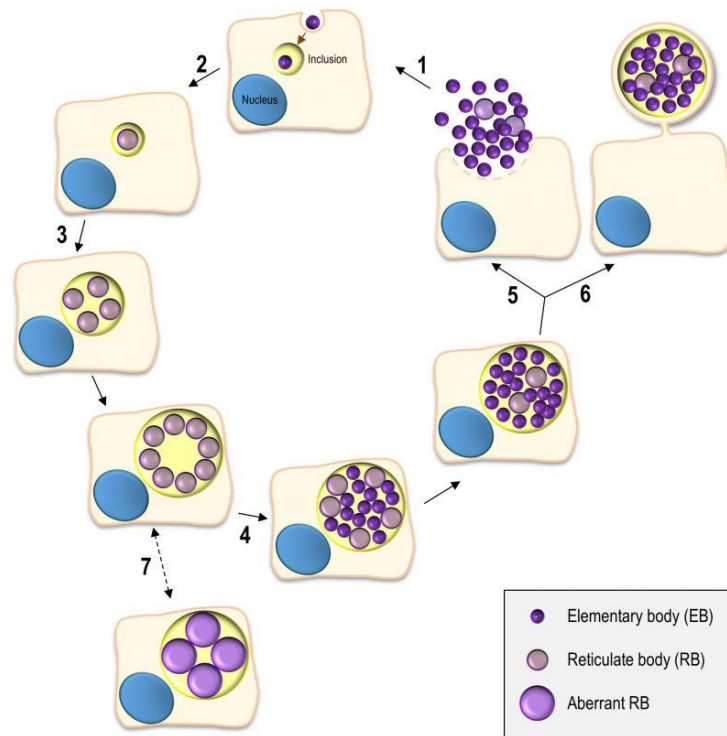


Figure 2: Development cycle of *C. pneumoniae* <sup>21</sup>

### 1.3. *Chlamydia pneumoniae* infection

*C. pneumoniae* is a common cause of acute respiratory infection, including community-acquired pneumonia (CAP), sinusitis, pharyngitis, bronchitis, and exacerbations of chronic bronchitis. *C. pneumoniae* is responsible for approximately 10% of all pneumonia cases<sup>22</sup>. Seropositivity of the populations shows that approximately 50-70% of the community have been infected with *C. pneumoniae* in a lifetime<sup>23-25</sup>. Moreover, *C. pneumoniae* infection has been associated with atherosclerosis<sup>26-28</sup>.

During the invasion of the upper and lower respiratory tract, phlegm is produced<sup>29,30</sup>. To facilitate the removal of the phlegm, mucolytics are often prescribed by physicians<sup>31</sup>.

### 1.4. The immune response against *C. pneumoniae*

The defence against chlamydial infection takes place on three platforms simultaneously. One element is the so-called cell-autonomous immunity, the second is the apoptosis and the last is the activation of the immune system.

There are several methods by which the infected cell can hinder the replication of the bacteria. Indoleamine 2,3 dioxygenase (IDO) is an IFN- $\gamma$  inducible enzyme that has two isoforms, IDO-1 and IDO-2<sup>32</sup>. This enzyme regulates the first and rate-limiting step in the catabolism process of L-tryptophan to N-formylkynurenine<sup>33</sup>. Chlamydiales are tryptophan auxotroph bacteria, thus the upregulation of the enzyme suppresses the replication of the bacteria. Earlier it has been described, that the induction of IDO-1,2 showed strong anti-chlamydial activity<sup>34–36</sup>.

Programmed cell death (PCD) is a mechanism that results in the death of the cells<sup>37</sup>. Apoptosis is a form of PCD, which happens throughout the body. There are two apoptotic pathways. The first one is the extrinsic pathway, which is mediated by death receptors (e.g. Fas (also called DR2, Apo-1 or CD95), TNFR-1(also called DR1, CD120a)) on the cell surface and the other is the intrinsic pathway, which is known to be the mitochondrial pathway<sup>38,39</sup>. In the intrinsic pathway, B-cell lymphoma 2 (Bcl-2) protein, which is found on the membrane of the mitochondria, plays a crucial role in inhibiting the pro-apoptotic proteins<sup>40</sup>. As a consequence of the intrinsic or extrinsic pathway activation, the cysteine-aspartic proteases (Caspase) (e.g. caspase-3, 6, 7) will be activated which leads to the apoptosis of the cell<sup>41</sup>. Moreover, it has been found that some stimuli (e.g. elevated intracellular  $\text{Ca}^{2+}$  concentration) can induce apoptosis, even if caspase inhibitors are added to the cells, resulting in caspase-independent apoptosis<sup>42,43</sup>. It is known that the members of the *Chlamydiaceae* try to evade host cell apoptosis by the stimulation of Raf/MEK/ERK pathways thereby inducing Bag1<sup>44–46</sup>. Bag1 binds to Bcl-2, thus sustaining its anti-apoptotic function<sup>47</sup>. However, it has been observed that at the late stage of the development cycle, *C. trachomatis* can activate caspase-3 thereby inducing apoptosis<sup>48</sup>.

Cytokines are secreted proteins or glycoproteins, which are involved in the signalling between the cells in the immune response<sup>49</sup>. Cytokines exert autocrine and/or paracrine functions as well<sup>50</sup>. Interleukins (IL) are a group of cytokines that are secreted by numerous cells (e.g., CD8<sup>+</sup> T-cells, CD4<sup>+</sup> T-cells, epithelial cells), and can provoke growth, differentiation, and immune response<sup>51</sup>. More than 50 ILs have been identified in the human genome thus far<sup>52</sup>. IL-12 is a heterodimeric cytokine, which is produced by dendritic cells (DC), activated macrophages, and neutrophil granulocytes. IL-12 has a role in the activation of natural killer (NK) cells, as well as the differentiation of naive T-cells to CD4<sup>+</sup> cells<sup>53,54</sup>. Moreover, it prompts the production of IFN- $\gamma$ , and together with IFN- $\gamma$  they promote the maturation of DCs<sup>53,54</sup>. It has been established, that the IL-12 is necessary for the DC to present the chlamydial proteins to the T-cells to have a proper immune response against *C. pneumoniae*<sup>55</sup>. Among the two major CD4<sup>+</sup> (Th1, Th2)

subsets, in 2005 a new subset of CD4<sup>+</sup> cells has been identified, and based on their ability to produce IL-17 were named as Th17<sup>56</sup>. IL-17 is a proinflammatory cytokine family, which consists of 6 members IL-17(A-F)<sup>57-59</sup>. It has been described that IL-17A mediates neutrophil infiltration during chlamydial lung infection by promoting chemokines expression<sup>60</sup>. At the molecular level, IL-17A upregulates MIP-2/CXCL2 and IL-6 which induce neutrophil infiltration in the lungs<sup>60,61</sup>. It has been shown that IL-23 is essential for inducing the *C. pneumoniae* specific Th17 response<sup>62,63</sup>. However, taking into account that IL-23 is a redundant cytokine, in IL-23 deficient mouse the incursion of Th1 and innate immune cells into genital tract was not compromised in the case of *C. muridarum* infection<sup>62</sup>. Meaning, that IL-23 does not play a central role in the defence of the body in case of *C. muridarum* genital tract infection<sup>62</sup>.

IFN- $\gamma$  is a cytokine belonging to the type II class of interferons, is produced by CD4<sup>+</sup>, CD8<sup>+</sup>, and NK cells<sup>64</sup>. IFN- $\gamma$  plays a crucial role both in innate and adaptive immunity (e.g. stimulates TNF production of macrophages, upregulates MHC expression thereby aiding the antigen presentation, facilitates phagosome-lysosome fusion, and induces several IFN- $\gamma$  inducible GTPase)<sup>34,35,65-67</sup>. Moreover, several IFN- $\gamma$  inducible GTPase have a pivotal role in the eradication of *C. pneumoniae* from the cell, such as p47, Irga6, Irgb10, IDO1,2<sup>68,69</sup>.

Surfactant proteins (SP) consist of four proteins (SP A-D), from which SP-A and SP-D have a role in the defence of the lungs<sup>70</sup>. SP-A and SP-D act as an opsonin, facilitate uptake of the bacteria by the alveolar macrophages and can aggregate bacteria<sup>71,72</sup>. SP-B and SP-C play a crucial role in the proper maintenance of lung homeostasis, which includes the reduction of surface tension<sup>71</sup>. Furthermore, SP-B is dependent on SP-C, and the absence of these proteins can result in serious diseases such as respiratory distress syndrome or interstitial lung disease<sup>73,74</sup>.

## 1.5. Characteristics of mucolytics

### N-acetyl-L-cysteine

N-acetyl-L-cysteine (NAC) (Acetylcysteine) is a thiol group-containing commonly used agent in the healthcare profession (**Figure 3**). It has multiple therapeutic uses in psychiatry including bipolar disorder, major depressive disorder, schizophrenia and is useful in the case of an acetaminophen overdose<sup>75–79</sup>. However, most often NAC is used as a mucolytic. Mechanism of action in the body occur in three ways: either thiol group can reduce disulphide bonds, therefore decreasing the viscosity of the mucus in the lungs or NAC can be the substrate of glutathione synthesis or it can directly neutralize oxidants<sup>80</sup>.

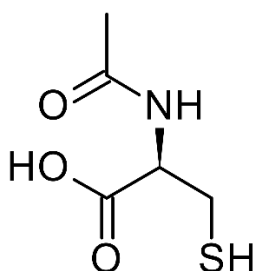


Figure 3: Skeletal formula of NAC

In Germany, NAC was the second most popular drug as mucolytics with 23.5% of the Over-the-counter (OTC) expectorant market<sup>31</sup>. Under the basis data that the National Health Insurance Fund of Hungary has provided us, little over 1 million units of NAC was sold in 2016 in Hungary, making NAC the most used mucolytics in Hungary (**Figure 4**).

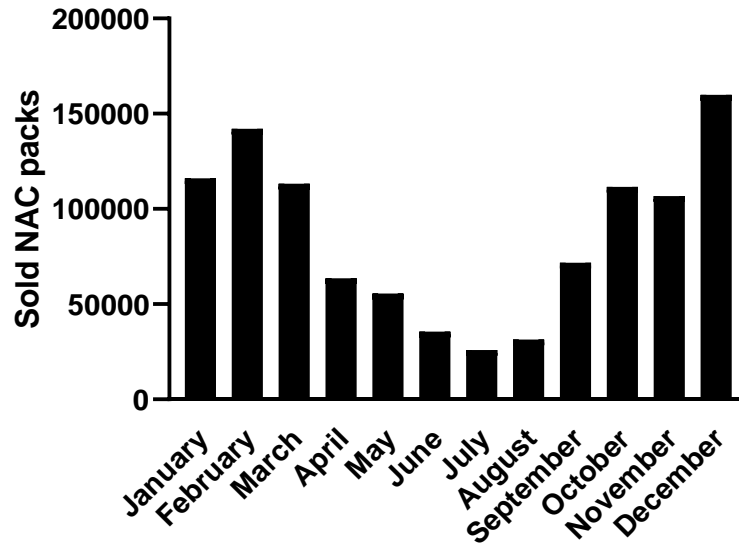


Figure 4: Consumption of NAC in Hungary 2016 <sup>81</sup>

The direct antimicrobial role of NAC is not well defined, but there are data regarding its inhibitory effect on biofilm formation. NAC displayed a direct antimicrobial effect against extracellular pathogens, but the concentrations applied by different authors varied greatly (0.003–80 mg/ml)<sup>82–84</sup>. In the case of tuberculosis, NAC was found to play a part in inhibiting the growth of intracellular *Mycobacterium tuberculosis* through bacteriostatic mechanisms<sup>85</sup>.

## Ambroxol

Ambroxol (Ax; 2-amino-3,5-dibromo-N-(trans-4-hydroxycyclohexyl) benzylamine) is widely used in the treatment of respiratory infections, chronic bronchitis, and neonatal respiratory distress syndrome due to its mucus viscosity-altering effect and has been shown to be a relatively safe drug (**Figure 4**)<sup>86,87</sup>. Furthermore, Ax shows beneficial effects on the course of Parkinson's disease by modifying glucocerebrosidase chaperon activity<sup>88</sup>.

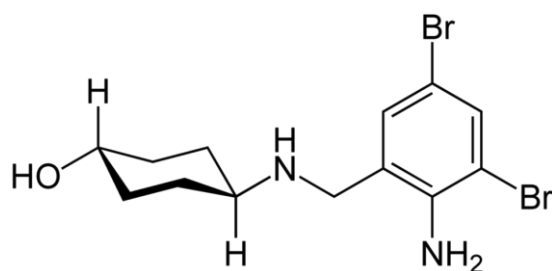


Figure 4: Skeletal formula of Ax

Ax exhibits pro-inflammatory properties by elevating IL-10, IL-12, and IFN- $\gamma$  expression; due to its aromatic moiety, Ax exhibits oxidant scavenger functions<sup>89,90</sup>. Moreover, it has been reported that Ax elevates SP production and can reverse the lipopolysaccharide(LPS)-stimulated induction of the extracellular signal-regulated kinase (ERK) 1/2 pathway<sup>91,92</sup>.

In Germany, Ax was the most popular drug as mucolytics with 24 % of the OTC expectorant market<sup>31</sup>. Under the basis of data that the National Health Insurance Fund of Hungary has provided us, little over 605000 units of Ax was sold in 2016 in Hungary, making Ax the second most used mucolytics in Hungary (**Figure 5**).

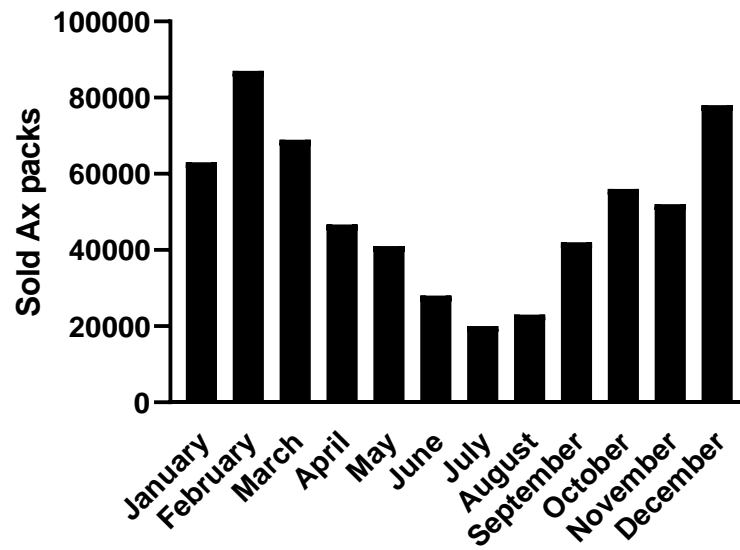


Figure 5: Consumption of Ax in Hungary 2016<sup>81</sup>

In addition, Ax is used for the symptomatic treatment of sore throat during viral infections, as it shows local anaesthetic effects<sup>93,94</sup>.

## 2. Aims and objectives

- Investigating the effect of NAC on *C. pneumoniae* replication in *in vitro*
- Examining the effect of short term and long-term treatment of NAC on *C. pneumoniae* replication in *in vivo* in mice
- Determining the mechanism of NAC on *C. pneumoniae* replication
- Finding a replaceable mucolytics of NAC
- Investigating the effect of higher concentration of Ax on *C. pneumoniae* replication in *in vivo* in mice
- Examining the potential effect of Ax on the gene expression profile in known anti-chlamydial gene *in vivo* in mice
- Verifying the impact of Ax on IFN- $\gamma$  and IL-6 production at the protein level *in vivo* in mice
- Analysing the effect of SP-A and SP-D protein on *C. pneumoniae* attachment and replication on mouse cell line
- Proving the effect of Ax treatment on ERK pathway regulation

### 3. Material and Methods

#### 3.1. Propagation of *C. pneumoniae*

In our experiments, the CWL029 strain of *C. pneumoniae* from the ATCC (Manassas, VA, USA) was used. *C. pneumoniae* was propagated in HEp-2 cells (ATCC), as described previously<sup>95,96</sup>. The titre of the infectious EBs was determined by an indirect immunofluorescence assay. Serial dilutions of the EB preparation were inoculated onto McCoy cells (ECACC, London UK), and after being cultured for 48 h, the cells were fixed with acetone and stained with a monoclonal anti-Chlamydia lipopolysaccharide antibody (AbD Serotec, Oxford, UK) and FITC-labelled anti-mouse IgG (Sigma, St Louis, MO, USA). The number of *C. pneumoniae* inclusions was counted under a UV microscope, and the titre was expressed as inclusion-forming units IFU/ml.

#### 3.2. *In vitro* effect of NAC and Ax

McCoy (ATCC) cultures were grown in 24-well tissue culture plates containing a 13 mm cover glass in minimum essential medium Eagle with Earle's salts (Sigma), supplemented with 10% vol/vol foetal calf serum, 0.5% wt/vol glucose, l-glutamine 0.3 mg/ml, 4 mM HEPES and 25 µg/ml gentamycin. Five parallel wells of semi-confluent cultures were infected with  $2 \times 10^3$  /well *C. pneumoniae* or treated simultaneously with NAC (0.01–10 mg/ml) or Ax (0.002–0.05 mg/ml) at the time of infection. Separate cells were infected with *C. pneumoniae* pretreated (1 h) with different concentrations of NAC. Subsequently, *C. pneumoniae* EBs were pretreated with NAC or Ax by continuous shaking in the presence of NAC (0.1 mg/ml) or Ax (0.05 mg/ml) at room temperature, and after 1 h these drugs were washed out using a culture medium and centrifugation at 13800g for 15 min (Heraeus Fresco 17) or left unwashed. NAC- or Ax-treated *C. pneumoniae* or non-treated *C. pneumoniae* were inoculated onto cells on cover glasses in 24-well plates and centrifuged at 800g for 1 h. After incubation for 48 h, the cells on the cover glasses were fixed with acetone and stained as described above in the 'Propagation of *C. pneumoniae*' section to visualize the inclusions of *C. pneumoniae*. To detect the effect of NAC or Ax on the attachment of chlamydial EBs to host cells, McCoy or A549 (ATCC) cells were infected with NAC- or Ax-treated *C. pneumoniae* EBs and after a 1 h incubation period and centrifugation the cells were washed and fixed and the bound EBs were stained by indirect immunofluorescence, as described above.

Fluorescence signals were analysed via Olympus UV microscopy. The immunofluorescence of non-infected or *C. pneumoniae*-infected cells, or cells infected with drug-treated *C. pneumoniae* was analysed quantitatively by ImageQuantTL 8.1 software as follows: 6–6 equally sized circular areas covering the cells were randomly selected on each image, and then the background signals of the selected areas were eliminated by a threshold set-up and the fluorescence intensity/pixel values of the randomly selected cells were quantified.

### 3.3. Mice and infection conditions

Pathogen-free 6-week-old female BALB/c mice were obtained from Charles River Laboratories (Hungary). The mice were maintained under standard husbandry conditions at the animal facility of the Department of Medical Microbiology and Immunobiology, University of Szeged, and were provided with food and water ad libitum. Before infection, the mice were mildly sedated with an intraperitoneal injection of 200 µl of sodium pentobarbital (7.5 mg/ml). They were then infected intranasally with  $2 \times 10^5$  IFU *C. pneumoniae* in 20 µl sucrose/phosphate/glutamic acid (SPG) buffer.

Four *in vivo* experiments were conducted:

1. From the second day post-infection (*p.i.*) mice were treated with 10 mg/kg NAC (Sigma) in a volume of 50 µl drinking water *per os* daily. Mice were anaesthetized and sacrificed on 7 days *p.i.*.
2. The above-described experiment was repeated, but mice were treated until 19 days *p.i.*, and sacrificed on 20 days *p.i.*.
3. In a separate study, *C. pneumoniae*-infected mice were treated similarly as above but with 1.25 mg/kg Ax (Sigma) and sacrificed 7 days after infection.
4. From the first day *p.i.*, the mice were administered daily with 5 mg/kg Ax. The mice were anaesthetized and euthanized on 7 days *p.i.*.

In every experiment: behaviour and weight were monitored daily; control mice received the same amount of water via oral administration using a pipette to mimic the stress of the treatment process. The sera were harvested via cardiac puncture, lungs were removed and homogenized

using acid-purified sea sand (Fluka Chemie AG, Buchs, Switzerland). Half of the homogenized tissue sample was processed for RNA extraction, whereas the other half was suspended in 1 ml of SPG for the detection of viable Chlamydia and to measure the cytokine levels.

This study was approved by the National Scientific Ethical Committee on Animal Experimentation of Hungary (August, 10 August 2016; III./3072/2016) and the Animal Welfare Committee of the University of Szeged. This study conformed to the Directive 2010/63/EU of the European Parliament.

### **3.4. Cultivation of *C. pneumoniae* from the lungs of mice**

After two freeze-thaw cycles, the homogenized lungs from individual mice were centrifuged (10 min, 400g) and serial dilutions of the supernatants were inoculated onto McCoy cell monolayers. These samples were then centrifuged (1 h, 800g), and after a 48 h culture, the cells were fixed with acetone and stained as described above in the 'Propagation of *C. pneumoniae*' section to visualize the inclusions of *C. pneumoniae*.

### **3.5. RNA extraction from the cells**

One-day-old semi-confluent McCoy cells in six-well plates were infected with *C. pneumoniae* using a multiplicity of infection (MOI) of 4. The cells were then left untreated, or NAC 0.1 mg/ml or Ax 0.05 mg/ml were added to the medium. Total RNA was extracted after a 1-day with Tri Reagent according to the manufacturer's protocol (Sigma). RNA concentrations were measured at 260 nm via a NanoDrop spectrophotometer (Thermo Scientific, Waltham, MA, USA).

### **3.6. RNA extraction from the lungs of mice**

Half of the homogenized lung sample acquired in Section 3.3 was processed with Tri Reagent and the extraction were conducted as described in Section 3.5,

### **3.7. cDNA synthesis**

After the RNA extraction protocol, 1 µg of total RNA was reverse transcribed using Maxima Reverse Transcriptase according to the manufacturer's protocol with random hexamer primer (Thermo Fisher Scientific, Inc. Waltham, MA, USA).

### 3.8. Quantitative PCR (qPCR) of the *Ido1*, *Ido2*, *Il12*, *Il17a*, *Il17f*, *Il23*, *Ifng*, *Sftpa*, *Sftpb*, *Sftpc*, *Sftpd*, *Actb*

qPCR was performed in a Bio-Rad CFX96 real-time system by using a SsoFast EvaGreen qPCR Supermix (Bio-Rad, Hercules, CA, USA) master mix and the murine-specific primer pairs. All of the primers were designed using PrimerQuest Tool (IDT) software and synthesized by Integrated DNA Technologies, Inc. (Montreal, Quebec, Canada). To check the amplification specificity, the qPCR was followed by a melting curve analysis. Threshold cycles (Ct) were calculated for the *Ido1*, *Ido2*, *Il12*, *Il23*, *Il17a*, *Il17f*, *Ifng*, *Sftpa*, *Sftpb*, *Sftpc*, *Sftpd* and *Actb* and the relative gene expressions were calculated by the  $\Delta\Delta C_t$  method (**Table 1**). Student's t-test was used to compare the statistical differences of  $\Delta C_t$  values between the infected and control samples, or One-way analysis of variance with repeated measures (ANOVA RM) and planned comparisons were used to compare the statistical differences in the  $\Delta C_t$  values between the infected and control samples, as described previously, with a level of significance of  $p < 0.05$ .

Primer	Sequence
<i>Ido1</i> sense	5'-GCTTCTTCCTCGTCTCTCTATT G-3'
<i>Ido1</i> antisense	5'-TCTCCAGACTGGTAGCTATGT-3'
<i>Ido2</i> sense	5'-CCTGGACTGCAGATTCCTAAAG-3'
<i>Ido2</i> antisense	5'-CCAAGTTCCTGG ATACCTCAAC-3'
<i>Il12 p40</i> sense	5'-ACATCAAGAGCAGTAGCAGTTC-3'
<i>Il12 p40</i> antisense	5'-AGTTGGGCAGGTGACATCC-3'
<i>Il17a</i> sense	5'-AAGGCAGCAGCGATCATCC-3'
<i>Il17a</i> antisense	5'-GGAACGGTTGAGGTAGTCTGAG-3'
<i>Il17f</i> sense	5'-AGCAAGAAATCCTGGTCCTTCGGA-3'
<i>Il17f</i> antisense	5'-CTTGACACAGGTGCAGCCAACTTT-3'
<i>Il23 p19</i> sense	5'-CCTGCTTGACTCTGACATCTT-3'
<i>Il23 p19</i> antisense	5'-TGGGCATCTGTTGGGTCTC-3'
<i>Ifng</i> sense	5'-CAAGTGGCATAGATGTGGAAGA-3'
<i>Ifng</i> antisense	5'-GCTGTTGCTGAAGAAGGTAGTA-3'
<i>Sftpa</i> sense	5'-GGTGTCTAAGAAGCCAGAGAAC-3'
<i>Sftpa</i> antisense	5'-CAAGATCCAGATCCAAGGAAGAG-3'
<i>Sftpb</i> sense	5'-CCACCTCCTCACAAAGATGAC-3'
<i>Sftpb</i> antisense	5'-TTGGGGTTAATCTGGCTCTGG-3'
<i>Sftpc</i> sense	5'-ATGGACATGAGTAGCAAAGAGGT-3'
<i>Sftpc</i> antisense	5'-CACGATGAGAAGGCGTTTGAG-3'
<i>Sftpd</i> sense	5'-TCTGAGCCACTGGAGGTAAA-3'
<i>Sftpd</i> antisense	5'-CAACATACAGGTCTGAGCCATAG-3'
<i>Actb</i> sense	5'-TGGAATCCTGTGGCATCCATGAAAC-3'
<i>Actb</i> antisense	5'-TAAAACGCAGCTCAGTAACAGTCCG-3'

Table 1: Sequence of used primers

### 3.9. Enzyme-linked immunosorbent assay (ELISA)

Standard sandwich mouse IL-6 and mouse IFN- $\gamma$  ELISA kits (BD OptEIA TM; BD Biosciences, Franklin Lakes, NJ, USA) were used to determine the IL-6 and IFN- $\gamma$  concentrations in the lung supernatants. Prior to use, the stored lung samples were thawed immediately, and the assay was performed according to the manufacturer's instructions at 10 $\times$  dilution for IL-6 and at 50 $\times$  dilution for IFN- $\gamma$ . The dynamic range of the kits was between 10 and 1000 pg/ml. Plates were analysed using the Biochrom Anthos 2010 microplate reader (Biochrom, Cambridge, UK). Samples were assayed in duplicate.

### 3.10. Western blotting analysis of ERK pathway

To investigate the levels of phosphorylation in RAF proto-oncogene serine/threonine-protein kinase (c-Raf), as well as dual specificity mitogen-activated protein kinase (MEK)1/2, ERK1/2, P90RSK1/2, and mitogen- and stress-activated protein kinase 1 (MSK-1) proteins, McCoy cells were grown in 6-well plates and treated with Ax (0.05 mg/ml) and/or infected with *C. pneumoniae* simultaneously at 0.01 MOI or left untreated and/or uninfected. After a 12-h incubation period, the cells were washed twice with ice-cold phosphate-buffered saline, scraped, and collected in a homogenization buffer (1 $\times$  radioimmunoprecipitation buffer supplemented with phosphatase inhibitors and a protease inhibitor cocktail) (Cell Signaling, Danvers, MA, USA). Cells were sonicated using an ultrasonic homogenizer (10 s, 4 °C), followed by centrifugation of the homogenate (14000g, 10 min, 4 °C). The bicinchoninic acid assay was performed to determine the protein concentration in the homogenates<sup>98</sup>. Samples containing 20  $\mu$ g of protein were boiled for 5 min. After preparation, the samples were subjected to sodium dodecyl sulphate-polyacrylamide gel electrophoresis (SDS-PAGE) using 10% polyacrylamide gels<sup>98</sup>. After separation, the proteins were transferred onto 0.45- $\mu$ m pore-sized nitrocellulose membranes (Amersham, Buckinghamshire, UK) (35 V, 1.5 h, room temperature (RT)). Nonspecific binding was blocked via incubation (1 h, RT) in 0.05% (v/v) Tris-buffered saline–Tween-20 containing 1% bovine serum albumin (BSA; v/v) (Sigma). In all experiments, the membranes were cut horizontally according to the molecular weights of the investigated proteins. Membranes were incubated with specific primary antibodies against phosphorylated forms of Raf (1:1000), MEK (1:2000), p90 (1:1500), ERK (1:2000), and MSK (1:1000) (Cell Signaling), as well as a housekeeping protein/loading control GAPDH (1:10,000) in 1% BSA solution containing 0.1% Tween-20 (overnight, 4 °C). After washing (Tris-buffered saline

containing 0.05% Tween-20, Sigma), the membranes were incubated with horseradish peroxidase-conjugated goat anti-rabbit secondary antibodies (Cell Signaling Technology) for 45 min at RT. A chemiluminescence analysis was performed using the LumiGLO 20× reagent (Cell Signaling), followed by exposure of the membranes to X-ray films. All films were scanned (Epson Perfection V19 Scanner, Epson, Suwa, Nagano, Japan) (8-bit, 400 dpi), and the density of the protein bands was quantified using Quantity One software (Bio-Rad)<sup>99</sup>. The 90-kDa form of MSK-1 was used for the calculation of the protein contents of the bands according to the protocol.

### **3.11. Apoptosis assay and flow cytometry**

Caspase 3/7 activity assays were performed using the FAM FLICA™ Caspase-3/7 Kit (Bio-Rad) combined with propidium iodide (PI). McCoy cells were divided into 4 experimental groups. Half of the McCoy cells were infected with 0.01 MOI *C. pneumoniae*, while the other half were left uninfected. Both the infected and uninfected groups were subdivided into those treated with 0.05-mg/ml Ax or left untreated. After 12 h of incubation, the apoptosis assay was performed according to the manufacturer's instructions, and the cells were analysed via flow cytometry. The assay discriminated between viable (caspase 3/7–/PI–), early apoptotic (caspase 3/7+/PI–), and late apoptotic (caspase 3/7+/PI+) cells. The fluorescence of the cell populations was analysed immediately using a BD fluorescence-activated cell sorting Aria Fusion flow cytometer (BD Biosciences).

### **3.12. *In vitro* effects of SP-A and SP-D on *C. pneumoniae* proliferation and attachment**

McCoy cells were seeded ( $2.5 \times 10^5$  cells) to form a monolayer in 24-well plates and incubated overnight. *C. pneumoniae* (0.01 MOI) was diluted in 1 ml medium in the presence of either SP-A (1 µg/ml) (Abcam, Cambridge, UK), SP-D (1 µg/ml) (Abcam), or neither. The mixtures were shaken at 37 °C for 1 h and then centrifuged at 800g for 1 h; at 48 h *p.i.*, the cells were fixed using acetone and stained, as described in Section 3.1. To detect the effect of SP-A and SP-D proteins on the attachment of *C. pneumoniae* to J-774 cells (ATCC), the experiment described above was repeated with the following modification. After 1 h of centrifugation, the cells were stained immediately, as described earlier.

Fluorescence signals were analysed using the Olympus IX83 Live Cell Imaging system and scanR High-Content Screening Station microscopy. The immunofluorescence of cells infected with nontreated *C. pneumoniae*, SP-A-pretreated *C. pneumoniae*, or SP-D-pretreated *C. pneumoniae* was analysed quantitatively using ImageQuantTL 8.1 as described in Section 3.2.

### **3.13. Statistical analysis**

Welch's t-test or one-way ANOVA RM with planned comparisons was performed using GraphPad Prism 8.0.1 software (GraphPad Software, San Diego, CA, USA). Data were expressed as the mean  $\pm$  standard deviation (SD). A value of  $p < 0.05$  was considered significant.

## 4. Results

### 4.1. NAC increases the *in vitro* replication of *C. pneumoniae*

Initially, we wanted to check the potential anti-chlamydial effect of NAC under *in vitro* conditions. During our experiments, different concentrations of NAC were applied using two approaches. First, a decreasing concentration of NAC was mixed directly with *C. pneumoniae*, and the host cells were immediately infected. Among the concentrations applied, doses of 10 mg/ml and 2 mg/ml NAC were toxic to the cells. Surprisingly, 0.1 mg/ml NAC resulted in a nearly sixfold increase in the number of *C. pneumoniae* inclusions in McCoy cells as compared to the number observed after infection with untreated *C. pneumoniae* (**Figure 6**). Accordingly, we chose this concentration in later studies. In the second approach, *C. pneumoniae* was preincubated with NAC at the respective three concentrations by shaking the mixture of *C. pneumoniae* and NAC continuously for 1 h before infecting the cells. As shown in (**Figure 6**), there was no significant difference in the infectivity of *C. pneumoniae* pretreated for 1 h with NAC and *C. pneumoniae* treated with 0.1 mg/ml NAC immediately before inoculation of the cells ( $p > 0.05$ ).

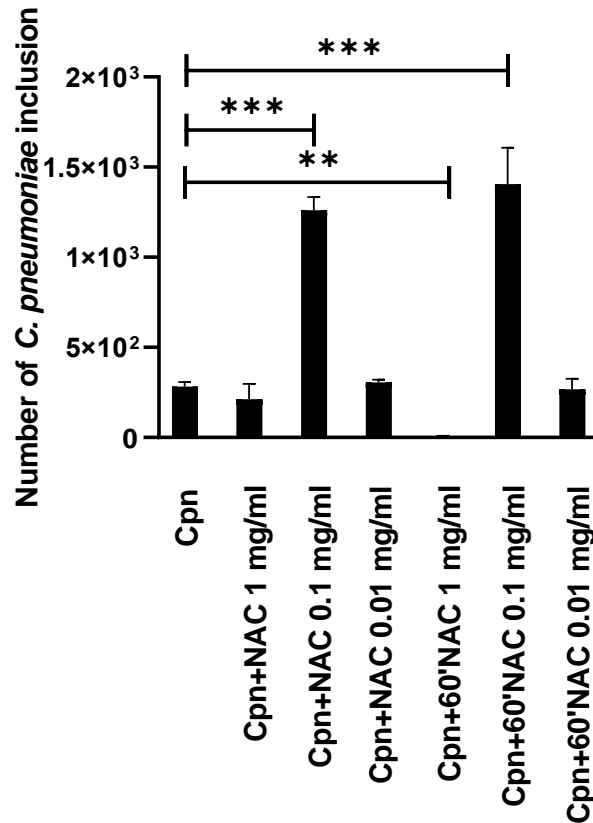


Figure 6: The effect of different concentrations of NAC and different treatment conditions on *C. pneumoniae* replication. McCoy cells were infected with *C. pneumoniae* treated with different concentrations (0.01–1 mg/ml) of NAC at the time of inoculation or infected with *C. pneumoniae* pretreated with NAC. *C. pneumoniae* inclusions were counted under a UV microscope after indirect immunofluorescence staining. Bars denote the mean $\pm$ SD of the results on five parallel tissue wells Cpn=*C. pneumoniae* (\*\*  $p < 0.01$ , and \*\*\*  $p < 0.001$ ).

#### 4.2. NAC increases the binding of *C. pneumoniae* to the host cell

To investigate whether NAC is able to influence the attachment of *C. pneumoniae*, McCoy and the more relevant A549 epithelial cells of human respiratory origin were infected with NAC-treated *C. pneumoniae* or with untreated *C. pneumoniae*. As shown in (Figure 7. a, b, d), NAC-treated *C. pneumoniae* produced a significantly higher fluorescence intensity as compared to the untreated *C. pneumoniae* in McCoy cells. A similar effect was observed in the A549 cells (Figure 7e, f, j). The control cells did not display any fluorescence (Figure 7. c, g).

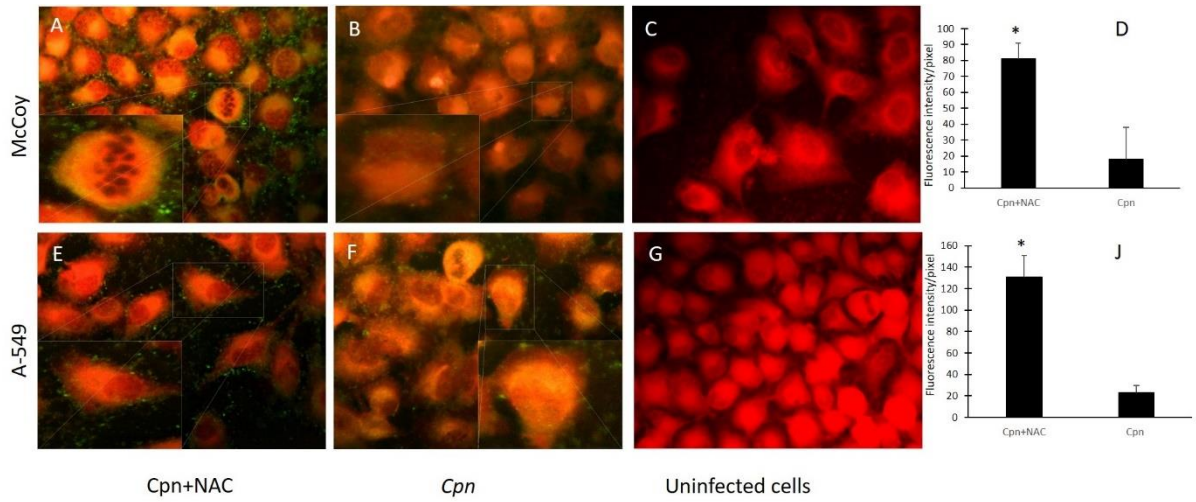


Figure 7: The effect of NAC treatment on *C. pneumoniae* attachment. McCoy or A549 cells were infected with NAC-treated (0.1 mg/ml) (a, e) or untreated *C. pneumoniae* (Cpn) (b, f). After the incubation period, the cells were stained as described above in the Methods section. Fluorescence signals were analysed via UV microscopy, and the immunofluorescence of non-infected, *C. pneumoniae*-infected or drug-treated *C. pneumoniae*-infected cells was analysed quantitatively by ImageQuantTL 8.1 software. The results are expressed as the mean $\pm$ SD of the data from three independent experiments, (\* $p < 0.05$  (d, j)).

Subsequent experiments indicated that the removal of NAC with the culture medium from *C. pneumoniae* did not significantly modify the number of replicating *C. pneumoniae* as compared to the outcome of the infection with unwashed *C. pneumoniae* (**Figure 8**). Adding NAC to the cells 6 or 24 h after *C. pneumoniae* infection did not change the number of inclusions formed by *C. pneumoniae* (**Figure 8**). Furthermore, preincubation of the host cells with NAC for 48 h before infection with *C. pneumoniae* did not modify the replication of *C. pneumoniae* (data not shown).

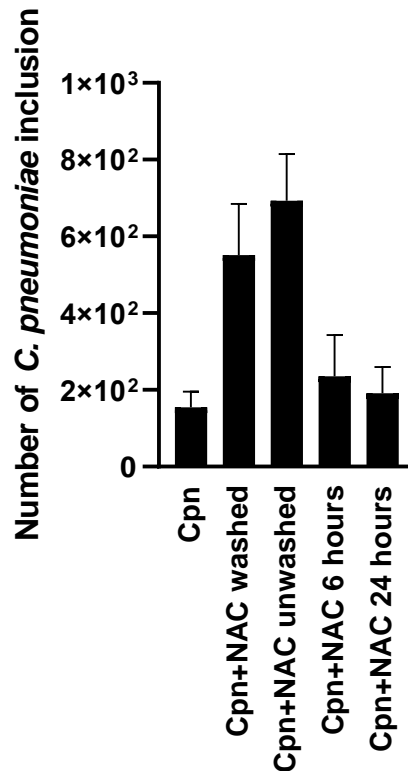


Figure 8: The effect of pre- or post-infection exposure to NAC on *C. pneumoniae* replication. The number of *C. pneumoniae* inclusions were counted in McCoy cells infected with untreated *C. pneumoniae* (Cpn), cells infected with *C. pneumoniae* preincubated for 1 h with (0.1 mg/ml) NAC and subsequently washed via high-speed centrifugation (Cpn+NAC washed), cells infected with NAC-treated but unwashed *C. pneumoniae* (Cpn+NAC unwashed) and cells infected with untreated *C. pneumoniae* to which NAC was added 6 h (Cpn+NAC 6 h) or 24 h (Cpn+NAC 24 h) *p.i.*. The *C. pneumoniae* inclusions were revealed by indirect immunofluorescence. The means of the titres are expressed as IFU in five parallel cultures and the  $\pm$ SD are shown.

#### 4.3. Exposure to NAC not only increases the chlamydial lung burden but also prolongs the infection in mice

Here, we investigated whether NAC might aggravate the chlamydial infection in the short term. Twenty mice were infected with *C. pneumoniae*, and 10 were treated with 10 mg/kg NAC *per os* at the same concentration as that applied for human respiratory infections as a mucolytic drug for 6 days. On the seventh day, the mice were sacrificed; the lungs were removed for the determination of recoverable *C. pneumoniae*. We found that after 6 days of exposure to NAC the severity of the *C. pneumoniae* infection increased. The number of recoverable chlamydial

inclusions was approximately three times higher in the NAC-treated group than in the *C. pneumoniae*-infected mice without NAC treatment (**Figure 9**). Next, we investigated whether NAC prolongs the clearance of *C. pneumoniae* from the lungs. Sixteen mice were infected with *C. pneumoniae*, and eight mice were treated with NAC for 19 days. On the twentieth day, the mice were sacrificed, and their lungs were removed for the detection of viable *C. pneumoniae* (**Figure 10**). All of the mice were *C. pneumoniae* culture-positive in the NAC-treated group and the number of *C. pneumoniae* inclusions was 2.5 times higher than that in the control group. Moreover, in the control group, two mice became culture-negative (the sensitivity of our method was  $<40$  IFU/lung), suggesting recovery from the disease. The data for these mice were not included in Figure 10.

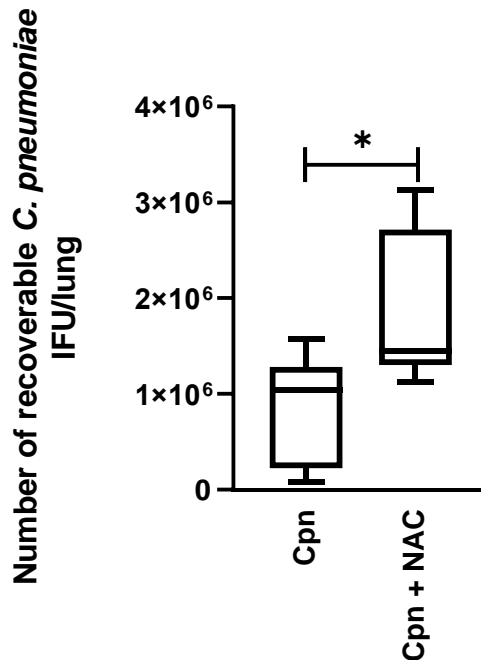


Figure 9: Recoverable IFU in *C. pneumoniae*-infected mice with or without oral NAC treatment. Mice were sacrificed on 7 days *p.i.*, Box = 25th percentile, median, and 75th percentiles; bars = min and max values (\*  $p < 0.05$ )

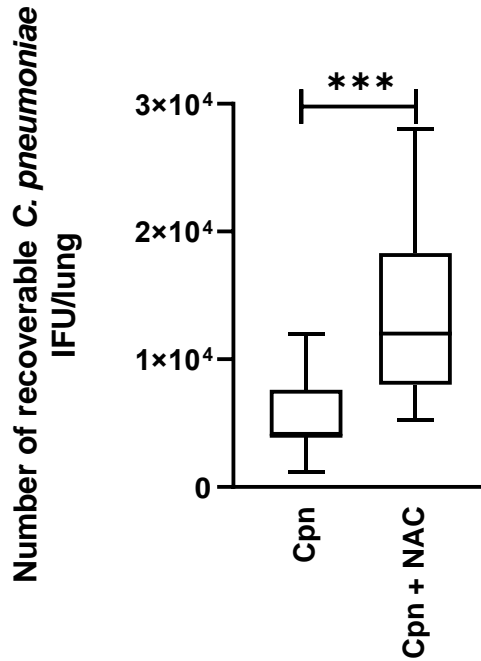


Figure 10: Recoverable IFU in *C. pneumoniae*-infected mice with or without oral NAC treatment. Mice were sacrificed on 20 days *p.i.*. Box = 25th percentile, median, and 75th percentiles; bars = min and max values (\*\*\*)  $p < 0.001$ ).

#### 4.4. Ax does not increase the number of infective *C. pneumoniae*

To look for a better alternative to NAC, the effect of Ax on *C. pneumoniae* replication was tested in *in vitro* and *in vivo* systems. Using concentrations of 0.002 and 0.01 mg/ml, Ax did not cause any significant changes in bacterial replication in McCoy cells, but 0.05 mg/ml Ax had a strong antimicrobial effect, and this reduced the number of *C. pneumoniae* to approximately one-fifth of that observed with untreated cells (**Figure 11**). None of the applied concentrations of Ax influenced host cell viability (data not shown). Increasing the dose to 0.25 mg/ml Ax proved to be toxic to the cells (data not shown). We then wanted to determine the reason for the antimicrobial activity of Ax. An identical experiment to that performed with NAC was conducted. Ax-treated and untreated *C. pneumoniae* were inoculated onto McCoy and A549 cells, and the cells were stained using the immunofluorescence method. An altered immunofluorescence was not observed in this case, and we inferred that the Ax treatment did not modify the number of *C. pneumoniae* EBs attached to the cell membrane (data not shown). We then tested whether Ax might influence the expression of IDO1,2. Ax caused a 2.5-fold increase in IDO-2 expression in *C. pneumoniae*-infected cells as compared to the expression in untreated cells. In our experiments, NAC treatment did not influence the expression of IDO1,2

in *C. pneumoniae*-infected cells (data not shown). To further investigate the role of Ax during *C. pneumoniae* infection, our mice were infected with *C. pneumoniae* and from the second day were treated with tap water-diluted Ax at the same concentration as is applied for human respiratory infections when it is used as a mucolytic drug (1.25 mg/kg). The control mice were given tap water. During the 7-day period, the behaviour (activity and appetite) and weight of the animals did not change significantly between groups (data not shown). The mice were sacrificed 7 days after the infection and the number of recoverable *C. pneumoniae* was counted from the lungs by indirect immunofluorescence. As shown in (Figure 12) the number of recoverable *C. pneumoniae* did not change significantly in the Ax-treated and untreated *C. pneumoniae*-infected group of mice.

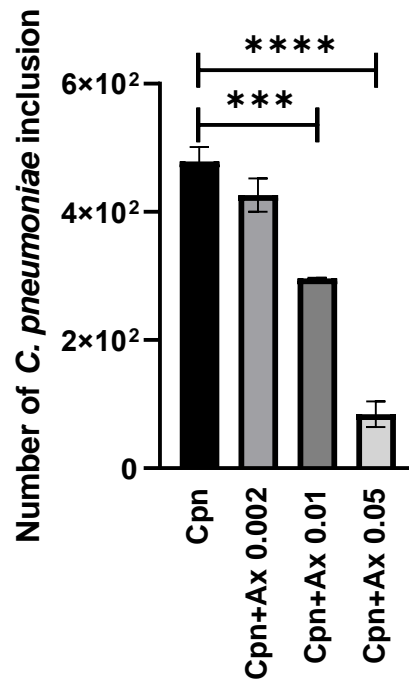


Figure 11: Effect of increasing concentration of Ax on *in vitro* *C. pneumoniae* replication. McCoy cells were infected with *C. pneumoniae* ( $2 \times 10^3$  IFU/well) and simultaneously treated with different amounts of Ax (0.002–0.05 mg/ml). *C. pneumoniae* inclusions were detected by indirect immunofluorescence. Data are presented as the mean  $\pm$  SD of the results in five parallel cultures. (\*\*\*)  $p < 0.001$ , and (\*\*\*\*)  $p < 0.0001$ .

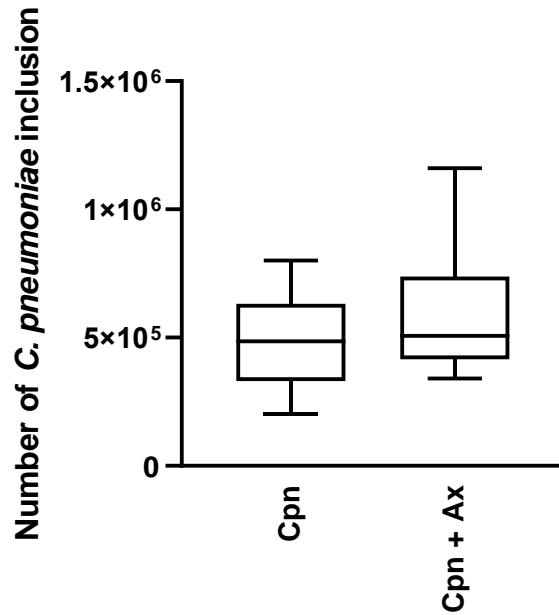


Figure 12: Effect of 1.25 mg/kg Ax on *C. pneumoniae* replication in *in vivo* mice. A group of 10 *C. pneumoniae*-infected mice were treated *per os* with Ax (1.25 mg/kg). The mice were sacrificed 7 days after infection and the number of infective *C. pneumoniae* was detected in the homogenized lungs by inoculation onto McCoy cells and staining using indirect immunofluorescence. Box = 25th percentile, median, and 75th percentiles; bars = min and max values.

#### 4.5. Ax treatment at elevated concentration suppressed *C. pneumoniae* proliferation in mouse lungs

Subsequently, our aim was to determine whether a relatively higher concentration of Ax would influence the chlamydia replication. Therefore, the mice were infected with *C. pneumoniae* ( $2 \times 10^5$  IFU/mouse); half of the mice were treated daily from day 1 *p.i.* with a  $4 \times$  higher concentration of Ax (5 mg/kg) than the dose used as a mucolytic in common respiratory infections, as we used earlier Section 4.4. Seven days *p.i.*, the mice were euthanized, and the lungs were removed for detection of viable *C. pneumoniae*. A significant difference was found between the number of recoverable *C. pneumoniae* between the Ax-treated and untreated groups. The mean numbers of viable *C. pneumoniae* IFUs in the Ax-treated and untreated groups were  $3.1 \times 10^4$  and  $7.3 \times 10^4$  IFU/lung, respectively (**Figure 13**). The mice in the Ax-treated group exhibited less severe symptoms than those in the control group.

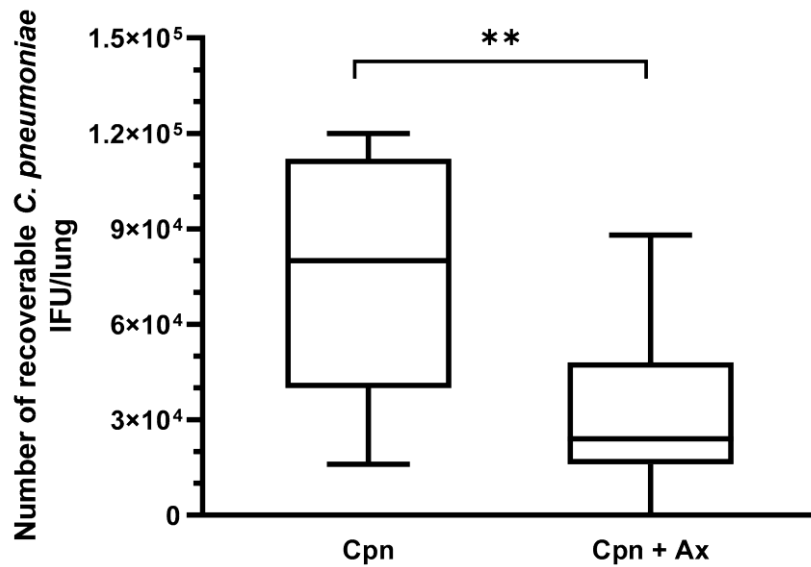


Figure 13. Recoverable *C. pneumoniae* IFU in infected mice ( $n = 20$ ) with and without Ax treatment. Ax-treated mice daily received 5 mg/kg Ax for 6 days. The supernatant of the lung homogenates was inoculated onto a McCoy cell monolayer and cultured for 2 days, followed by fixation and staining, and the number of inclusions was determined via indirect immunofluorescence assay. (\*\*  $p = 0.0049$ ). Box = 25th percentile, median, and 75th percentiles; bars = min and max values. IFU, inclusion-forming unit; Cpn, *C. pneumoniae*-infected mice; Cpn + Ax, *C. pneumoniae*-infected mice treated with Ax.

#### 4.6. Ax treatment altered the gene expression and protein level of IFN- $\gamma$ in the lungs of *C. pneumoniae*-infected mice

We investigated whether gene expression was altered during Ax treatment, concerning the cytokine profile in *C. pneumoniae* infection. We found that the relative expression of IL-12, IL-23, IL-17A, and IFN- $\gamma$  was significantly higher in the *C. pneumoniae*-infected/Ax-treated group than in the *C. pneumoniae*-infected group without treatment (2.22-, 3.07-, 2.46-, and 2.27-fold, respectively) (**Figure 14a**).

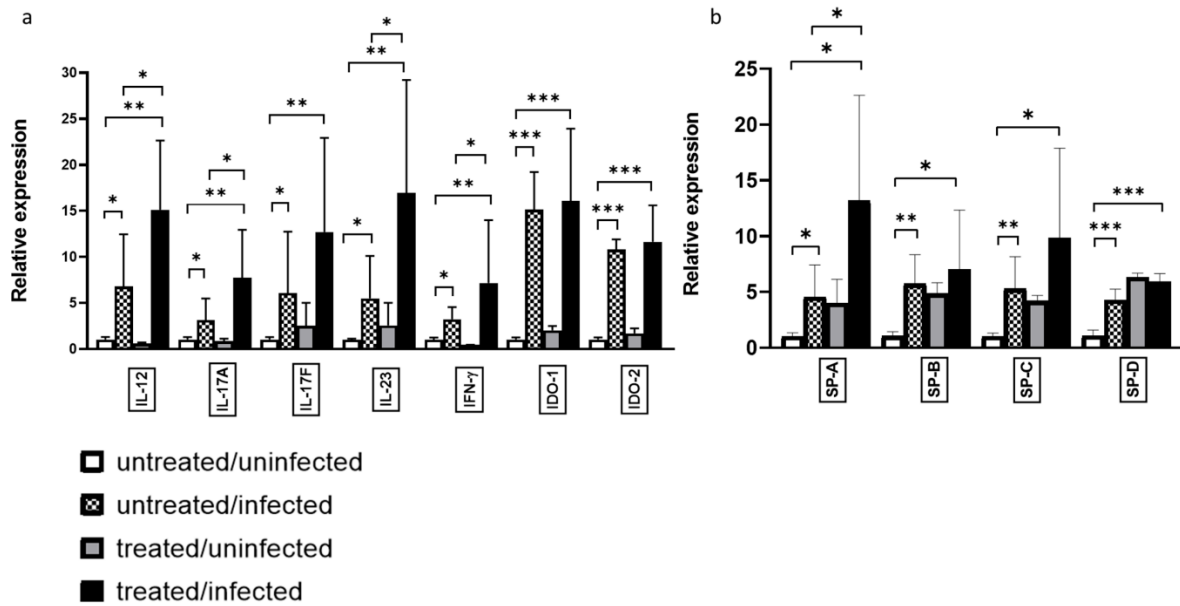


Figure 14: Relative expression of genes influences by *C. pneumoniae* infection and Ax treatment. Mice were either infected with *C. pneumoniae* (or remained uninfected as a control), followed by treatment with Ax (5mg/kg) (or remained untreated, for the control). RNA was extracted from the lungs followed by cDNA synthesis. Gene expression was analysed via qPCR for (a) IL-12, IL-23, IL-17A, IL-17F, IFN- $\gamma$ , IDO-1, and IDO-2 and (b) SP-A, SP-B, SP-C, and SP-D. Bars denote the mean  $\pm$ SD of the expression levels for triplicate measurements (\*  $p < 0.05$ , \*\*  $p < 0.01$ , and \*\*\*  $p < 0.001$ ).

We previously reported that Ax treatment elevates the expression of the known anti-chlamydial enzyme IDO-2 in the A549 cell line; however, this elevation is not significant when a human equivalent mg/kg dose is administered to *C. pneumoniae*-infected mice<sup>100</sup>. Therefore, we determined whether an elevated dose of Ax increased IDO-1 and IDO-2 expression in mice. We observed no significant difference in expression levels between *C. pneumoniae*-infected mice and *C. pneumoniae*-infected/Ax-treated mice. However, in accordance with the findings of Virok et al., which showed that IDO-1 and IDO-2 are active in *C. pneumoniae*-infected mice<sup>35</sup>, in contrast to earlier findings<sup>101</sup>, we also found significant increases in both IDO-1 and IDO-2 expression levels during *C. pneumoniae* infection compared to those of the untreated/uninfected group (15.14- and 10.81-fold, respectively) (**Figure 14a**).

SPs play a crucial role in maintaining lung homeostasis; moreover, SP-D shows an anti-*C. trachomatis* activity in a genital mouse model<sup>102–105</sup>. Therefore, we determined the relative expression of SPs in the lungs of the mice. We found that all SPs were significantly upregulated in the untreated/infected mice compared to that of the uninfected/untreated group (SP-A, 4.55-

fold; SP-B, 5.72-fold; SP-C, 5.28-fold; SP-D, 4.26-fold), suggesting that these anti-chlamydial mechanisms occur naturally in *C. pneumoniae*-infected mouse lungs. Notably, we observed a significant elevation in SP-A expression levels of mice in the treated/infected group compared to those of the untreated/infected group (2.89-fold) (**Figure 14b**).

After determining that the relative mRNA expression of *Ifng* was significantly higher in Ax-treated/infected mice than in untreated/infected mice, we investigated the protein expression levels of IFN- $\gamma$ . We measured the cytokine concentrations in lung supernatants and found that IFN- $\gamma$  levels were significantly higher in the *C. pneumoniae*-infected/Ax-treated group than in the untreated/infected group ( $p = 0.0041$ ) (**Figure 15**). We also measured the level of the pro-inflammatory cytokine IL-6; however, we did not observe significant differences between the expression levels of *C. pneumoniae*-infected and *C. pneumoniae*-infected/Ax-treated groups (**Figure 15**).

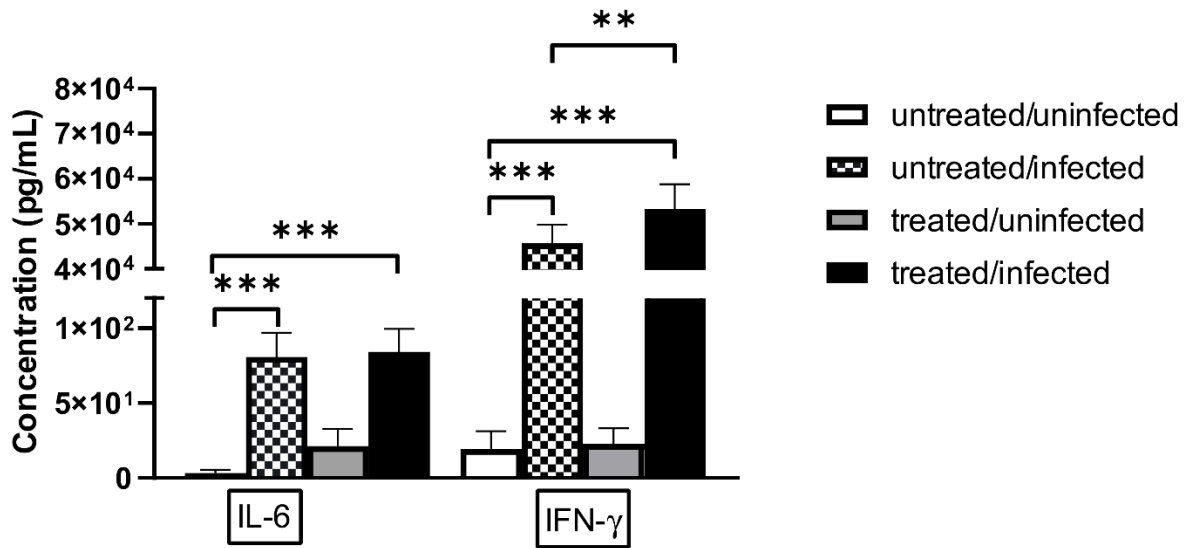


Figure 15: Concentrations of IL-6 and IFN- $\gamma$  in lung supernatants. Mice were infected intranasally with *C. pneumoniae* and treated with 5 mg/kg Ax for 6 days or left untreated and uninfected. On the seventh day *p.i.* the mice were euthanized and the concentrations of IL-6 and IFN- $\gamma$  in the supernatants of the lungs were measured via ELISA. Each bar denotes the mean  $\pm$  SD for 10 mice (\*\*  $p < 0.01$ , and \*\*\*  $p < 0.001$ ).

#### 4.7. SP treatment increased the attachment of *C. pneumoniae* to macrophages and decreased bacterial proliferation

After showing that Ax treatment increased the relative expression of SPs in the lungs of *C. pneumoniae*-infected mice (**Figure 14b**), we investigated the effect of anti-chlamydial SP proteins on *C. pneumoniae* replication and attachment to macrophages *in vitro*. We found that the pretreatment of EBs with SP-A or SP-D significantly reduced the number of *C. pneumoniae* inclusions (0.18-fold) ( $p = 0.021$ ) and (0.57-fold) ( $p = 0.034$ ), respectively, in infected cells. This anti-chlamydial effect was more prominent in SP-A treatment than in SP-D treatment (**Figure 16**). These results correspond to the findings of Oberley et al.<sup>102,105</sup>, who showed that SP-A and SP-D can aggregate Chlamydia, thereby inhibiting the infection of cells.

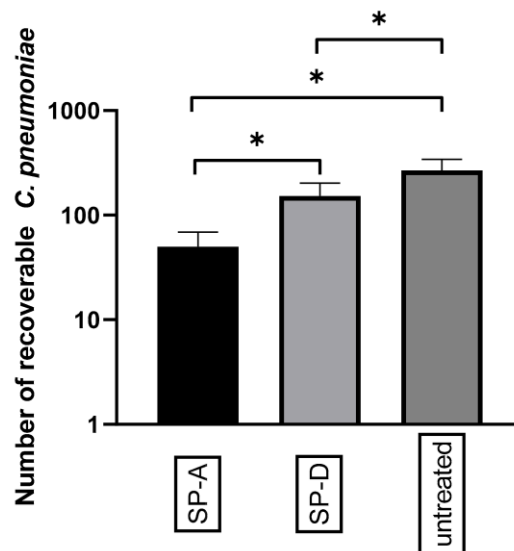


Figure 16. Anti-chlamydial effect of SP-A and SP-D. *C. pneumoniae* EBs were treated with either SP-A, SP-D, or left untreated. After 1 h of incubation, the samples were inoculated onto McCoy cells and fixed 48 h post-infection. The number of *C. pneumoniae* inclusions was determined via indirect immunofluorescence staining. Each bar denotes the mean number of inclusions in three parallel cultures  $\pm$  SD (\*  $p < 0.05$ ).

Next, we wanted to investigate whether *C. pneumoniae* EBs treated with SP-A or SP-D are taken up with higher efficiency by J-774 murine macrophage cells. Consequently *C. pneumoniae* EBs were treated with SP-A or SP-D and then, the samples were inoculated onto J-774 cells. After 1 h of centrifugation, we stained the cells with Chlamydia-specific immunofluorescent antibodies, and it was found that the average pixel intensity of FITC was significantly elevated after treatment with both types of SPs compared to that seen in cells

infected with untreated EBs. This indicated that a relatively larger number of *C. pneumoniae* cells were recognized by J-774 cells after SP treatment. This effect was more prominent in SP-A-treated *C. pneumoniae* than in SP-D-treated *C. pneumoniae* (SP-A 2.74-fold ( $p = 0.014$ )) and (SP-D 2.05-fold ( $p = 0.024$ )) (**Figure 17**). The results were in agreement with Oberley et al., who demonstrated that SP-A-or SP-D-treated Chlamydia are recognized by THP-1 human monocytic cells with higher efficiency than untreated bacteria <sup>102</sup>.

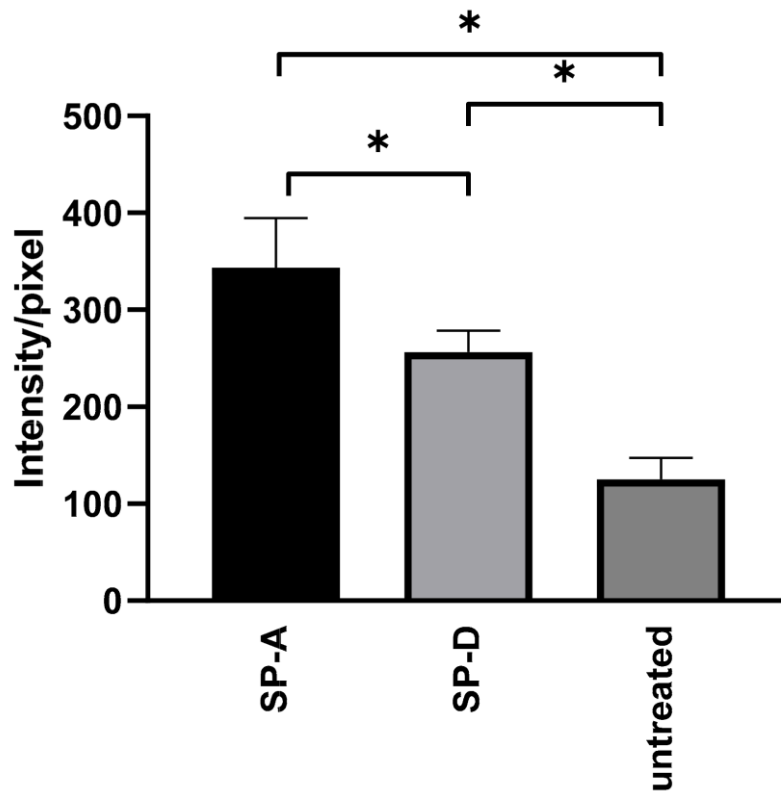


Figure 17. Effect of SP-A and SP-D treatment on *C. pneumoniae* attachment to J-774 cells. *C. pneumoniae* EBs were incubated with either SP-A or SP-D, or they were left untreated. After 1 h of incubation, the samples were inoculated onto J-774 cells, and then, 1 h *p.i.* the cells were fixed and stained via immunofluorescence. The average FITC intensity/pixel was measured. The results are expressed as the mean  $\pm$  SD of the data from three independent experiments (\*  $p < 0.05$ ).

#### 4.8. Ax treatment did not induce apoptosis via the Caspase-dependent pathway but decreased ERK 1/2 activation in *C. pneumoniae*-infected cells

It has been shown that *C. pneumoniae* can prevent the occurrence of host cell apoptosis<sup>44,46,106</sup> therefore, we investigated whether Ax treatment affected host cell death during *C. pneumoniae* infection. According to Galle et al., the assessment of apoptosis in *C. pneumoniae*-infected cells via annexin V staining is not accurate due to the *C. pneumoniae*-induced externalization of phosphatidylserine on the host cell membrane, which provides a binding site for annexin V and creates a false-positive apoptosis signal<sup>107</sup>. Therefore, we determined caspase 3/7 activity using flow cytometry. The analysis revealed that caspase 3/7 activity did not differ significantly between the treated/infected group and the untreated/infected group (Figure 18).

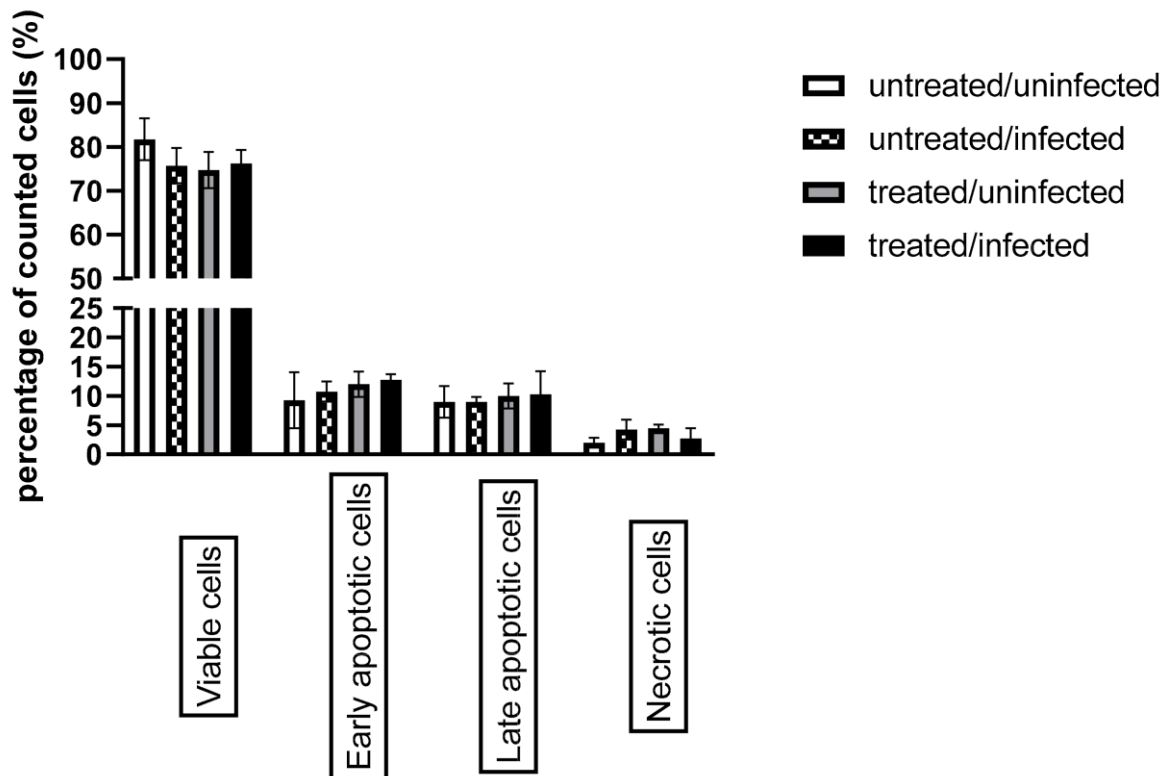


Figure 18: Evaluation of host cell apoptosis based on caspase 3/7 activity combined with propidium iodide staining. McCoy cells were infected with 0.01 MOI of *C. pneumoniae* and/or treated with 0.05 g/ml Ax or left untreated/uninfected. Flow cytometric analysis was performed 12 h *p.i.* to determine the status of apoptosis. The results are expressed as the mean  $\pm$  SD of the data from three independent experiments. ( $p > 0.05$ ).

*C. pneumoniae* activates the ERK 1/2 pathway to acquire several essential molecules from host cells and avoid host cell apoptosis<sup>106,108</sup>. Therefore, we investigated the effect of Ax treatment on the MAPK/ERK activity in *C. pneumoniae*-infected cells. Western blotting analysis showed that the ERK-1 (1.49-fold;  $p < 0.05$ ) and ERK-2 (2.04-fold;  $p < 0.05$ ) protein expression levels were significantly increased in untreated/infected cells compared to those in untreated/uninfected cells (**Figure 19**). We also observed that *C. pneumoniae* infection significantly increased the MSK-1 levels (2.25-fold) in untreated/infected cells compared to those in untreated/uninfected cells. MSK-1 is responsible for the activation of nuclear factor kappa-enhancer of B-cells and induction of early genes such as *c-fos*, *junB*, and *mkp-1*<sup>109</sup>. The Ax treatment of *C. pneumoniae*-infected cells significantly decreased the levels of c-RAF (0.42-fold), ERK-1 (0.16-fold), ERK-2 (0.15-fold), P90RSK1 (0.61-fold), P90RSK2 (0.67-fold), and MSK-1 (0.19-fold) ( $p < 0.05$ ) compared to those of the untreated/infected group (**Figure 19**).

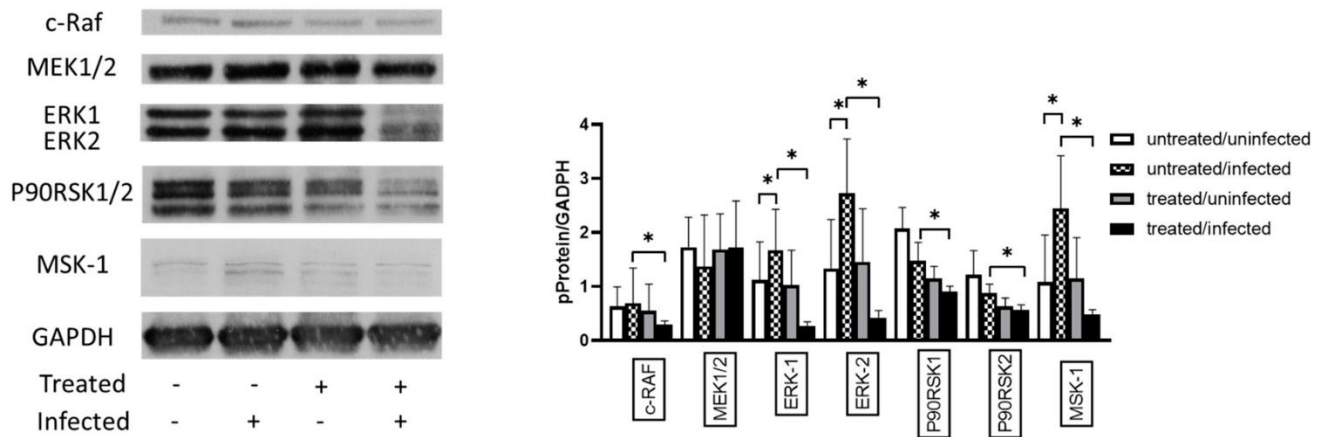


Figure 19. Analysis of the expression of proteins related to the MAPK/ERK pathway. McCoy cells were infected with 0.01 MOI *C. pneumoniae*, treated with 0.05 mg/ml Ax, infected with 0.01 MOI *C. pneumoniae* and treated with 0.05 mg/ml Ax, or left untreated. The cells were scraped at 12 h *p.i.*. Subsequently, proteins in the cell lysates were separated via SDS-PAGE and then blotted onto nitrocellulose membranes. Membranes were incubated with specific primary antibodies against phosphorylated forms of c-RAF, MEK1/2, P90RSK1/2, ERK1/2, MSK-1, and a housekeeping protein/loading control GAPDH. Horseradish-peroxidase-conjugated goat anti-rabbit IgG was used as secondary antibody. Chemiluminescence analysis was performed using the LumiGLO reagent, followed by the exposure of membranes to X-ray films. All films were scanned, and density of the protein bands was quantified using the Quantity One software. The ratio of phosphorylated protein/GAPDH was determined. The results are expressed as the mean  $\pm$  SD of the data from three independent experiments. The

shown Western blot is representative of parallel Western blots (\*  $p < 0.05$ ). MAPK, mitogen-activated protein kinase; ERK, extracellular signal-regulated kinase; c-RAF, RAF proto-oncogene serine/threonine-protein kinase; MEK1, dual specificity mitogen-activated protein kinase; MSK-1, mitogen- and stress-activated protein kinase 1; GAPDH, glyceraldehyde 3-phosphate dehydrogenase.

## 5. Discussion

NAC is a multifaceted drug that is used in the treatment of different diseases, mainly as a mucolytic agent. It is relatively inexpensive and commercially available as an OTC medicine. It has been shown to increase the level of GSH, the body's major antioxidant, by increasing glutathione S-transferase activity. It is a powerful antioxidant and has the potential to treat diseases characterized by the generation of free oxygen radicals<sup>110</sup>. For instance, NAC is a therapeutic option in chronic obstructive pulmonary disease. In an open-label study of 1392 patients, NAC reduced the viscosity of expectorated sputum, reduced cough severity and improved the ease of expectoration in patients after 2 months of treatment<sup>111</sup>. Furthermore, NAC dramatically attenuated influenza symptoms in a group of patients as compared with a placebo-treated group<sup>112</sup>. In our study, we found that instead of decreasing bacterial replication, NAC actually increased the number of replicating *C. pneumoniae* in both *in vitro* and *in vivo* infections.

Based on our *in vitro* experiment, we disclosed that NAC increased the attachment of the pathogens to the host cells. Lazarev et al. investigated the role of intracellular GSH in *C. trachomatis* infection, and they found that the treatment of cells with buthionine sulfoximine, which causes the irreversible inhibition of GSH biosynthesis or hydrogen peroxide-induced oxidation of GSH, decreased the number of *C. trachomatis* inclusions. In contrast with this finding, the treatment of cells with NAC increased the number of chlamydial inclusions. The researchers concluded that GSH plays a crucial role in chlamydial replication. However in their experiments, NAC was used as a GSH precursor, and they did not attempt to investigate the anti-chlamydial effect of NAC<sup>113</sup>. However, it is well known that the infectivity of Chlamydia species depends on the reduced status of the cell membrane protein OmcB<sup>114</sup>. In agreement with our hypothesis, NAC treatment of the EBs increases the attachment directly, probably by reducing OmcB, which could not have been from an increased level of GSH, because NAC was removed from the culture medium in some of our experiments.

According to our *in vivo* results, NAC significantly increased *C. pneumoniae* replication both in early phase of acute infection and late phase of acute infection and in chronic infection. During the experiment the mice showed more severe signs of infection (e.g. changes in weight, posture, behaviour) in NAC treated group compared to untreated group, which indicates that the infection was more severe.

Aside from the negative effect of NAC on acute *C. pneumoniae* infection, we need to take into account another possible effect of this drug. *C. trachomatis*, which belongs to the family *Chlamydiaceae*, is one of the most common sexually transmitted pathogens. Unfortunately, the infection is asymptomatic in up to 70 % of the cases. The severe consequences of chronic *C. trachomatis* infection are ectopic pregnancy, infertility, or a pelvic inflammatory disease <sup>115</sup>. In the worst-case scenario, NAC applied simultaneously in the treatment of ongoing respiratory diseases may not only increase the growth of *C. pneumoniae* but stimulate the growth of *C. trachomatis* as well. In order to circumvent NAC's aggravating effect on *C. pneumoniae* infection, we looked for a better mucolytic agent that does not increase the severity of the respiratory disease. In our *in vitro* study, Ax displayed significant anti-chlamydial activity that was not associated with decreased binding of the pathogen to the host cells. The complete antimicrobial mechanism of Ax was not analysed, but Ax treatment increased the expression of the anti-chlamydial IDO-2, which may in part cause a reduction in the number of pathogens. In our first *in vivo* experiment, mice were infected with *C. pneumoniae* and then treated with Ax. Using a human equivalent Ax/body weight dose we found no significant difference in the number of recoverable *C. pneumoniae* between the treated and the untreated groups. Yang et al. found that Ax 10 mg/kg/day (which is eight times higher than the normal dose in a human) significantly reduced the mortality of mice infected with a lethal dose of H3N2 influenza virus <sup>94</sup>.

*C. pneumoniae* is a common respiratory pathogen and unfortunately it is not always diagnosed correctly, and if a doctor suggests NAC as a mucolytic agent, it might worsen and delay the patient's recovery. Based on the prevalence of *C. pneumoniae*, many patients could suffer prolonged respiratory disease because of NAC. Overall, on the basis of our results, we can state that NAC can aggravate and prolong the infection caused by *C. pneumoniae* in an animal model. This information will be useful for physicians who recommend NAC as a mucolytic drug in respiratory diseases with a non-identified aetiology. In the case of a *C. pneumoniae* infection, a correct laboratory diagnosis is imperative, because in its absence the use of NAC may worsen the patient's chance of recovery. It is important that clinical studies to prove our results are implemented.

Ax, a metabolite of bromhexine, is considered a relatively safe OTC drug. It is primarily recommended as a secretory agent for the treatment of various respiratory diseases that are associated with extensive mucus production. Ax treatment increases surfactant synthesis and facilitates their secretion from type II pneumocytes <sup>116,117</sup>. Furthermore, Ax exhibits voltage-

dependent sodium channel inhibitory properties, which can be beneficial in cases of diseases associated with sore throat by incorporating Ax in lozenges <sup>93,118</sup>. Ax can also be used in the treatment of Gaucher disease and is considered a supplemental medication for treating Parkinson's disease, as it increases glucocerebrosidase activity <sup>88,119</sup>. Additionally, a recently published study suggested that when Ax is administered together with antibiotics, a relatively higher antibiotic concentration can be obtained in the lungs due to its secretion-supporting function <sup>120</sup>. Several studies have shown that Ax exhibits antimicrobial characteristics. Ax treatment reverses the resistance of *Candida albicans* to fluconazole <sup>121</sup>. Moreover, it inhibits the mucoid conversion of *Pseudomonas aeruginosa*, facilitates the bactericidal activity of ciprofloxacin against biofilms, and exhibits synergy with vancomycin for the elimination of catheter-related *Staphylococcus epidermidis* biofilms both *in vitro* and *in vivo* <sup>122</sup>. Furthermore, Ax impedes the rhinovirus infection in primary cultures of human tracheal epithelial cells <sup>123</sup>. Ax also shows antibiofilm properties; the biofilm formed by *Pseudomonas aeruginosa* treated with Ax for 7 days is thinner and more fragmented than that formed by untreated cells <sup>124</sup>.

It is known that Ax has a well-balanced and favourable risk-benefit profile <sup>87</sup>; therefore, we investigated the effect of a four-fold increase in Ax dose on *C. pneumoniae* infection. In our *in vivo* study, we found that 5mg/kg Ax significantly decreased the number of viable *C. pneumoniae* IFUs in the lungs of mice. We found several significantly elevated cytokine gene expressions, which has a crucial role in the defence of *C. pneumoniae* infection. IL-17A is associated with a neutrophil influx in the lungs; mice infected with *C. pneumoniae* and treated with anti-IL-17A antibodies have a relatively higher *C. pneumoniae* burden <sup>125,126</sup>. IL-23 has been described to be essential for inducing the *C. pneumoniae*-specific Th17 response <sup>62</sup>. In our study, Ax treatment in *C. pneumoniae*-infected mice significantly increased the relative expression levels of IFN- $\gamma$ , IL-12, IL-17A, and IL-23 compared to those of the untreated/infected mice; additionally, the IFN- $\gamma$  levels were higher in the lungs of the Ax-treated *C. pneumoniae*-infected mice than in infected/untreated mice. These results suggest that Ax treatment may enhance inflammation in the lungs and promote the anti-chlamydial response, thus resulting in a reduction in bacterial burden.

Furthermore, additional factors may contribute to a decreased number of recoverable *C. pneumoniae* inclusions. SP-A and SP-D are known to play an immunological role in maintaining lung homeostasis. It has been shown that these proteins are able to aggregate *C. pneumoniae* and *C. trachomatis* and can facilitate the uptake of bacteria by human macrophages <sup>102,105</sup>. Our qPCR results suggest elevated SP-A levels that might also contribute

to the improved elimination of bacteria in Ax-treated mice. Our *in vitro* results are in agreement with this phenomenon, as we found that the pretreatment of *C. pneumoniae* with SP-A or SP-D decreased the number of *C. pneumoniae* inclusion in the McCoy cell line, probably due the aggregating effect of SP-A and SP-D, thus resulting in a smaller proportion of *C. pneumoniae* infected cells. According to our results, SP-A and SP-D increased *C. pneumoniae* attachment to mouse macrophage cells, similar to the findings in human macrophage cells<sup>102</sup>.

It is known that *C. pneumoniae* inhibit cell apoptosis in the early phase of the infection, however, in the late phase of infection pro-apoptotic process will dominate<sup>44,46,106</sup>. Indeed, our research group has been established also that pro and anti-apoptotic processes simultaneously emerge in the Chlamydia infected cells. Murine epithelial cells were infected with *C. trachomatis* and were treated with IFN- $\gamma$ , afterwards, transcriptome analysis was carried out with DNA chip analysis. It has been found that both positive and negative regulation of apoptosis were highly enriched, which overall resulted lack of apoptosis in *C. trachomatis* infected and IFN- $\gamma$  treated cells<sup>127</sup>. Our results are in agreement with these findings, as we could not detect elevated caspase 3/7 activity at 12 h *p.i.*<sup>44,48,106</sup>. Additionally, *C. pneumoniae* stimulates the ERK 1/2 pathway activity to prevent caspase-independent apoptosis. Similarly, we found that *C. pneumoniae* infection significantly enhanced the ERK 1/2 pathway activity compared to that in uninfected/untreated cells<sup>44,108</sup>. Notably, we observed a novel possible mechanism via which *C. pneumoniae* prevents host cell apoptosis: *C. pneumoniae* significantly elevates the levels of phosphorylated MSK-1, which can also promote BCL-2-associated agonist of cell death (BAD) phosphorylation and lead to the repression of BAD-induced apoptosis<sup>128,129</sup>. Contrary, when the cells were treated with Ax in *C. pneumoniae*-treated cells, MAPK/ERK activity was significantly reduced. This result suggests that the anti-chlamydial activity of Ax may be partially attributed to the reduced MAPK/ERK 1/2 activity. The MAPK/ERK 1/2 pathway also plays a crucial role in the nourishment of proliferating bacteria, and inhibition of this process is fatal to the pathogen; it has been shown that MAPK inhibitors can inhibit *C. pneumoniae* infection<sup>44,130</sup>. The level of the P90RSK1/2 protein was also found to be significantly decreased; this protein is crucial for the phosphorylation of several antiapoptotic proteins such as death-associated protein kinase 1 and BAD<sup>131</sup>. Additionally, the levels of phosphorylated MSK-1 decrease significantly, which are known to result in apoptosis. These findings suggest that Ax treatment may induce apoptosis in *C. pneumoniae*-infected cells, thereby inhibiting bacterial proliferation.

The results of a phase 2 clinical trial showed that Ax is well-tolerated beyond its standard administration at 1.25 mg/kg<sup>132</sup>. Given the coronavirus disease 2019 (COVID-19) pandemic, several studies have shown that Ax can be used as a supplemental medication for treating COVID-19<sup>133–135</sup>. Notably, MAPK/ERK activation plays a pivotal role in additional bacterial infections, including *Coxiella burnetii* infections, which are similar to Chlamydia infections. Therefore, we think it may be worth to investigate the role of Ax in *C. burnetii* infections.

## 6. Conclusion

NAC and Ax have been used as a medication for a long time for treating respiratory infection with phlegm production; however, they can influence the outcome of *C. pneumoniae* infection.

We demonstrated that NAC increases *C. pneumoniae* replication *in vitro* and *in vivo* in mice. Related to our hypothesis, NAC is able to reduce disulphide bridges in the membrane of the *C. pneumoniae* EBs, which concordantly leads to more efficient binding of EBs to the host cell's membrane resulting higher reproduction rate of the bacteria. Moreover, we tested the Ax's mucolytic activity on bacterial replication. Ax exhibited anti-chlamydial activity partly due to the elevated IDO-2 gene expression, however, it was shown that Ax, at a normal dose used for humans, has no influence on *C. pneumoniae* proliferation in mice.

We found that *C. pneumoniae*-infected mice treated with four times higher doses of Ax than normal contained significantly fewer viable *C. pneumoniae* IFUs than those in untreated mice. The mRNA expression levels of IL-12, IL-23, IL-17F, IFN- $\gamma$ , and SP-A were significantly increased in infected mice treated with Ax compared to those in control mice. Moreover, we found that Ax treatment decreased the activity of the MAPK/ERK pathway, which may have induced apoptosis in infected cells.

Based on our results, a higher dose of Ax exhibits an anti-chlamydial effect in mice, probable due to its modulating effects on the immunologic and metabolic pathways.

According to our *in vivo* results, Ax should be the preferred mucolytic in a known *C. pneumoniae* infected patient. However, based on the immunological differences between mice and humans, further clinical experiments should be conducted to establish the effect of NAC or Ax in *C. pneumoniae* infected humans.

## 7. Summary

*Chlamydia pneumoniae* is an obligate intracellular pathogen with a biphasic cycle and is responsible for 10% of the community acquired pneumoniae. Furthermore, *C. pneumoniae* can cause sinusitis, pharyngitis, bronchitis. Proper identification of the bacteria is not always carried out, which is due to the fact that especially with mild symptoms, the self-medicating percentage of the population is high. Considering that *C. pneumoniae* infection can cause phlegm production, taking mucolytics is a common method to facilitate the removal of sputum.

During our research, we investigated the influence of the two most popular mucolytics in Europe, NAC and Ax, on the replication of *C. pneumoniae* *in vitro* and *in vivo* in mice. Surprisingly, we found that NAC actually increases *C. pneumoniae* replication *in vitro* and *in vivo* in mice and also prolongs the bacterial burden in mice. Based on this information, we were eager to find the underlying mechanism behind this phenomenon. We found that NAC probably reduces the OmcB disulphide bridges in *C. pneumoniae* EBs's membrane, thus facilitating EBs's entry into the cell and aiding the bacterial growth.

Next, we wanted to examine the effect of Ax on *C. pneumoniae* replication. We found that even though Ax had anti-chlamydial activity *in vitro*, at the concentration used in human infection Ax did not influence the replication of *C. pneumoniae* in mice. However, as we applied 4x higher concentration *in vivo* in mice that is used in human medicine, we observed anti-chlamydial activity. Ax had several anti-chlamydial mechanisms which could lead to the decrease of recoverable *C. pneumoniae* inclusion. qPCR revealed to us, that in *C. pneumoniae*-infected Ax-treated mice lungs IL-12, IL-17A, IL-23, IFN- $\gamma$  and SP-A expression was significantly elevated than in *C. pneumoniae*-infected mice lungs. Moreover, IFN- $\gamma$  protein concentration was significantly higher in *C. pneumoniae*-infected Ax-treated mice. Furthermore, we conducted several *in vitro* investigations to better understand the mechanism behind anti-chlamydial effect of Ax. We observed the presence of several key proteins that results in the decrease of *C. pneumoniae* survival. ERK-1, ERK-2, c-Raf, P90RSK2 and MSK1 were decreased significantly in *C. pneumoniae*-infected Ax-treated cells compared to *C. pneumoniae*-infected cells.

It is known that *C. pneumoniae* can utilize several mechanisms to avoid host cell apoptosis. During our experiments we found a novel mechanism, which *C. pneumoniae* can utilize in

human alveolar epithelial cell to avoid apoptosis, that is the upregulation of MSK-1 protein. Indeed, it has been significantly upregulated in *C. pneumoniae* infected cells compared to uninfected cell. This protein plays a crucial role in the repression of BAD induced apoptosis.

Altogether, our experiments provided novel information regarding the use of medications in *C. pneumoniae* infections. We found that a commonly used mucolytics, the NAC increases *C. pneumoniae* replication and prolongs the bacterial clearance from the lungs. Moreover, we established that Ax, another commonly used mucolytic, in a higher dose suppresses *C. pneumoniae* infection. Therefore, we believe that our results could impact the medication for unidentified pneumonia.

Considered novel findings:

1. NAC increases *C. pneumoniae* replication *in vitro*
2. NAC increases *C. pneumoniae* replication *in vivo* in mice and prolongs the clearance of the bacteria
3. NAC increases the attachment of EBs to the host cell membrane, which may lead to higher efficiency in the bacterial uptake in the cell, thus elevating the bacterial inclusion number.
4. Ax has anti-chlamydial activity *in vitro* partly due to the IDO-2 elevation
5. Ax does not have anti-chlamydial activity at the concentration used in human medicine *in vivo* in mice
6. Ax has anti-chlamydial activity at 4x higher concentration than it is used in human medicine *in vivo* in mice
7. Ax significantly elevates IL-12, IL-17A IL-23, IFN- $\gamma$  and SP-A expression in lungs of *C. pneumoniae*-infected mice, which indicates higher inflammation, thus a better chlamydia clearance
8. Ax significantly elevates IFN- $\gamma$  protein level in the supernatant of *C. pneumoniae*-infected mice lungs, which signals prompt cellular immune response
9. *C. pneumoniae* increases phosphorylated MSK-1 level, which results in anti-apoptotic processes
10. Ax decreases ERK1/2 activity, which lead to apoptosis of the host cell, thus decreasing the replicating *C. pneumoniae*.

## 8. Összefoglalás

A *Chlamydia pneumoniae* egy obligát intracelluláris kórokozó bifázisos ciklussal, és a közösségben szerzett tüdőgyulladások 10%-áért felelős. Ezenfelül a kórokozó képes arcüreggyulladást, torokgyulladást, hörghurutot okozni. A baktérium megfelelő azonosítása sajnálatos módon nem mindig történik meg, illetve a felnőtt populációnál enyhe tünetek esetében az öngyógyszerelés százaléka magas. Tekintettel arra, hogy a *C. pneumoniae* fertőzés váladéktermelést okozhat, a mukolitikumok szedése általános módszer a köpet eltávolításának elősegítésére.

Kutatásunk során az Európában két legnépszerűbb mukolitikum, a NAC és az Ax, hatását vizsgáltuk a *C. pneumoniae* fertőzésben *in vitro* és *in vivo* egerekben. Meglepő módon azt találtuk, hogy a NAC fokozza a *C. pneumoniae* szaporodását *in vitro* és *in vivo* egerekben, illetve meghosszabbítja a baktériumok kiürülését az egerek tüdejéből. Ezen információk alapján szerettük volna kideríteni a jelenség mögött meghúzódó mechanizmust. Azt találtuk, hogy a NAC fokozza a chlamydia gazdasejtbe való kötődését valószínűleg redukálva az OmcB-ben lévő diszulfid-hidakat a *C. pneumoniae* elementáris test membránjában, ezáltal megkönnyíti azok bejutását a sejtbe, és elősegíti a baktériumok szaporodását.

Ezt követően megvizsgáltuk az Ax hatását a *C. pneumoniae* replikációjára. Megállapítottuk, hogy bár az Ax anti-chlamydiális hatással rendelkezett *in vitro*, viszont a humán fertőzésben alkalmazott koncentrációban az Ax nem befolyásolta a *C. pneumoniae* egerekben történő szaporodását. A későbbiekben a humán gyógyászatban alkalmazottnál 4-szer magasabb koncentrációt alkalmaztunk *in vivo* egerekben, ebben a koncentrációban viszont chlamydiaellenes hatást figyeltünk meg. Az Ax számos anti-chlamydiális mechanizmussal rendelkezik, amelyek hozzájárulhattak a visszatenyészthető *C. pneumoniae* inklúziók csökkenéséhez. Az qPCR módszerrel kimutattuk, hogy a *C. pneumoniae* Ax-szal kezelt egerek tüdejében az IL-12, IL-17A, IL-23, IFN- $\gamma$  és SP-A expressziója szignifikánsan megemelkedett összehasonlítva a *C. pneumoniae*-vel fertőzött egerek tüdejében mértekkel. Ezenkívül az IFN- $\gamma$  fehérje szignifikánsan magasabb volt a *C. pneumoniae* Ax-szal kezelt egerekben. A továbbiakban számos *in vitro* vizsgálatot végeztünk, hogy jobban megértsük az Ax anti-chlamydiális hatása mögött meghúzódó mechanizmusokat.

Eredményeink szerint az Ax számos foszforilált fehérje relatív szintjét csökkentette. Western-blot módszerrel megállapítottuk, hogy az ERK-1, ERK-2, c-Raf, P90RSK2 és MSK1 esetében

szignifikáns csökkenést tapasztalhattunk *in vitro* *C. pneumoniae*-vel fertőzött Ax-kezelt sejtekben a *C. pneumoniae*-vel fertőzött sejtekhez képest. Ezen foszforilált fehérjék csökkenése részben hozzájárulhatott, hogy a *C. pneumoniae* szaporodása csökkent Ax kezelés hatására.

Ismert, hogy a *C. pneumoniae* számos mechanizmust alkalmaz a gazdasejt apoptózisának elkerülésére. Kísérleteink során azt találtuk, hogy a *C. pneumoniae*-vel fertőzött sejtekben az MSK-1 fehérje relatív szintje szignifikánsan emelkedett a nem fertőzött sejtekhez képest. Ez a fehérje döntő szerepet játszik a BAD által kiváltott apoptózis visszaszorításában.

Összességében kísérleteink új információkat szolgáltatottak a *C. pneumoniae* fertőzések gyógyszeres kezeléséről. Azt találtuk, hogy egy gyakran használt mukolitikum, a NAC fokozza a *C. pneumoniae* replikációját, és meghosszabbítja a baktériumok tüdőből való kiürülését. Megállapítottuk továbbá, hogy az Ax, egy másik gyakran használt nyákoldó, nagyobb dózisban anti-chlamydiális hatással rendelkezik.

## 9. Acknowledgement

I would like to express my gratitude to my supervisor **Burián Katalin**, who always supported me since I started to work in her laboratory in 2015 as a scientific student. She always listened to my ideas and gave helping hands when it was needed. Without her support, this thesis could not have been possible.

I would also like to thank our assistant **Müllerné Deák Györgyi**, who was always there when I started to drown in work.

I wish to thank my colleagues, **Endrész Valéria** and **Somogyvári Ferenc**, who have been a great help to me throughout my Ph.D.

I express my thanks to my friends and Ph.D. fellows, **Benkő Ernő** and **Lőrinczi Bálint**, on whom I could always count on.

I thank my **grandparents**, for the love they provided to me throughout my life.

I owe my greatest gratitude to my **mother** and my **father**, without their never-ending love and care I could have never achieved anything in life.

I express my special thanks to my **fiancée**, who always supported me throughout my Ph.D. studies.

My Ph.D. thesis is dedicated to my relatives, who can not be with us today: **Sarolta, János** and **Gabriella**

## 10. Reference

1. Bachmann, N. L., Polkinghorne, A. & Timms, P. Chlamydia genomics: providing novel insights into chlamydial biology. *Trends Microbiol* **22**, 464–472 (2014).
2. *Mandell, Douglas, and Bennett's principles and practice of infectious diseases.* (Churchill Livingstone/Elsevier, 2010).
3. Yu, H. *et al.* Comparison of Chlamydia outer membrane complex to recombinant outer membrane proteins as vaccine. *Vaccine* **38**, 3280–3291 (2020).
4. F, F. & P, C. DiANNA: a web server for disulfide connectivity prediction. *Nucleic acids research* **33**, (2005).
5. Disulfide connectivity prediction using secondary structure information and diresidue frequencies - PubMed. <https://pubmed.ncbi.nlm.nih.gov/15741247/>.
6. UCSF Chimera--a visualization system for exploratory research and analysis - PubMed. <https://pubmed.ncbi.nlm.nih.gov/15264254/>.
7. Jumper, J. *et al.* Highly accurate protein structure prediction with AlphaFold. *Nature* **596**, 583–589 (2021).
8. Varadi, M. *et al.* AlphaFold Protein Structure Database: massively expanding the structural coverage of protein-sequence space with high-accuracy models. *Nucleic Acids Research* gkab1061 (2021) doi:10.1093/nar/gkab1061.
9. Saka, H. A. *et al.* Quantitative proteomics reveals metabolic and pathogenic properties of Chlamydia trachomatis developmental forms. *Mol Microbiol* **82**, 1185–1203 (2011).
10. Cossé, M. M., Hayward, R. D. & Subtil, A. One Face of Chlamydia trachomatis: The Infectious Elementary Body. *Curr Top Microbiol Immunol* **412**, 35–58 (2018).
11. Moelleken, K. & Hegemann, J. H. The Chlamydia outer membrane protein OmcB is required for adhesion and exhibits biovar-specific differences in glycosaminoglycan binding. *Mol Microbiol* **67**, 403–419 (2008).

12. Elwell, C., Mirrashidi, K. & Engel, J. Chlamydia cell biology and pathogenesis. *Nat Rev Microbiol* **14**, 385–400 (2016).
13. K, M. & Jh, H. The Chlamydia outer membrane protein OmcB is required for adhesion and exhibits biovar-specific differences in glycosaminoglycan binding. *Molecular microbiology* **67**, (2008).
14. AbdelRahman, Y. M. & Belland, R. J. The chlamydial developmental cycle. *FEMS Microbiology Reviews* **29**, 949–959 (2005).
15. Bastidas, R. J., Elwell, C. A., Engel, J. N. & Valdivia, R. H. Chlamydial Intracellular Survival Strategies. *Cold Spring Harb Perspect Med* **3**, a010256 (2013).
16. Zuck, M. & Hybiske, K. The Chlamydia trachomatis Extrusion Exit Mechanism Is Regulated by Host Abscission Proteins. *Microorganisms* **7**, 149 (2019).
17. Koehler, L. *et al.* Ultrastructural and molecular analyses of the persistence of Chlamydia trachomatis (serovar K) in human monocytes. *Microbial Pathogenesis* **22**, 133–142 (1997).
18. Matsumoto, A. & Manire, G. P. Electron Microscopic Observations on the Effects of Penicillin on the Morphology of Chlamydia psittaci. *Journal of Bacteriology* (1970) doi:10.1128/jb.101.1.278-285.1970.
19. Coles, A. M., Reynolds, D. J., Harper, A., Devitt, A. & Pearce, J. H. Low-nutrient induction of abnormal chlamydial development: A novel component of chlamydial pathogenesis? *FEMS Microbiology Letters* **106**, 193–200 (1993).
20. Chlamydial Persistence: beyond the Biphasic Paradigm | Infection and Immunity. <https://journals.asm.org/doi/full/10.1128/IAI.72.4.1843-1855.2004>.
21. Bugalhão, J. N. & Mota, L. J. The multiple functions of the numerous Chlamydia trachomatis secreted proteins: the tip of the iceberg. *Microb Cell* **6**, 414–449 (2019).

22. Miyashita, N. Atypical pneumonia: Pathophysiology, diagnosis, and treatment. *Respiratory Investigation* (2021) doi:10.1016/j.resinv.2021.09.009.
23. Gundagurti, B., Dasari, P. & Singh, R. Association of Chlamydophila pneumoniae infection and hypertension during pregnancy - A case control study. *Clin Exp Hypertens* **43**, 793–799 (2021).
24. Al-Hajaya, T. S., Al-Zereini, W. A. & Al-Younes, H. M. Chlamydia pneumoniae infection in patients hospitalised for community-acquired pneumonia in Southern Jordan. *Indian J Med Microbiol* **38**, 338–343 (2020).
25. Miyashita, N., Fukano, H., Yoshida, K., Niki, Y. & Matsushima, T. Seroepidemiology of Chlamydia pneumoniae in Japan between 1991 and 2000. *J Clin Pathol* **55**, 115–117 (2002).
26. Khoshbayan, A., Taheri, F., Moghadam, M. T., Chegini, Z. & Shariati, A. The association of Chlamydia pneumoniae infection with atherosclerosis: Review and update of in vitro and animal studies. *Microb Pathog* **154**, 104803 (2021).
27. Miao, G. *et al.* TLR2/CXCR4 coassociation facilitates Chlamydia pneumoniae infection-induced atherosclerosis. *Am J Physiol Heart Circ Physiol* **318**, H1420–H1435 (2020).
28. Li, B., Xia, Y. & Hu, B. Infection and atherosclerosis: TLR-dependent pathways. *Cell Mol Life Sci* **77**, 2751–2769 (2020).
29. Ferrari, M. *et al.* Respiratory symptoms, asthma, atopy and Chlamydia pneumoniae IgG antibodies in a general population sample of young adults. *Infection* **30**, 203–207 (2002).
30. Rubin, B. K. The Role of Mucus in Cough Research. *Lung* **188**, 69–72 (2010).
31. Morice, A. & Kardos, P. Comprehensive evidence-based review on European antitussives. *BMJ Open Respiratory Research* **3**, e000137 (2016).
32. Panda, A. & Ganesan, S. Genomic and Immunologic Correlates of Indoleamine 2,3-Dioxygenase Pathway Expression in Cancer. *Front Genet* **12**, 706435 (2021).

33. Munn, D. H. & Mellor, A. L. Indoleamine 2,3 dioxygenase and metabolic control of immune responses. *Trends Immunol* **34**, 137–143 (2013).
34. Virok, D. P. *et al.* Indoleamine 2,3-Dioxygenase Cannot Inhibit Chlamydia trachomatis Growth in HL-60 Human Neutrophil Granulocytes. *Front Immunol* **12**, 717311 (2021).
35. Virok, D. P. *et al.* Indoleamine 2,3-Dioxygenase Activity in Chlamydia muridarum and Chlamydia pneumoniae Infected Mouse Lung Tissues. *Front Cell Infect Microbiol* **9**, 192 (2019).
36. Shima, K. *et al.* Interferon- $\gamma$  interferes with host cell metabolism during intracellular Chlamydia trachomatis infection. *Cytokine* **112**, 95–101 (2018).
37. Raff, M. Cell suicide for beginners. *Nature* **396**, 119–119 (1998).
38. The Fas Signaling Pathway: More Than a Paradigm.  
<https://www.science.org/doi/10.1126/science.1071553>.
39. Wang, X. The expanding role of mitochondria in apoptosis. *Genes Dev* **15**, 2922–2933 (2001).
40. Spitz, A. Z. & Gavathiotis, E. Physiological and pharmacological modulation of BAX. *Trends Pharmacol Sci* S0165-6147(21)00216–9 (2021) doi:10.1016/j.tips.2021.11.001.
41. Park, M. Y. *et al.* Differences of Key Proteins between Apoptosis and Necroptosis. *Biomed Res Int* **2021**, 3420168 (2021).
42. Kroemer, G. & Martin, S. J. Caspase-independent cell death. *Nat Med* **11**, 725–730 (2005).
43. Tait, S. W. G. & Green, D. R. Caspase-independent cell death: leaving the set without the final cut. *Oncogene* **27**, 6452–6461 (2008).
44. Kun, D., Xiang-lin, C., Ming, Z. & Qi, L. Chlamydia inhibit host cell apoptosis by inducing Bag-1 via the MAPK/ERK survival pathway. *Apoptosis* **18**, 1083–1092 (2013).

45. K, D. *et al.* Chlamydial antiapoptotic activity involves activation of the Raf/MEK/ERK survival pathway. *Current microbiology* **63**, (2011).
46. A, S. *et al.* Mechanisms of apoptosis inhibition in Chlamydia pneumoniae-infected neutrophils. *International journal of medical microbiology : IJMM* **305**, (2015).
47. Mariotto, E. *et al.* BAG1 down-regulation increases chemo-sensitivity of acute lymphoblastic leukaemia cells. *Journal of Cellular and Molecular Medicine* **25**, 9060–9065 (2021).
48. Matsuo, J. *et al.* Activation of caspase-3 during Chlamydia trachomatis-induced apoptosis at a late stage. *Can J Microbiol* **65**, 135–143 (2019).
49. Lin, J.-X. & Leonard, W. J. Fine-Tuning Cytokine Signals. *Annual Review of Immunology* **37**, 295–324 (2019).
50. Miyajima, A., Kitamura, T., Harada, N., Yokota, T. & Arai, K. Cytokine Receptors and Signal Transduction. *Annual Review of Immunology* **10**, 295–331 (1992).
51. Commins, S. P., Borish, L. & Steinke, J. W. Immunologic messenger molecules: cytokines, interferons, and chemokines. *J Allergy Clin Immunol* **125**, S53-72 (2010).
52. Brocker, C., Thompson, D., Matsumoto, A., Nebert, D. W. & Vasilou, V. Evolutionary divergence and functions of the human interleukin (IL) gene family. *Human Genomics* **5**, 30 (2010).
53. Trinchieri, G. Interleukin-12: A Proinflammatory Cytokine with Immunoregulatory Functions that Bridge Innate Resistance and Antigen-Specific Adaptive Immunity. *Annual Review of Immunology* **13**, 251–276 (1995).
54. Gately, M. K. *et al.* THE INTERLEUKIN-12/INTERLEUKIN-12-RECEPTOR SYSTEM: Role in Normal and Pathologic Immune Responses. *Annual Review of Immunology* **16**, 495–521 (1998).

55. Lu, H. & Zhong, G. Interleukin-12 Production Is Required for Chlamydial Antigen-Pulsed Dendritic Cells To Induce Protection against Live *Chlamydia trachomatis* Infection. *Infection and Immunity* (1999).
56. McGeachy, M. J. & Cua, D. J. Th17 Cell Differentiation: The Long and Winding Road. *Immunity* **28**, 445–453 (2008).
57. Weaver, C. T., Hatton, R. D., Mangan, P. R. & Harrington, L. E. IL-17 Family Cytokines and the Expanding Diversity of Effector T Cell Lineages. *Annual Review of Immunology* **25**, 821–852 (2007).
58. Majumder, S. & McGeachy, M. J. IL-17 in the Pathogenesis of Disease: Good Intentions Gone Awry. *Annual Review of Immunology* **39**, 537–556 (2021).
59. Korn, T., Bettelli, E., Oukka, M. & Kuchroo, V. K. IL-17 and Th17 Cells. *Annual Review of Immunology* **27**, 485–517 (2009).
60. Qiao, S. *et al.* Endogenous IL-17A mediated neutrophil infiltration by promoting chemokines expression during chlamydial lung infection. *Microb Pathog* **129**, 106–111 (2019).
61. Mursalin, M. H. *et al.* C-X-C Chemokines Influence Intraocular Inflammation During Bacillus Endophthalmitis. *Invest Ophthalmol Vis Sci* **62**, 14 (2021).
62. Frazer, L. C. *et al.* IL-23 induces IL-22 and IL-17 production in response to *Chlamydia muridarum* genital tract infection, but the absence of these cytokines does not influence disease pathogenesis. *Am J Reprod Immunol* **70**, (2013).
63. Khader, S. A. & Gopal, R. IL-17 in protective immunity to intracellular pathogens. *Virulence* **1**, 423–427 (2010).
64. Gray, P. W. & Goeddel, D. V. Structure of the human immune interferon gene. *Nature* **298**, 859–863 (1982).

65. Borges da Silva, H., Fonseca, R., Alvarez, J. M. & D'Império Lima, M. R. IFN- $\gamma$  Priming Effects on the Maintenance of Effector Memory CD4(+) T Cells and on Phagocyte Function: Evidences from Infectious Diseases. *J Immunol Res* **2015**, 202816 (2015).
66. J, G., P, F., P, F. & Aa, V. The role of interferon-gamma and interferon-gamma receptor in tuberculosis and nontuberculous mycobacterial infections. *International journal of mycobacteriology* **10**, (2021).
67. STAT1 regulates IFN-alpha beta- and IFN-gamma-dependent control of infection with *Chlamydia pneumoniae* by nonhemopoietic cells - PubMed.  
<https://pubmed.ncbi.nlm.nih.gov/16709859/>.
68. *Chlamydia muridarum* evades growth restriction by the IFN-gamma-inducible host resistance factor Irgb10 - PubMed. <https://pubmed.ncbi.nlm.nih.gov/18424746/>.
69. Ma, A.-Z., Hm, A.-Y., Pr, B., J, Z. & Tf, M. IFN-gamma-inducible Irga6 mediates host resistance against *Chlamydia trachomatis* via autophagy. *PloS one* **4**, (2009).
70. Griese, M. Pulmonary surfactant in health and human lung diseases: state of the art. 22.
71. Wright, J. R. Immunomodulatory functions of surfactant. **77**, 32 (1997).
72. Oberley, R. E. *et al.* A role for surfactant protein D in innate immunity of the human prostate. *Prostate* **65**, 241–251 (2005).
73. Tan, Y.-X. *et al.* Role of surfactant protein C in neonatal genetic disorders of the surfactant system: A case report. *Medicine (Baltimore)* **100**, e28201 (2021).
74. Basabe-Burgos, O., Landreh, M., Rising, A., Curstedt, T. & Jan Johansson, null. Treatment of Respiratory Distress Syndrome with Single Recombinant Polypeptides that Combine Features of SP-B and SP-C. *ACS Chem Biol* **16**, 2864–2873 (2021).
75. Ntamo, Y. *et al.* Drug-Induced Liver Injury: Clinical Evidence of N-Acetyl Cysteine Protective Effects. *Oxid Med Cell Longev* **2021**, 3320325 (2021).

76. Palaniyappan, L., Sabesan, P., Li, X. & Luo, Q. Schizophrenia Increases Variability of the Central Antioxidant System: A Meta-Analysis of Variance From MRS Studies of Glutathione. *Front Psychiatry* **12**, 796466 (2021).
77. Bartoli, F. *et al.* Repurposed drugs as adjunctive treatments for mania and bipolar depression: A meta-review and critical appraisal of meta-analyses of randomized placebo-controlled trials. *Journal of Psychiatric Research* **143**, 230–238 (2021).
78. Dean, O., Giorlando, F. & Berk, M. N-acetylcysteine in psychiatry: current therapeutic evidence and potential mechanisms of action. *J Psychiatry Neurosci* **36**, 78–86 (2011).
79. Berk, M., Malhi, G. S., Gray, L. J. & Dean, O. M. The promise of N-acetylcysteine in neuropsychiatry. *Trends in Pharmacological Sciences* **34**, 167–177 (2013).
80. Pedre, B., Barayeu, U., Ezeriņa, D. & Dick, T. P. The mechanism of action of N-acetylcysteine (NAC): The emerging role of H<sub>2</sub>S and sulfane sulfur species. *Pharmacology & Therapeutics* **228**, 107916 (2021).
81. Consumption of NAC and Ax in Hungary 2016, National Health Insurance Fund of Hungary. (2017).
82. Aslam, S., Trautner, B. W., Ramanathan, V. & Darouiche, R. O. Combination of tigecycline and N-acetylcysteine reduces biofilm-embedded bacteria on vascular catheters. *Antimicrob Agents Chemother* **51**, 1556–1558 (2007).
83. Zhao, T. & Liu, Y. N-acetylcysteine inhibit biofilms produced by *Pseudomonas aeruginosa*. *BMC Microbiology* **10**, 140 (2010).
84. Olofsson, A.-C., Hermansson, M. & Elwing, H. N-Acetyl-L-Cysteine Affects Growth, Extracellular Polysaccharide Production, and Bacterial Biofilm Formation on Solid Surfaces. *Applied and Environmental Microbiology* (2003)  
doi:10.1128/AEM.69.8.4814-4822.2003.

85. Allen, M. *et al.* Mechanisms of Control of Mycobacterium tuberculosis by NK Cells: Role of Glutathione. *Front Immunol* **6**, 508 (2015).
86. Germouty, J. & Jirou-Najou, J. L. Clinical efficacy of ambroxol in the treatment of bronchial stasis. Clinical trial in 120 patients at two different doses. *Respiration* **51 Suppl 1**, 37–41 (1987).
87. Cazan, D., Klimek, L., Sperl, A., Plomer, M. & Kölsch, S. Safety of ambroxol in the treatment of airway diseases in adult patients. *Expert Opin Drug Saf* **17**, 1211–1224 (2018).
88. Balestrino, R. & Schapira, A. H. V. Glucocerebrosidase and Parkinson Disease: Molecular, Clinical, and Therapeutic Implications. *Neuroscientist* **24**, 540–559 (2018).
89. Gillissen, A. *et al.* Oxidant scavenger function of ambroxol in vitro: a comparison with N-acetylcysteine. *Res Exp Med (Berl)* **196**, 389–398 (1997).
90. Aihara, M. *et al.* Effects of N-Acetylcysteine and Ambroxol on the Production of IL-12 and IL-10 in Human Alveolar Macrophages. *RES* **67**, 662–671 (2000).
91. He, W. *et al.* Pulmonary-Affinity Paclitaxel Polymer Micelles in Response to Biological Functions of Ambroxol Enhance Therapeutic Effect on Lung Cancer. *Int J Nanomedicine* **15**, 779–793 (2020).
92. Zhang, S. *et al.* Ambroxol inhalation ameliorates LPS-induced airway inflammation and mucus secretion through the extracellular signal-regulated kinase 1/2 signaling pathway. *European Journal of Pharmacology* **775**, 138–148 (2016).
93. de Mey, C., Koelsch, S., Richter, E., Pohlmann, T. & Sousa, R. Efficacy and Safety of Ambroxol Lozenges in the Treatment of Acute Uncomplicated Sore Throat - a Pooled Analysis. *Drug Res (Stuttg)* **66**, 384–392 (2016).
94. Yang, B. *et al.* Ambroxol suppresses influenza-virus proliferation in the mouse airway by increasing antiviral factor levels. *Eur. Respir. J.* **19**, 952–958 (2002).

95. Burián, K. *et al.* Chlamydophila (Chlamydia) pneumoniae induces histidine decarboxylase production in the mouse lung. *Immunol. Lett.* **89**, 229–236 (2003).
96. Caldwell, H. D., Kromhout, J. & Schachter, J. Purification and partial characterization of the major outer membrane protein of Chlamydia trachomatis. *Infect. Immun.* **31**, 1161–1176 (1981).
97. Hellemans, J., Mortier, G., De Paepe, A., Speleman, F. & Vandesompele, J. qBase relative quantification framework and software for management and automated analysis of real-time quantitative PCR data. *Genome Biol* **8**, R19 (2007).
98. Gáspár, R. *et al.* The cytoprotective effect of biglycan core protein involves Toll-like receptor 4 signaling in cardiomyocytes. *J Mol Cell Cardiol* **99**, 138–150 (2016).
99. Szabó, M. R. *et al.* Hypercholesterolemia Interferes with Induction of miR-125b-1-3p in Preconditioned Hearts. *Int J Mol Sci* **21**, (2020).
100. Kókai, D., Mosolygó, T., Virók, D. P., Endrész, V. & Burián, K. N-acetyl-cysteine increases the replication of Chlamydia pneumoniae and prolongs the clearance of the pathogen from mice. *J Med Microbiol* **67**, 702–708 (2018).
101. Roshick, C., Wood, H., Caldwell, H. D. & McClarty, G. Comparison of gamma interferon-mediated antichlamydial defense mechanisms in human and mouse cells. *Infect Immun* **74**, 225–238 (2006).
102. Oberley, R. E. *et al.* Surfactant proteins A and D enhance the phagocytosis of Chlamydia into THP-1 cells. *Am J Physiol Lung Cell Mol Physiol* **287**, L296-306 (2004).
103. Wang, Z. *et al.* Air particulate matter pollution and circulating surfactant protein: A systemic review and meta-analysis. *Chemosphere* **272**, 129564 (2021).
104. Johansson, J. & Curstedt, T. Synthetic surfactants with SP-B and SP-C analogues to enable worldwide treatment of neonatal respiratory distress syndrome and other lung diseases. *J Intern Med* **285**, 165–186 (2019).

105. Oberley, R. E., Goss, K. L., Ault, K. A., Crouch, E. C. & Snyder, J. M. Surfactant protein D is present in the human female reproductive tract and inhibits Chlamydia trachomatis infection. *Mol. Hum. Reprod.* **10**, 861–870 (2004).
106. Sharma, M. & Rudel, T. Apoptosis resistance in Chlamydia-infected cells: a fate worse than death? *FEMS Immunol. Med. Microbiol.* **55**, 154–161 (2009).
107. Galle, J. N., Fechtner, T., Eierhoff, T., Römer, W. & Hegemann, J. H. A Chlamydia pneumoniae adhesin induces phosphatidylserine exposure on host cells. *Nature Communications* **10**, 4644 (2019).
108. Su, H. *et al.* Activation of Raf/MEK/ERK/cPLA2 Signaling Pathway Is Essential for Chlamydial Acquisition of Host Glycerophospholipids. *J. Biol. Chem.* **279**, 9409–9416 (2004).
109. McCOY, C. E., Campbell, D. G., Deak, M., Bloomberg, G. B. & Arthur, J. S. C. MSK1 activity is controlled by multiple phosphorylation sites. *Biochem J* **387**, 507–517 (2005).
110. Mokhtari, V., Afsharian, P., Shahhoseini, M., Kalantar, S. M. & Moini, A. A Review on Various Uses of N-Acetyl Cysteine. *Cell J* **19**, 11–17 (2017).
111. Tattersall, A. B., Bridgman, K. M. & Huitson, A. Acetylcysteine (Fabrol) in chronic bronchitis--a study in general practice. *J Int Med Res* **11**, 279–284 (1983).
112. De Flora, S., Grassi, C. & Carati, L. Attenuation of influenza-like symptomatology and improvement of cell-mediated immunity with long-term N-acetylcysteine treatment. *Eur Respir J* **10**, 1535–1541 (1997).
113. Lazarev, V. N. *et al.* The role of intracellular glutathione in the progression of Chlamydia trachomatis infection. *Free Radic. Biol. Med.* **49**, 1947–1955 (2010).
114. Abromaitis, S. & Stephens, R. S. Attachment and Entry of Chlamydia Have Distinct Requirements for Host Protein Disulfide Isomerase. *PLoS Pathog* **5**, (2009).

115. Haggerty, C. L. *et al.* Risk of sequelae after Chlamydia trachomatis genital infection in women. *J Infect Dis* **201 Suppl 2**, S134-155 (2010).
116. Seifart, C. *et al.* Cell-specific modulation of surfactant proteins by ambroxol treatment. *Toxicology and Applied Pharmacology* **203**, 27–35 (2005).
117. Fois, G. *et al.* A new role for an old drug: Ambroxol triggers lysosomal exocytosis via pH-dependent  $\text{Ca}^{2+}$  release from acidic  $\text{Ca}^{2+}$  stores. *Cell Calcium* **58**, 628–637 (2015).
118. Weiser, T. Comparison of the effects of four  $\text{Na}^+$  channel analgesics on TTX-resistant  $\text{Na}^+$  currents in rat sensory neurons and recombinant Nav1.2 channels. *Neuroscience Letters* **395**, 179–184 (2006).
119. McNeill, A. *et al.* Ambroxol improves lysosomal biochemistry in glucocerebrosidase mutation-linked Parkinson disease cells. *Brain* **137**, 1481–1495 (2014).
120. Deretic, V. & Timmins, G. S. Enhancement of lung levels of antibiotics by ambroxol and bromhexine. *Expert Opin Drug Metab Toxicol* **15**, 213–218 (2019).
121. Li, X. *et al.* Ambroxol Hydrochloride Combined with Fluconazole Reverses the Resistance of Candida albicans to Fluconazole. *Front Cell Infect Microbiol* **7**, 124 (2017).
122. Zhang, Y. *et al.* Synergy of ambroxol with vancomycin in elimination of catheter-related Staphylococcus epidermidis biofilm in vitro and in vivo. *J. Infect. Chemother.* **21**, 808–815 (2015).
123. Yamaya, M. *et al.* Ambroxol inhibits rhinovirus infection in primary cultures of human tracheal epithelial cells. *Arch. Pharm. Res.* **37**, 520–529 (2014).
124. Cataldi, M., Sblendorio, V., Leo, A. & Piazza, O. Biofilm-dependent airway infections: A role for ambroxol? *Pulmonary Pharmacology & Therapeutics* **28**, 98–108 (2014).

125. Mosolygó, T. *et al.* Chlamydomonas pneumoniae re-infection triggers the production of IL-17A and IL-17E, important regulators of airway inflammation. *Inflamm. Res.* **62**, 451–460 (2013).
126. Linden, A. Neutrophils, interleukin-17A and lung disease. *European Respiratory Journal* **25**, 159–172 (2005).
127. Burian, K. *et al.* Transcriptome Analysis Indicates an Enhanced Activation of Adaptive and Innate Immunity by Chlamydia-Infected Murine Epithelial Cells Treated with Interferon  $\gamma$ . *The Journal of Infectious Diseases* **202**, 1405–1414 (2010).
128. She, Q.-B., Ma, W.-Y., Zhong, S. & Dong, Z. Activation of JNK1, RSK2, and MSK1 is involved in serine 112 phosphorylation of Bad by ultraviolet B radiation. *J Biol Chem* **277**, 24039–24048 (2002).
129. Cook, S. J., Stuart, K., Gilley, R. & Sale, M. J. Control of cell death and mitochondrial fission by ERK1/2 MAP kinase signalling. *FEBS J* **284**, 4177–4195 (2017).
130. Kortesoja, M., Trofin, R. E. & Hanski, L. A platform for studying the transfer of Chlamydia pneumoniae infection between respiratory epithelium and phagocytes. *Journal of Microbiological Methods* **171**, 105857 (2020).
131. Lara, R., Seckl, M. J. & Pardo, O. E. The p90 RSK family members: common functions and isoform specificity. *Cancer Res* **73**, 5301–5308 (2013).
132. Mullin, S. *et al.* Ambroxol for the Treatment of Patients With Parkinson Disease With and Without Glucocerebrosidase Gene Mutations: A Nonrandomized, Noncontrolled Trial. *JAMA Neurol* **77**, 427–434 (2020).
133. Olaleye, O. A., Kaur, M. & Onyenaka, C. C. Ambroxol Hydrochloride Inhibits the Interaction between Severe Acute Respiratory Syndrome Coronavirus 2 Spike Protein's Receptor Binding Domain and Recombinant Human ACE2. *bioRxiv* (2020) doi:10.1101/2020.09.13.295691.

134. Alkotaji, M. Azithromycin and ambroxol as potential pharmacotherapy for SARS-CoV-2. *Int J Antimicrob Agents* **56**, 106192 (2020).
135. Bradfute, S. B. *et al.* Ambroxol and Ciprofloxacin Show Activity Against SARS-CoV2 in Vero E6 Cells at Clinically-Relevant Concentrations. *bioRxiv* (2020)  
doi:10.1101/2020.08.11.245100.

## **11. Annexes**

### **I.**

# N-acetyl-cysteine increases the replication of *Chlamydia pneumoniae* and prolongs the clearance of the pathogen from mice

Dávid Kókai, Tímea Mosolygó, Dezső P. Virók, Valéria Endrész and Katalin Burián\*

## Abstract

**Purpose.** Within the community, 10 % of acquired pneumonia is caused by *Chlamydia pneumoniae*. N-acetyl-cysteine (NAC) is one of the most commonly used mucolytics in respiratory diseases, but its effect on *C. pneumoniae* infection has not yet been investigated. In this study, our aim was to investigate whether NAC influences the replication of *C. pneumoniae*. After determining that NAC does have an effect on *C. pneumoniae* replication, the effect of an alternative drug called Ambroxol (Ax) was investigated.

**Methodology.** The *in vitro* effect of NAC and Ax was studied on *C. pneumoniae*-infected A549 and McCoy cells. Furthermore, the influence of NAC and Ax was examined in mice infected intranasally with *C. pneumoniae*.

**Results.** NAC treatment resulted in approximately sixfold more efficient *C. pneumoniae* growth in tissue culture compared to the untreated control cells, and this effect was shown to be based on the increased binding of the bacterium to the host cells. The *C. pneumoniae*-infected mice to which NAC was given had prolonged and more severe infections than the control mice. Ax decreased *C. pneumoniae* replication *in vitro*, which was partially associated with the increased expression of indolamine 2,3-dioxygenase. In animals, using the adapted usual human dose, Ax did not alter the number of recoverable *C. pneumoniae*.

**Conclusion.** Based on our results, it might be recommended that a mucolytic agent other than NAC, such as Ax, be used in respiratory diseases suspected to be caused by *C. pneumoniae*.

## INTRODUCTION

N-acetyl-cysteine (NAC) is a commonly used agent in the healthcare profession. It has multiple therapeutic uses in psychiatry and is useful in the case of an acetaminophen overdose. Moreover, NAC is used as a mucolytic agent in respiratory diseases, where its free thiol group breaks down the disulphide bonds in mucus, thereby decreasing its viscosity. NAC is mostly taken *per os*, except when it is taken to combat acetaminophen intoxication [1]. Ambroxol (Ax) is another mucolytic and expectorant drug that is used to treat different respiratory diseases. In addition to the effects of Ax on mucus regulation and its local anaesthetic effects, a wide range of pharmacological anti-inflammatory properties of Ax have been described *in vitro* and *in vivo* [2, 3].

*Chlamydia pneumoniae*, belonging to the family *Chlamydiaceae*, is a Gram-negative obligate intracellular bacterium. It is a common cause of acute respiratory infection,

including community-acquired pneumonia, sinusitis, pharyngitis, bronchitis and exacerbations of chronic bronchitis. *C. pneumoniae* is responsible for approximately 10 % of pneumonia cases [4]. The infectivity of *Chlamydia* species depends on the reduced state of a cysteine-rich protein [5]. There is a cysteine-rich, strongly disulphide cross-linked protein of the family *Chlamydiaceae* that is called OmcB, and this is indispensable for binding [6]. *C. pneumoniae* and *Chlamydia trachomatis* carry OmcB protein in their outer membrane, where the reduction of its disulphide bonds can be achieved by glutathione (GSH) [7] and by the host cell's protein disulphide isomerase [5]. The influence of NAC, a potent reducing agent, on *C. pneumoniae* replication has not yet been investigated. On the basis of our hypothesis, the reduction of OmcB (which has the highest disulphide content among the structural proteins in *C. pneumoniae*) by NAC can increase binding and consequently increase the replication of *C. pneumoniae*. In this study, we found that

Received 4 January 2018; Accepted 27 February 2018

**Author affiliation:** Department of Medical Microbiology and Immunobiology, University of Szeged, Dóm tér 10, 6720 Szeged, Hungary.

**\*Correspondence:** Katalin Burián, burian.katalin@med.u-szeged.hu

**Keywords:** *Chlamydia pneumoniae*; N-acetyl-cysteine; ambroxol; mouse model.

**Abbreviations:** Ax, ambroxol; GSH, glutathione; IDO 1,2, indolamine 2,3-dioxygenase 1,2; NAC, N-acetyl-cysteine.

NAC promotes *C. pneumoniae* growth *in vitro* and aggravates the severity of pneumonia in mice.

## METHODS

### Propagation of *C. pneumoniae*

In our experiments, the CWL029 strain of *C. pneumoniae* from the ATCC (Manassas, VA, USA) was used. *C. pneumoniae* was propagated in HEp-2 cells (ATCC), as described previously [8, 9]. The titre of the infectious elementary bodies (EBs) was determined by indirect immunofluorescence assay. Serial dilutions of the EB preparation were inoculated onto McCoy cells (ECACC, London UK), and after being cultured for 48 h, the cells were fixed with acetone and stained with a monoclonal anti-*Chlamydia* lipopolysaccharide antibody (AbD Serotec, Oxford, UK) and FITC-labelled anti-mouse IgG (Sigma, St Louis, MO, USA). The number of *C. pneumoniae* inclusions was counted under a UV microscope, and the titre was expressed as inclusion-forming units/ml (i.f.u. ml<sup>-1</sup>).

### *In vitro* effect of NAC and Ax

McCoy and A549 (ATCC) cultures were grown in 24-well tissue culture plates containing a 13 mm cover glass in minimum essential medium Eagle with Earle's salts (Sigma), supplemented with 10 % vol/vol foetal calf serum, 0.5 % wt/vol glucose, 0.3 mg of L-glutamine ml<sup>-1</sup>, 4 mM HEPES and 25 µg of gentamycin ml<sup>-1</sup>. Five parallel wells of semi-confluent cultures were infected with  $2 \times 10^3$  well<sup>-1</sup> *C. pneumoniae* or treated simultaneously with NAC (0.01–10 mg ml<sup>-1</sup>) or Ax (0.002–0.05 mg ml<sup>-1</sup>) at the time of infection. Separate cells were infected with *C. pneumoniae* pretreated (1 h) with different concentrations of NAC. Subsequently, *C. pneumoniae* EBs were pretreated with NAC or Ax by continuous shaking in the presence of NAC (0.1 mg ml<sup>-1</sup>) or Ax (0.05 mg ml<sup>-1</sup>) at room temperature, and after 1 h these drugs were washed out using a culture medium and centrifugation at 13 800 g for 15 min (Heraeus Fresco 17) or left unwashed. NAC- or Ax-treated *C. pneumoniae* or non-treated *C. pneumoniae* were inoculated onto cells on cover glasses in 24-well plates and centrifuged at 800 g for 1 h. After incubation for 48 h, the cells on the cover glasses were fixed with acetone and stained as described above in the 'Propagation of *C. pneumoniae*' section to visualize the inclusions of *C. pneumoniae*. In order to detect the effect of NAC or Ax on the attachment of chlamydial EBs to host cells, McCoy or A549 cells were infected with NAC- or Ax-treated *C. pneumoniae* EBs and after a 1 h incubation period and centrifugation the cells were washed and fixed and the bound EBs were stained by indirect immunofluorescence, as described above.

Fluorescence signals were analysed via Olympus UV microscopy. The immunofluorescence of non-infected or *C. pneumoniae*-infected cells, or cells infected with drug-treated *C. pneumoniae* was analysed quantitatively by ImageQuantTL 8.1 software as follows: 6–6 equally sized circular areas covering the cells were randomly selected on each image, and then the background signals of the selected

areas were eliminated by a threshold set-up and the fluorescence intensity/pixel values of the randomly selected cells were quantified.

### Mice and infection conditions

Pathogen-free 6-week-old female BALB/c mice were obtained from Charles River Laboratories (Hungary). The mice were maintained under standard husbandry conditions at the animal facility of the Department of Medical Microbiology and Immunobiology, University of Szeged, and were provided with food and water *ad libitum*. Before infection, the mice were mildly sedated with an intraperitoneal injection of 200 µl of sodium pentobarbital (7.5 mg ml<sup>-1</sup>). They were then infected intranasally with  $2 \times 10^5$  i.f.u. *C. pneumoniae* in 20 µl sucrose/phosphate/glutamic acid (SPG) buffer, and from the second day post-infection they were treated with 0.2 mg NAC (Sigma) in a volume of 50 µl drinking water *per os* daily. Mice were anaesthetized and sacrificed 7 days, or in another experiment 20 days, after the infection. Blood was then taken by cardiac puncture. In a separate study, *C. pneumoniae*-infected mice were treated in a similar way as above with 25 µg Ax (Sigma) and sacrificed 7 days after infection. The control mice received the same amount of tap water by oral administration using a Gilson pipette to mimic the stress of the watering process. After euthanization, the lungs of the mice were removed and homogenized with acid-purified sea sand (Fluka Chemie AG, Buchs, Switzerland). The homogenized lungs were suspended in 1 ml of SPG for the detection of viable *C. pneumoniae*. The experiments were approved by the Animal Welfare Committee of the University of Szeged and they conformed to Directive 2010/63/EU of the European Parliament.

### The culturing of *C. pneumoniae* from the lungs of mice

After two freeze-thaw cycles, the homogenized lungs from individual mice were centrifuged (10 min, 400 g) and serial dilutions of the supernatants were inoculated onto McCoy cell monolayers. These samples were then centrifuged (1 h, 800 g), and after a 48 h culture the cells were fixed with acetone and stained as described above in the 'Propagation of *C. pneumoniae*' section to visualize the inclusions of *C. pneumoniae*.

### Total RNA extraction and cDNA synthesis

One-day-old semi-confluent McCoy cells in six-well plates were infected with *C. pneumoniae* using a multiplicity of infection (m.o.i.) of 4. The cells were then left untreated or NAC (0.1 mg ml<sup>-1</sup>) or Ax (0.05 mg ml<sup>-1</sup>) were added to the medium. Total RNA was extracted after a 1-day incubation from three parallel wells of each condition with Tri Reagent according to the manufacturer's protocol (Sigma). RNA concentrations were measured at 260 nm via a NanoDrop spectrophotometer (Thermo Scientific, Waltham, MA, USA). The purity of the RNA samples was given as the ratio of the RNA absorbance at 260 and 280 nm, which was higher than 2 in each sample. Afterwards, 1 µg of total RNA was reverse-transcribed using Maxima Reverse Transcriptase according to the

manufacturer's protocol with random hexamer priming (Thermo Fisher Scientific, Inc. Waltham, MA, USA).

### Quantitative PCR (qPCR) of the indolamine 2,3-dioxygenase 1,2 (*IDO1,2*)

qPCR was performed in a Bio-Rad CFX96 real-time system by using a SsoFast EvaGreen qPCR Supermix (Bio-Rad, Hercules, CA, USA) master mix and the murine-specific primer pairs *IDO1*: 5'-GCTTCTTCCTCGTCTCTCTATTG-3', 5'-TCTCCAGACTGGTAGCTATGT-3'; *IDO2*: 5'-CC TGGACTGCAGATTCTAAAG-3', 5'-CCAAGTTCCTGG ATACCTCAAC-3'; beta-actin: 5'-TGGAATCCTGTGGCA TCCATGAAAC-3', 5'-TAAAACGCAGCTCAGTAACAG TCCG-3'. All of the primers were designed using Primer-Quest Tool (IDT) software and synthesized by Integrated DNA Technologies, Inc. (Montreal, Quebec, Canada). To check the amplification specificity, the qPCR was followed by a melting curve analysis. Threshold cycles (*Ct*) were calculated for the *IDO1*, *IDO2* and beta-actin genes, and the relative gene expressions were calculated by the  $\Delta\Delta C_t$  method. Student's *t*-test was used to compare the statistical differences of  $\Delta C_t$  values between the infected and control samples, as described previously [10], with a significance level of  $P < 0.05$ .

### Statistical analysis

The data are expressed as mean  $\pm$  standard deviation (SD). Student's *t*-test was applied using Microsoft Office Excel and a *P* value of less than 0.05 indicated a statistically significant difference.

## RESULTS

### NAC increases the *in vitro* replication of *C. pneumoniae*

Initially, we wanted to check the potential anti-chlamydial effect of NAC under *in vitro* conditions. During our experiments, different concentrations of NAC were applied using two approaches. First, a decreasing concentration of NAC was mixed directly with *C. pneumoniae*, and the host cells were immediately infected. Among the concentrations applied, doses of 10 mg ml<sup>-1</sup> and 2 mg ml<sup>-1</sup> NAC were toxic to the cells. Surprisingly, 0.1 mg ml<sup>-1</sup> NAC resulted in a nearly sixfold increase in the number of *C. pneumoniae* inclusions in McCoy cells as compared to the number observed after infection with untreated *C. pneumoniae* ( $P < 0.05$ ; Fig. 1). Accordingly, we chose this concentration in later studies. In the second approach, *C. pneumoniae* was preincubated with NAC at the respective three concentrations by shaking the mixture of *C. pneumoniae* and NAC continuously for 1 h before infecting the cells. As shown in Fig. 1, there was no significant difference in the infectivity of *C. pneumoniae* pretreated for 1 h with NAC and *C. pneumoniae* treated with 0.1 mg ml<sup>-1</sup> NAC immediately before inoculation of the cells ( $P > 0.05$ ).

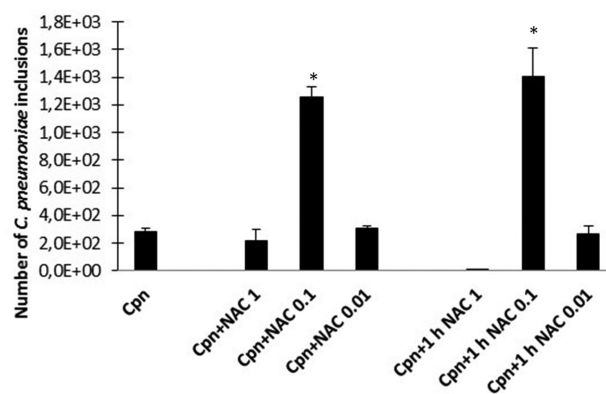


**Fig. 1.** The effect of different concentrations of NAC and different treatment conditions on *C. pneumoniae* replication. McCoy cells were infected with *C. pneumoniae* treated with different concentrations (0.01–1 mg ml<sup>-1</sup>) of NAC at the time of inoculation or infected with *C. pneumoniae* pretreated with NAC. *C. pneumoniae* inclusions were counted under a UV microscope after indirect immunofluorescence staining. Here, the bars denote the means and sds of the results on five parallel tissue wells (\* $P < 0.05$ ).

### NAC increases the binding of *C. pneumoniae* to the host cell

To investigate whether NAC is able to influence the attachment of *C. pneumoniae*, McCoy and the more relevant A549 epithelial cells of human respiratory origin were infected with NAC-pretreated *C. pneumoniae* or with untreated *C. pneumoniae*. As shown in Fig. 2(a, b, d), NAC-treated *C. pneumoniae* produced a significantly higher fluorescence intensity as compared to the untreated *C. pneumoniae* in McCoy cells. A similar effect was observed in the A549 cells (Fig. 2e, f, j). The control cells did not display any fluorescence (Fig. 2c, g).

Subsequent experiments indicated that the removal of NAC with the culture medium from *C. pneumoniae* did not significantly modify the number of replicating *C. pneumoniae* as compared to the outcome of the infection with unwashed *C. pneumoniae* ( $P > 0.05$ ; Fig. 3). Adding NAC to the cells 6 or 24 h after *C. pneumoniae* infection did not change the number of inclusions formed by *C. pneumoniae* (Fig. 3). Furthermore, preincubation of the host cells with NAC for 48 h before infection with *C. pneumoniae* did not modify the replication of *C. pneumoniae* (data not shown).

### Exposure to NAC not only increases the chlamydial lung burden, but also prolongs the infection in mice

Here, we investigated whether NAC might aggravate the chlamydial infection in the short term. Twenty mice were infected with *C. pneumoniae*, and 10 were treated with 10 mg kg<sup>-1</sup> NAC *per os* at the same concentration as that applied for human respiratory infections as a mucolytic drug for 6 days. On the seventh day, the mice were sacrificed; the lungs were removed for the determination of recoverable *C. pneumoniae*. We found that after 6 days of exposure to NAC the severity

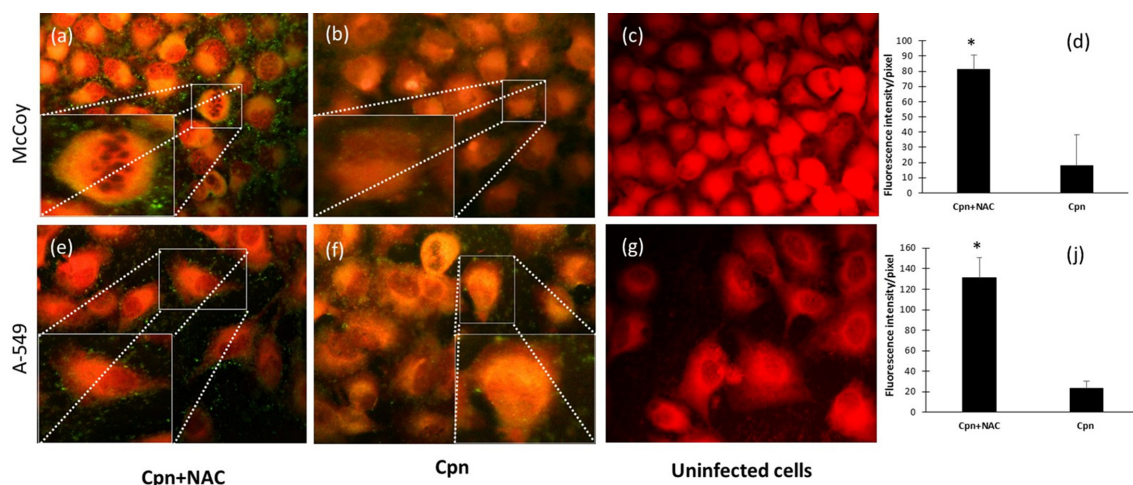


**Fig. 2.** The effect of NAC treatment on *C. pneumoniae* attachment. McCoy or A549 cells were infected with NAC-treated ( $0.1 \text{ mg ml}^{-1}$ ) (a, e) or untreated *C. pneumoniae* (Cpn) (b, f). After the incubation period, the cells were stained as described above in the Methods section. Fluorescence signals were analysed via UV microscopy, and the immunofluorescence of non-infected, *C. pneumoniae*-infected or drug-treated *C. pneumoniae*-infected cells was analysed quantitatively by ImageQuantTL 8.1 software. The results are expressed as the mean $\pm$ SD of the data from three independent experiments, \* $P<0.05$  (d, j).

of the *C. pneumoniae* infection increased. The number of recoverable chlamydial inclusions was approximately three times higher in the NAC-treated group than in the *C. pneumoniae*-infected mice without NAC treatment (Fig. 4a). Next, we investigated whether NAC prolongs the clearance of *C. pneumoniae* from the lungs. Sixteen mice were infected with *C. pneumoniae* and eight mice were treated with NAC

for 19 days. On the twentieth day, the mice were sacrificed and their lungs were removed for the detection of viable *C. pneumoniae*. All of the mice were *C. pneumoniae* culture-positive in the NAC-treated group and the number of *C. pneumoniae* inclusions was 2.5 times higher than that in the control group. Moreover, in the control group two mice became culture-negative (the sensitivity of our method was  $<40 \text{ i.f.u./lung}$ ), suggesting recovery from the disease. The data for these mice were not included in Fig. 4(b).

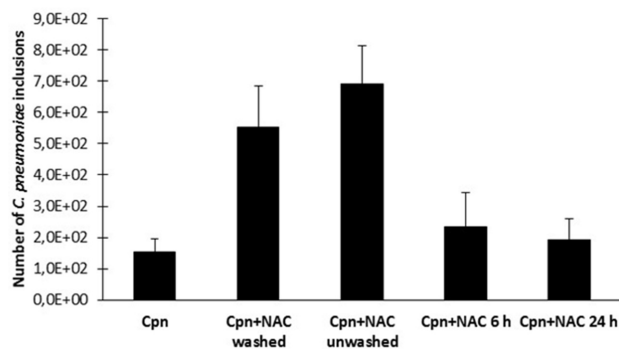


**Fig. 3.** The effect of pre- or post-infection exposure to NAC on *C. pneumoniae* replication. The number of *C. pneumoniae* inclusions were counted in McCoy cells infected with untreated *C. pneumoniae* (Cpn), cells infected with *C. pneumoniae* preincubated for 1 h with ( $0.1 \text{ mg ml}^{-1}$ ) NAC and subsequently washed via high-speed centrifugation (Cpn+NAC washed), cells infected with NAC-treated but unwashed *C. pneumoniae* (Cpn+NAC unwashed) and cells infected with untreated *C. pneumoniae* to which NAC was added 6 h (Cpn+NAC 6 h) or 24 h (Cpn+NAC 24 h) post-infection. The *C. pneumoniae* inclusions were revealed by indirect immunofluorescence days post-infection. The means of the titres are expressed as i.f.u.  $\text{ml}^{-1}$  in five parallel cultures and the SDs are shown.

### Ax does not increase the number of infective *C. pneumoniae*

To look for a better alternative to NAC, the effect of Ax on *C. pneumoniae* replication was tested in *in vitro* and *in vivo* systems. Using concentrations of  $0.002$  and  $0.01 \text{ mg ml}^{-1}$ , Ax did not cause any significant changes in bacterial replication in McCoy cells, but  $0.05 \text{ mg ml}^{-1}$  Ax had a strong antimicrobial effect and this reduced the number of *C. pneumoniae* to approximately one-fifth of that observed with untreated cells ( $P<0.05$ ; Fig. 5a). As shown in Fig. 5(b), none of the applied concentrations of Ax influenced host cell viability. Increasing the dose to  $0.25 \text{ mg ml}^{-1}$  Ax proved to be toxic to the cells (data not shown). We then wanted to determine the reason for the antimicrobial activity of Ax. An identical experiment to that performed with NAC was conducted. Ax-treated and untreated *C. pneumoniae* were inoculated onto McCoy and A549 cells, and the cells were stained using the immunofluorescence method. A decrease in immunofluorescence was not observed in this case, and we inferred that the Ax treatment did not modify the number of *C. pneumoniae* EBs attached to the cell membrane (data not shown). It is well documented that IDO1,2 shows antimicrobial activity that metabolizes the tryptophan, which is essential in chlamydial replication. We then tested whether Ax might

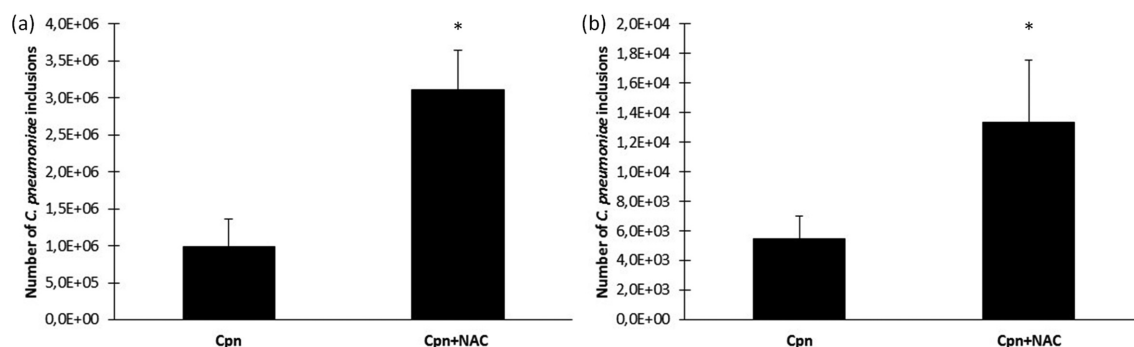


**Fig. 4.** Recoverable i.f.u. in *C. pneumoniae*-infected mice with or without oral NAC treatment. The lung homogenates of infected (Cpn) or infected and NAC-treated ( $10 \text{ mg kg}^{-1}$ ) (Cpn+NAC) mice on day 7 (a) or on day 20 (b) post-infection were inoculated onto McCoy cell monolayers, and *C. pneumoniae* inclusions were detected by indirect immunofluorescence. Here, the data are the means  $\pm$  SD of the number of *C. pneumoniae* inclusions (i.f.u./lung) in the lung homogenates of individual mice (\* $P < 0.05$ ).

influence the expression of IDO1,2. Ax caused a 2.5-fold increase in IDO2 expression in *C. pneumoniae*-infected cells as compared to the expression in untreated cells. In our experiments, NAC treatment did not influence the expression of IDO1,2 in *C. pneumoniae*-infected cells (data not shown). To further investigate the role of Ax during *C. pneumoniae* infection, our mice were infected with *C. pneumoniae* and from the second day were treated with tap water-diluted Ax at the same concentration as is applied for human respiratory infections when it is used as a mucolytic drug ( $1.25 \text{ mg kg}^{-1}$ ). The control mice were given tap water. During the 7-day period, the behaviour (activity and appetite) and weight of the animals did not change significantly between groups (data not shown). The mice were sacrificed 7 days after the infection and the number of recoverable *C. pneumoniae* was counted from the lungs by indirect immunofluorescence. As shown in Fig. 5(c), the number of recoverable *C. pneumoniae* did not change significantly in the Ax-treated and un-treated *C. pneumoniae*-infected group of mice.

## DISCUSSION

NAC is a multifaceted drug that is used in the treatment of different diseases, mainly as a mucolytic agent. It is relatively inexpensive and commercially available as an over-the-counter (OTC) medicine. It has been shown to increase the level of GSH, the body's major antioxidant, by increasing glutathione S-transferase activity. It is a powerful antioxidant and has the potential to treat diseases characterized by the generation of free oxygen radicals [1]. For instance, NAC is a therapeutic option in chronic obstructive pulmonary disease. In an open-label study of 1392 patients, NAC reduced the viscosity of expectorated sputum, reduced cough severity and improved the ease of expectoration in patients after 2 months of treatment [11]. Furthermore, NAC dramatically attenuated influenza symptoms in a group of patients as compared with a placebo-treated group [12].

The direct antimicrobial role of NAC is not well defined, but there are data regarding its inhibitory effect on biofilm

formation. NAC displayed a direct antimicrobial effect against extracellular pathogens, but the concentrations applied by different authors varied greatly ( $0.003\text{--}80 \text{ mg ml}^{-1}$ ) [13–15]. In the case of tuberculosis, NAC was found to play a part in inhibiting the growth of intracellular *Mycobacterium tuberculosis* through bacteriostatic mechanisms [16]. In our study, we found that instead of decreasing bacterial replication, NAC actually increased the number of replicating *C. pneumoniae* in both *in vitro* and *in vivo* infections. Based on our *in vitro* experiment, we disclosed that NAC increased the attachment of the pathogens to the host cells (Fig. 2). Lazarev *et al.* investigated the role of intracellular GSH in *C. trachomatis* infection, and they found that the treatment of cells with buthionine sulfoximine, which causes the irreversible inhibition of GSH biosynthesis or hydrogen peroxide-induced oxidation of GSH, decreased the number of *C. trachomatis* inclusions. In contrast with this finding, the treatment of cells with NAC increased the number of chlamydial inclusions. The researchers concluded that GSH plays a crucial role in chlamydial replication. In their experiments NAC was used as a GSH precursor, and they did not attempt to investigate the anti-chlamydial effect of NAC [7]. However, it is well known that the infectivity of *Chlamydia* species depends on the reduced status of the cell membrane proteins [5]. In agreement with our hypothesis, NAC treatment of the EBs increases the attachment directly, probably by reducing OmcB, which could not have been from an increased level of GSH, because NAC was removed from the culture medium in some of our experiments. It would be worth examining other reducing agents, such as ascorbic acid (vitamin C), to find out whether they influence the binding of *C. pneumoniae* EBs onto host cells.

Aside from the negative effect of NAC on acute *C. pneumoniae* infection, we need to take into account another possible effect of this drug. *C. trachomatis*, which belongs to the family *Chlamydiaceae*, is one of the most common sexually transmitted pathogens. Unfortunately, the infection is asymptomatic in up to 70 % of the cases. This means that the infections usually go unrecognized. The severe consequences of chronic

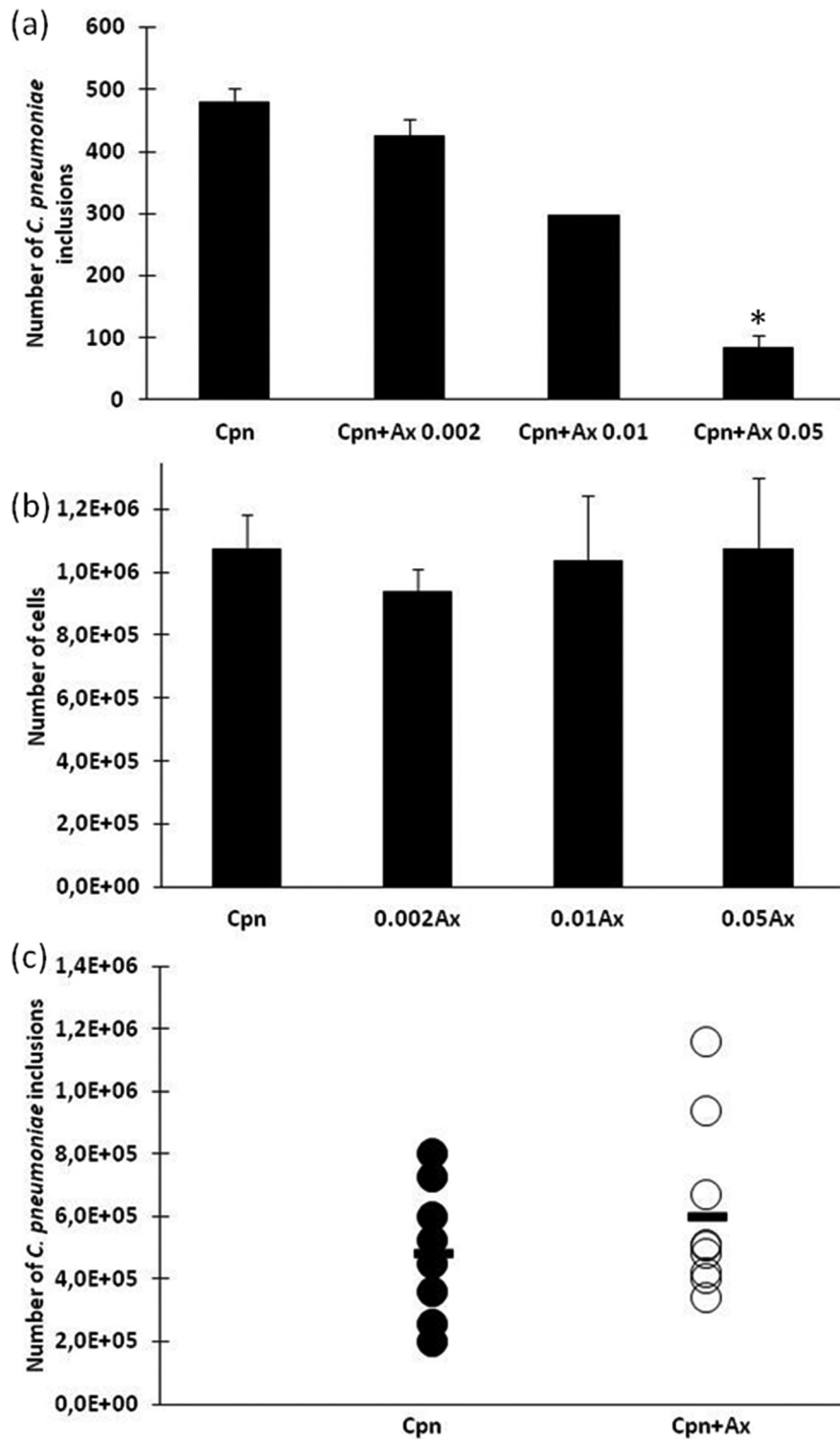


**Fig. 5.** The effect of Ax treatment on *in vitro* and *in vivo* *C. pneumoniae* infection. (a) McCoy cells were infected with *C. pneumoniae* ( $2 \times 10^3$  i.f.u.) and simultaneously treated with different amounts of Ax (0.002–0.05 mg ml<sup>-1</sup>). *C. pneumoniae* inclusions were detected by indirect immunofluorescence. Here, the data are presented as the means  $\pm$  SD of the results in five parallel cultures. (b) The cell numbers for different concentrations of Ax. Five parallel wells of viable cells were counted under a light microscope using trypan blue dye. (c) A group of 10 *C. pneumoniae*-infected mice were treated *per os* with Ax (1.25 mg kg<sup>-1</sup>). The mice were sacrificed 7 days after infection and the number of infective *C. pneumoniae* was detected in the homogenized lungs by inoculation onto McCoy cells and staining using indirect immunofluorescence. The symbols (●, *C. pneumoniae*-infected; ○, *C. pneumoniae*-infected+Ax-treated) stand for individual mice. The bars represent the means of the recoverable *C. pneumoniae* inclusions in the groups.

*C. trachomatis* infection are ectopic pregnancy, infertility, or a pelvic inflammatory disease [17]. In the worst-case scenario, NAC applied simultaneously in the treatment of ongoing respiratory diseases may not only increase the growth of *C. pneumoniae*, but stimulate the growth of *C. trachomatis* as well.

In order to circumvent NAC's aggravating effect on *C. pneumoniae* infection, we looked for a better mucolytic agent that does not increase the severity of the respiratory disease. In our *in vitro* study, Ax displayed significant anti-chlamydial activity that was not associated with decreased binding of the pathogen to the host cells. The complete antimicrobial mechanism of Ax was not analysed, but Ax treatment increased the expression of the anti-chlamydial IDO2, which may in part cause a reduction in the number of pathogens. In our *in vivo* experiment, mice were infected with *C. pneumoniae* and then treated with Ax. Using a human equivalent Ax/body weight dose we found no significant difference in the number of recoverable *C. pneumoniae* between the treated and the untreated groups. The limitation of our study is that despite the promising *in vitro* results, we did not check to see whether a higher dose of Ax has an anti-chlamydial effect *in vivo*. Yang *et al.* found that  $10 \text{ mg kg}^{-1} \text{ day}^{-1}$  (which is eight times higher than the normal dose in a human) significantly reduced the mortality of mice infected with a lethal dose of H3N2 influenza virus [18]. Further experiments are needed to investigate the possible anti-chlamydial effects of Ax at a higher dose.

In Germany, NAC is the second most popular drug for acute coughs, with 23.5 % of the OTC expectorant market share in 2015 (Ax is first with 24 %) [19]. *C. pneumoniae* is a common respiratory pathogen and unfortunately it is not always diagnosed correctly, and if a doctor suggests NAC as a mucolytic agent it might worsen and delay the patient's recovery. Based on the prevalence of *C. pneumoniae*, many patients could suffer prolonged respiratory disease because of NAC.

Overall, on the basis of our results, we can state that NAC can aggravate and prolong the infection caused by *C. pneumoniae* in an animal model. This information will be useful for physicians who recommend NAC as a mucolytic drug in respiratory diseases with a non-identified aetiology. In the case of a *C. pneumoniae* infection, a correct laboratory diagnosis is imperative, because in its absence the use of NAC may worsen the patient's chance of recovery. It is important that clinical studies to prove our results are implemented. Instead of NAC, Ax might be recommended, as it does not support the growth of *C. pneumoniae* in the mouse model.

#### Funding information

This work was supported by GINOP-2.3.2-15-2016-00012 and Human Resources Development Operational Program EFOP-3.6.1-16-2016-00008.

#### Acknowledgements

We would like to thank Györgyi Müllerné Deák for her excellent technical support. We also thank the anonymous blogger who inspired our experiments. He had pneumonia caused by *C. pneumoniae* and

complained about his worsening status after taking NAC prescribed by a physician.

#### Conflicts of interest

The authors declare that there are no conflicts of interest.

#### Ethical statement

The experiments were approved by the Animal Welfare Committee of the University of Szeged and they conformed to Directive 2010/63/EU of the European Parliament.

#### References

- Mokhtari V, Afsharian P, Shahhoseini M, Kalantar SM, Moini A. A review on various uses of N-acetyl cysteine. *Cell J* 2017;19:11–17.
- Beeh KM, Beier J, Esperester A, Paul LD. Antiinflammatory properties of ambroxol. *Eur J Med Res* 2008;13:557–562.
- Stetinová V, Herout V, Kvetina J. *In vitro* and *in vivo* antioxidant activity of ambroxol. *Clin Exp Med* 2004;4:152–158.
- Choroszy-Król I, Frej-Mądrzak M, Hober M, Sarowska J, Jama-Kmiecik A. Infections caused by *Chlamydomydia pneumoniae*. *Adv Clin Exp Med Off Organ Wroclaw Med Univ* 2014;23:123–126.
- Abromaitis S, Stephens RS. Attachment and entry of Chlamydia have distinct requirements for host protein disulfide isomerase. *PLoS Pathog* 2009;5:e1000357.
- Moelleken K, Hegemann JH. The Chlamydia outer membrane protein OmcB is required for adhesion and exhibits biovar-specific differences in glycosaminoglycan binding. *Mol Microbiol* 2008;67:403–419.
- Lazarev VN, Borisenko GG, Shkarupeta MM, Demina IA, Serebryakova MV *et al.* The role of intracellular glutathione in the progression of Chlamydia trachomatis infection. *Free Radic Biol Med* 2010;49:1947–1955.
- Burián K, Hegyesi H, Buzás E, Endrész V, Kis Z *et al.* Chlamydomydia (*Chlamydia*) pneumoniae induces histidine decarboxylase production in the mouse lung. *Immunol Lett* 2003;89:229–236.
- Caldwell HD, Kromhout J, Schachter J. Purification and partial characterization of the major outer membrane protein of Chlamydia trachomatis. *Infect Immun* 1981;31:1161–1176.
- Yuan JS, Reed A, Chen F, Stewart CN. Statistical analysis of real-time PCR data. *BMC Bioinformatics* 2006;7:85.
- Tattersall AB, Bridgman KM, Huitson A. Acetylcysteine (Fabrol) in chronic bronchitis—a study in general practice. *J Int Med Res* 1983;11:279–284.
- de Flora S, Grassi C, Carati L. Attenuation of influenza-like symptomatology and improvement of cell-mediated immunity with long-term N-acetylcysteine treatment. *Eur Respir J* 1997;10:1535–1541.
- Aslam S, Trautner BW, Ramanathan V, Darouiche RO. Combination of tigecycline and N-acetylcysteine reduces biofilm-embedded bacteria on vascular catheters. *Antimicrob Agents Chemother* 2007;51:1556–1558.
- Zhao T, Liu Y. N-acetylcysteine inhibit biofilms produced by *Pseudomonas aeruginosa*. *BMC Microbiol* 2010;10:140.
- Olofsson AC, Hermansson M, Elwing H. N-acetyl-L-cysteine affects growth, extracellular polysaccharide production, and bacterial biofilm formation on solid surfaces. *Appl Environ Microbiol* 2003;69:4814–4822.
- Allen M, Bailey C, Cahatol I, Dodge L, Yim J *et al.* Mechanisms of control of Mycobacterium tuberculosis by NK cells: role of glutathione. *Front Immunol* 2015;6:508.
- Haggerty CL, Gottlieb SL, Taylor BD, Low N, Xu F *et al.* Risk of sequelae after Chlamydia trachomatis genital infection in women. *J Infect Dis* 2010;201:134–155.
- Yang B, Yao DF, Ohuchi M, Ide M, Yano M *et al.* Ambroxol suppresses influenza-virus proliferation in the mouse airway by increasing antiviral factor levels. *Eur Respir J* 2002;19:952–958.
- Morice A, Kardos P. Comprehensive evidence-based review on European antitussives. *BMJ Open Respir Res* 2016;3:e000137.

**II.**

## Article

# Ambroxol Treatment Suppresses the Proliferation of *Chlamydia pneumoniae* in Murine Lungs

Dávid Kókai <sup>1,\*</sup>, Dóra Paróczai <sup>1</sup>, Dezső Peter Virok <sup>1</sup>, Valéria Endrész <sup>1</sup>, Renáta Gáspár <sup>2</sup>, Tamás Csont <sup>2</sup>, Renáta Bozó <sup>3</sup> and Katalin Burián <sup>1</sup>

<sup>1</sup> Department of Medical Microbiology and Immunobiology, University of Szeged, Dóm Square 10, 6720 Szeged, Hungary; paroczai.dora@med.u-szeged.hu (D.P.); virok.dezso.peter@med.u-szeged.hu (D.P.V.); endresz.valeria@med.u-szeged.hu (V.E.); burian.katalin@med.u-szeged.hu (K.B.)

<sup>2</sup> Metabolic Diseases and Cell Signaling (MEDICS) Research Group, Interdisciplinary Center of Excellence, Department of Biochemistry, University of Szeged, Dóm Square 9, 6720 Szeged, Hungary; gaspar.renata@med.u-szeged.hu (R.G.); csont.tamas@med.u-szeged.hu (T.C.)

<sup>3</sup> Department of Dermatology and Allergology, University of Szeged, Dóm Square 10, 6720 Szeged, Hungary; bozo.renata@med.u-szeged.hu

\* Correspondence: kokai.david@med.u-szeged.hu; Tel.: +36-62-545-115; Fax: 36-62-545-113

**Abstract:** Ambroxol (Ax) is used as a mucolytics in the treatment of respiratory tract infections. Ax, at a general dose for humans, does not alter *Chlamydia pneumoniae* growth in mice. Therefore, we aimed to investigate the potential anti-chlamydial effect of Ax at a concentration four times higher than that used in human medicine. Mice were infected with *C. pneumoniae* and 5-mg/kg Ax was administered orally. The number of recoverable *C. pneumoniae* inclusion-forming units (IFUs) in Ax-treated mice was significantly lower than that in untreated mice. mRNA expression levels of several cytokines, including interleukin 12 (IL-12), IL-23, IL-17F, interferon gamma (IFN- $\gamma$ ), and surfactant protein (SP)-A, increased in infected mice treated with Ax. The IFN- $\gamma$  protein expression levels were also significantly higher in infected and Ax-treated mice. Furthermore, the in vitro results suggested that the ERK 1/2 activity was decreased, which is essential for the *C. pneumoniae* replication. SP-A and SP-D treatments significantly decreased the number of viable *C. pneumoniae* IFUs and significantly increased the attachment of *C. pneumoniae* to macrophage cells. Based on our results, a dose of 5 mg/kg of Ax exhibited an anti-chlamydial effect in mice, probably an immunomodulating effect, and may be used as supporting drug in respiratory infections caused by *C. pneumoniae*.

**Keywords:** *Chlamydia pneumoniae*; ambroxol; anti-chlamydial; mouse model; extracellular signal-regulated kinase pathway; surfactant proteins



**Citation:** Kókai, D.; Paróczai, D.; Virok, D.P.; Endrész, V.; Gáspár, R.; Csont, T.; Bozó, R.; Burián, K. Ambroxol Treatment Suppresses the Proliferation of *Chlamydia pneumoniae* in Murine Lungs. *Microorganisms* **2021**, *9*, 880. <https://doi.org/10.3390/microorganisms9040880>

Academic Editor:  
Sofia Costa-de-Oliveira

Received: 5 March 2021

Accepted: 16 April 2021

Published: 20 April 2021

**Publisher's Note:** MDPI stays neutral with regard to jurisdictional claims in published maps and institutional affiliations.



**Copyright:** © 2021 by the authors. Licensee MDPI, Basel, Switzerland. This article is an open access article distributed under the terms and conditions of the Creative Commons Attribution (CC BY) license (<https://creativecommons.org/licenses/by/4.0/>).

## 1. Introduction

Ambroxol (Ax; 2-amino-3,5-dibromo-N-(trans-4-hydroxycyclohexyl) benzylamine) is widely used in the treatment of respiratory infections, chronic bronchitis, and neonatal respiratory distress syndrome due to its mucus viscosity-altering effect and has been shown to be a relatively safe drug [1,2]. Furthermore, Ax shows beneficial effects on the course of Parkinson's disease by modifying glucocerebrosidase chaperon activity [3]. Ax exhibits proinflammatory properties by elevating interleukin-10 (IL-10), IL-12, and interferon gamma (IFN- $\gamma$ ) expression; due to its aromatic moiety, Ax exhibits oxidant scavenger functions [4,5]. Moreover, it has been reported that Ax elevates surfactant protein (SP) production and can reverse the lipopolysaccharide-stimulated induction of the extracellular signal-regulated kinase (ERK) 1/2 pathway [6,7]. In addition, Ax is used for the symptomatic treatment of sore throat during viral infections, as it shows local anesthetic effects [8,9].

*Chlamydia pneumoniae*, belonging to the *Chlamydiaceae* family, is a Gram-negative obligate intracellular bacterium with a specific biphasic lifestyle. It has been shown that

two species of this family that are major human pathogens (*Chlamydia trachomatis* and *C. pneumoniae*), and they are partially dependent on ERK pathway activity during their growth cycle [10,11]. As demonstrated previously by Oberley et al., SPcan enhance the engulfment of Chlamydiae by human THP-1 cells [12]. Moreover, it has been reported that *C. pneumoniae* and *C. trachomatis* interfere with host cell apoptosis in a time-dependent manner via pro- and antiapoptotic processes [10,13]. *C. pneumoniae* is a common cause of acute respiratory infections, such as pharyngitis, bronchitis, and sinusitis, and is responsible for approximately 10% of community-acquired pneumonia cases, in addition to being associated with nonrespiratory diseases, including atherosclerosis [14–16]. In our previous study, we demonstrated that N-acetyl cysteine, a commonly used mucolytic, increases the proliferation of *C. pneumoniae* in vitro and in vivo, and Ax treatment induces the expression of the anti-chlamydial enzyme indoleamine 2,3-dioxygenase 2 (IDO-2) at the transcriptional level in vitro. However, in vivo experiments in mice indicated that commonly used therapeutic concentrations of Ax do not affect *C. pneumoniae* proliferation [17]. Yang et al. reported that an elevated dose of 10-mg/kg Ax (eight-fold greater than the therapeutic concentration for humans) significantly decreases the mortality of mice administered with a lethal dose of the H3N2 virus [9]. Therefore, we hypothesized that a dose of Ax four-fold higher than normal may alter the *C. pneumoniae* proliferation in mouse lungs.

The aim of this study was to verify this hypothesis and to determine the underlying immunological mechanisms induced by Ax that contribute to the elimination of *C. pneumoniae* in mice.

## 2. Materials and Methods

### 2.1. Cultivation of *C. pneumoniae*

Human epithelial type 2 (HEp-2) cells obtained from the American Type Culture Collection (ATCC, Manassas, VA, USA) were used to cultivate *C. pneumoniae* CWL029 (ATCC), as described previously [18,19]. After partial purification and concentration, aliquots of elementary bodies (EBs) were added to sucrose-phosphate-glutamic acid buffer (SPG) and stored at  $-80^{\circ}\text{C}$  until use [20]. An indirect immunofluorescence assay was performed to determine the titer of infectious *C. pneumoniae* EBs. Ten-fold serial dilutions of the purified EBs were inoculated into McCoy cells (ECACC, London, UK), and after 48 h of incubation, the infected cells were fixed with acetone at  $-20^{\circ}\text{C}$  and stained with monoclonal anti-*Chlamydia* lipopolysaccharide antibodies (AbD Serotec, Oxford, UK) and fluorescein isothiocyanate (FITC)-labeled anti-mouse IgG (Sigma-Aldrich, St. Louis, MO, USA). Cells were analyzed using an Olympus UV microscope; the titer of *C. pneumoniae* was expressed as inclusion-forming units (IFU)/mL.

### 2.2. Infection of Mice and Preparation of Lung Tissues

Female pathogen-free BALB/c mice (6 weeks old) were purchased from Charles River Laboratories (Veszprém, Hungary). Animals were provided with food and water ad libitum and maintained under standard husbandry conditions at the animal facility of the Department of Medical Microbiology and Immunobiology at the University of Szeged. The mice were divided into four groups: untreated/uninfected, untreated/infected, treated/uninfected, and treated/infected (10 mice/group). Prior to infection, the mice were mildly sedated via an intraperitoneal injection of 200  $\mu\text{L}$  of sodium pentobarbital (7.5 mg/mL), followed by the intranasal administration of  $2 \times 10^5$  IFU of *C. pneumoniae* in 20- $\mu\text{L}$  SPG buffer.

From the first day post-infection (pi), the mice were administered daily with 5-mg/kg Ax (Sigma-Aldrich, Darmstadt, Germany) dissolved in water (2 g/L). Control mice received the same amount of water via oral administration using a pipette to mimic the stress of the treatment process. Behavior and weight were monitored daily. The mice were anesthetized and euthanized 7 days pi. The sera were harvested via cardiac puncture. The lungs were removed and homogenized using acid-purified sea sand (Fluka Chemie AG, Buchs, Switzerland). Half of the homogenized tissue sample was processed for RNA extraction

and quantitative reverse-transcription polymerase chain reaction (RT-qPCR), whereas the other half was suspended in 1 mL of SPG for the detection of viable *Chlamydia* and to measure the cytokine levels.

This study was approved by the National Scientific Ethical Committee on Animal Experimentation of Hungary (August, 10 August 2016; III./3072/2016) and Animal Welfare Committee of the University of Szeged. This study conformed to the Directive 2010/63/EU of the European Parliament.

### 2.3. Culturing of *C. pneumoniae* from Murine Lungs

One half of the homogenized lung sample derived from individual mice was centrifuged (10 min,  $400 \times g$ ) (Sorvall® RT6000B, DuPont, Wilmington, DE, USA), after which, the serial dilutions of the supernatants were inoculated into McCoy cell monolayers and centrifuged (1 h,  $800 \times g$ ). After 48 h of culturing, the cells were fixed and visualized, and the inclusions were enumerated as described previously [21].

### 2.4. Total RNA Extraction and cDNA Synthesis

The remaining half of the homogenized lung sample was processed using the TRI reagent (Sigma-Aldrich) according to the manufacturer's protocol for performing total RNA extraction. RNA concentrations were measured at 260 nm using a NanoDrop spectrophotometer (Thermo Fisher Scientific, Waltham, MA, USA). The purity of the RNA samples was determined based on the ratio of RNA absorbance at 260 and 280 nm, which was  $> 2$  for all samples. Subsequently, 1 µg of total RNA was reverse-transcribed using Maxima Reverse Transcriptase according to the manufacturer's instructions using random hexamer primers (Thermo Fisher Scientific).

### 2.5. qPCR Amplification of *Ido1*, *Ido2*, *Il12*, *Il23*, *Il17a*, *Il17f*, *Ifng*, *Sftpa*, *Sftpb*, *Sftpc*, and *Sftpd*

qPCR was performed using a Bio-Rad CFX96 real-time system with the SsoFast™ EvaGreen® qPCR Supermix (Bio-Rad, Hercules, CA, USA) and the following murine-specific primer pairs: *Ido1*: 5'-GCTTCTTCCTCGTCTCTCTATTG-3' and 5'-TCTCCAGACTGGTAGCTA TGT-3', *Ido2*: 5'-CCTGGACTGCAGATTCCTAAAG-3' and 5'-CCAAGTTCCTGGATACCTCAA C-3', *Actb* encoding beta-actin: 5'-TGGAATCCTGTGGCATCCATGAAAC-3' and 5'-TAAAACG CAGCTCAGTAACAGTCCG-3', *Ifng*: 5'-CAAGTGGCATAGATGTGGAAGA-3' and 5'-GCTGT TGCTGAAGAAGGTAGTA-3', *Il12* p40 homodimer: 5'-ACATCAAGAGCAGTAGCAGTTC-3' and 5'-AGTTGGGCAGGTGACATCC-3', *Il23* p19: 5'-CCTGCTTGACTCTGACATCTT-3' and 5'-TGGGCATCTGTTGGGTCTC-3', *Il17a*: 5'-AAGGCAGCAGCGATCATCC-3' and GGAACGGTTGAGGTAGTCTGAG-3', *Il17f*: 5'-AGCAAGAAATCCTGGTCTTCGGA-3' and 5'-CTTGACACAGGTGCAGCCAACCTT-3', *Sftpa*: 5'-GGTGTCTAAGAAGCCAGAGAAC-3' and 5'-CAAGATCCAGATCCAAGGAAGAG-3', *Sftpb*: 5'-CCACCTCCTCACAAGATGAC-3' and 5'-TTGGGGTTAATCTGGCTCTGG-3', *Sftpc*: 5'-ATGGACATGAGTAGCAAAGAGGT-3' and 5'-CACGATGAGAAGGCGTTTGGAG-3', and *Sftpd*: 5'-TCTGAGCCACTGGAGGTAAA-3' and 5'-CAACATACAGGTCTGAGCCATAG-3'. All primers were designed using the PrimerQuest Tool software and synthesized by Integrated DNA Technologies Inc. (Coralville, IA, USA). A melting curve analysis was performed to verify the amplification specificity. Threshold cycles (Ct) were determined for *Ido1*, *Ido2*, *Il12*, *Il23*, *Il17a*, *Il17f*, *Ifng*, *Sftpa*, *Sftpb*, *Sftpc*, *Sftpd*, and *Actb*, and the relative gene expression was calculated via the  $2^{-(\Delta\Delta Ct)}$  method. One-way analysis of variance with repeated measures (ANOVA RM) and planned comparisons were used to compare the statistical differences in the  $\log_2(\Delta\Delta Ct)$  values between the infected and control samples, as described previously, with a level of significance of  $p < 0.05$  [22].

### 2.6. Enzyme-Linked Immunosorbent Assay (ELISA)

Standard sandwich mouse IL-6 and mouse IFN-γ ELISA kits (BD OptEIA™; BD biosciences, Franklin Lakes, NJ, USA) were used to determine the IL-6 and IFN-γ concentrations in the lung supernatants. Prior to use, the stored lung samples were thawed immediately, and the assay was performed according to the manufacturer's instructions

at 10× dilution for IL-6 and at 50× dilution for IFN-γ. The dynamic range of the kits was between 10 and 1000 pg/mL. Plates were analyzed using the Biochrom Anthos 2010 microplate reader (Biochrom, Cambridge, UK). Samples were assayed in duplicate.

### 2.7. Western Blotting Analysis of ERK

To investigate the levels of phosphorylation in RAF proto-oncogene serine/threonine-protein kinase (c-Raf), as well as dual specificity mitogen-activated protein kinase (MEK)1/2, ERK1/2, P90RSK1/2, and mitogen- and stress-activated protein kinase 1 (MSK-1) proteins, McCoy cells were grown in 6-well plates and treated with Ax (0.05 mg/mL) and/or infected with *C. pneumoniae* simultaneously at 0.01 multiplicity of infection (MOI) or left untreated and/or uninfected. After a 12-h incubation period, the cells were washed twice with ice-cold phosphate-buffered saline, scraped, and collected in a homogenization buffer (1× radioimmunoprecipitation buffer supplemented with phosphatase inhibitors and a protease inhibitor cocktail) (Cell Signaling, Danvers, MA, USA). Cells were sonicated using an ultrasonic homogenizer (10 s, 4 °C), followed by centrifugation of the homogenate (14000× g, 10 min, 4 °C). The bicinchoninic acid assay was performed to determine the protein concentration in the homogenates [23]. Samples containing 20 µg of protein were boiled for 5 min. After preparation, the samples were subjected to sodium dodecyl sulfate-polyacrylamide gel electrophoresis (SDS-PAGE) using 10% polyacrylamide gels [23]. After separation, the proteins were transferred onto 0.45-µm pore-sized nitrocellulose membranes (Amersham, Buckinghamshire, UK) (35 V, 1.5 h, room temperature (RT)). Nonspecific binding was blocked via incubation (1 h, RT) in 0.05% (v/v) Tris-buffered saline–Tween-20 containing 1% bovine serum albumin (BSA; v/v) (Sigma, St. Louis, MO, USA). In all experiments, the membranes were cut horizontally according to the molecular weights of the investigated proteins. Membranes were incubated with specific primary antibodies against phosphorylated forms of Raf (1:1000), MEK (1:2000), p90 (1:1500), ERK (1:2000), and MSK (1:1000) (Cell Signaling), as well as a housekeeping protein/loading control GAPDH (1:10,000) in 1% BSA solution containing 0.1% Tween-20 (overnight, 4 °C). After washing (Tris-buffered saline containing 0.05% Tween-20, Sigma), the membranes were incubated with horseradish peroxidase-conjugated goat anti-rabbit secondary antibodies (Cell Signaling Technology) for 45 min at RT. A chemiluminescence analysis was performed using the LumiGLO 20× reagent (Cell Signaling), followed by exposure of the membranes to X-ray films. All films were scanned (Epson Perfection V19 Scanner, Epson, Suwa, Nagano, Japan) (8-bit, 400 dpi), and the density of the protein bands was quantified using Quantity One software (Bio-Rad) [24]. The 90-kDa form of MSK-1 was used for the calculation of the protein contents of the bands according to the protocol.

### 2.8. Apoptosis Assay and Flow Cytometry

Caspase 3/7 activity assays were performed using the FAM FLICA™ Caspase-3/7 Kit (Bio-Rad) combined with propidium iodide (PI). McCoy cells were divided into 4 experimental groups. Half of the McCoy cells were infected with 0.01 MOI *C. pneumoniae*, while the other half were left uninfected. Both the infected and uninfected groups were subdivided into those treated with 0.05-mg/mL Ax or left untreated. After 12 h of incubation, the apoptosis assay was performed according to the manufacturer's instructions, and the cells were analyzed via flow cytometry. The assay discriminated between viable (caspase 3/7−/PI−), early apoptotic (caspase 3/7+/PI−), and late apoptotic (caspase 3/7+/PI+) cells. The fluorescence of the cell populations was analyzed immediately using a BD fluorescence-activated cell sorting Aria Fusion flow cytometer (BD biosciences).

### 2.9. In Vitro Effects of SP-A and SP-D on *C. pneumoniae* Proliferation and Attachment

McCoy cells were seeded ( $2.5 \times 10^5$  cells) to form a monolayer in 24-well plates and incubated overnight. *C. pneumoniae* (0.01 MOI) was diluted in 1-mL medium in the presence of either SP-A (1 µg/mL) (Abcam, Cambridge, UK), SP-D (1 µg/mL) (Abcam), or neither. The mixtures were shaken at 37 °C for 1 h and then centrifuged at 800× g for 1 h; at 48 h pi,

the cells were fixed using acetone and stained, as described in Section 2.1. To detect the effect of SP-A and SP-D proteins on the attachment of *C. pneumoniae* to J-774 cells (ATCC), the experiment described above was repeated with the following modification. After 1 h of centrifugation, the cells were stained immediately, as described earlier.

Fluorescence signals were analyzed using the Olympus IX83 Live Cell Imaging system and scanR High-Content Screening Station microscopy. The immunofluorescence of cells infected with nontreated *C. pneumoniae*, SP-A-pretreated *C. pneumoniae*, or SP-D-pretreated *C. pneumoniae* was analyzed quantitatively using ImageQuantTL 8.1; Image analysis software, GE Healthcare Bio-Sciences AB, Uppsala, Sweden, 2011 as follows: in three parallel cultures, 6–6 equally sized circular areas covering the cells were randomly selected on each image, and then, the background signals of the selected areas were eliminated via a threshold set-up, and the fluorescence intensity/pixel values of the randomly selected cells were quantitated.

#### 2.10. Statistical Analysis

Welch's *t*-test or one-way ANOVA RM with planned comparisons was performed using GraphPad Prism 8.0.1 software (GraphPad Software, San Diego, CA, USA). Data were expressed as the mean  $\pm$  standard deviation. A value of  $p < 0.05$  was considered significant.

### 3. Results

#### 3.1. Ax Treatment at Elevated Concentration Suppressed *C. pneumoniae* Proliferation in Mouse Lungs

Previously, we found that Ax treatment at a therapeutic dose for humans does not affect the severity of *C. pneumoniae* infection in mice [17]. Our current aim was to determine whether a relatively higher concentration of Ax would suppress the chlamydia replication. Therefore, the mice were infected with *C. pneumoniae* ( $2 \times 10^5$  IFU/mouse); half of the mice were treated daily from day 1 pi with a  $4\times$  higher concentration of Ax (5 mg/kg) than the dose used as a mucolytics in common respiratory infections. Seven days pi, the mice were euthanized, and the lungs were removed for detection of viable *C. pneumoniae*. A significant difference was found between the number of recoverable *C. pneumoniae* between the Ax-treated and untreated groups. The mean numbers of viable *C. pneumoniae* IFUs in the Ax-treated and untreated groups were  $3.1 \times 10^4$  and  $7.3 \times 10^4$  IFU/lung, respectively (Figure 1). The mice in the Ax-treated group exhibited less severe symptoms than those in the control group.

#### 3.2. Ax Treatment Altered the Gene Expression and Protein Level of IFN- $\gamma$ in the Lungs of *C. pneumoniae*-Infected Mice

We investigated whether gene expression was altered during Ax treatment, with respect to the cytokine profile in *C. pneumoniae* infection. We found that the relative expression of IL-12, IL-23, IL-17A, and IFN- $\gamma$  was significantly higher in the *C. pneumoniae*-infected/Ax-treated group than in the *C. pneumoniae*-infected group without treatment (2.22-, 3.07-, 2.46-, and 2.27-fold, respectively) (Figure 2a).

We previously reported that Ax treatment elevates the expression of the known anti-chlamydial enzyme IDO-2 in the A-549 cell line; however, this elevation is not significant when a human equivalent mg/kg dose is administered to *C. pneumoniae*-infected mice [17]. Therefore, we determined whether an elevated dose of Ax increased IDO-1 and IDO-2 expression in mice. We observed no significant difference in expression levels between *C. pneumoniae*-infected mice and *C. pneumoniae*-infected/Ax-treated mice. However, in accordance with the findings of Virok et al., which showed that IDO-1 and IDO-2 are active in *C. pneumoniae*-infected mice [25], in contrast to earlier findings [26], we also found significant increases in both IDO-1 and IDO-2 expression levels during *C. pneumoniae* infection compared to those of the untreated/uninfected group (15.14- and 10.81-fold, respectively) (Figure 2a).

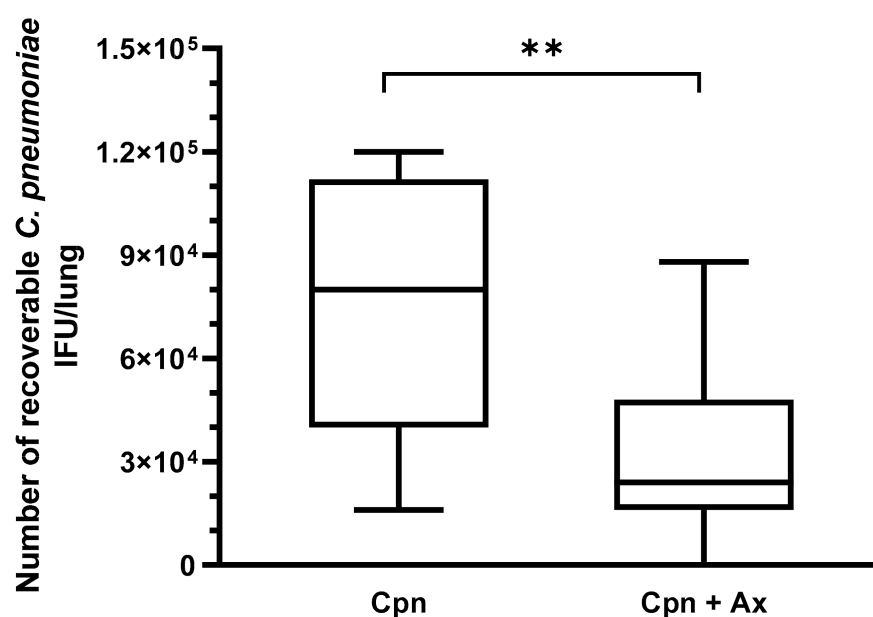


**Figure 1.** Recoverable *C. pneumoniae* IFU in infected mice ( $n = 20$ ) with and without Ax treatment. Ax-treated mice daily received 5-mg/kg Ax for 6 days. The supernatant of the lung homogenates was inoculated into a McCoy cell monolayer and cultured for 2 days, followed by fixation and staining, and the number of inclusions was determined via indirect immunofluorescence assay. (\*\*  $p = 0.0049$ ). Box = 25th percentile, median, and 75th percentiles; bars = min and max values. IFU, inclusion-forming unit; Cpn, *C. pneumoniae*-infected mice; Cpn + Ax, *C. pneumoniae*-infected mice treated with Ambroxol.

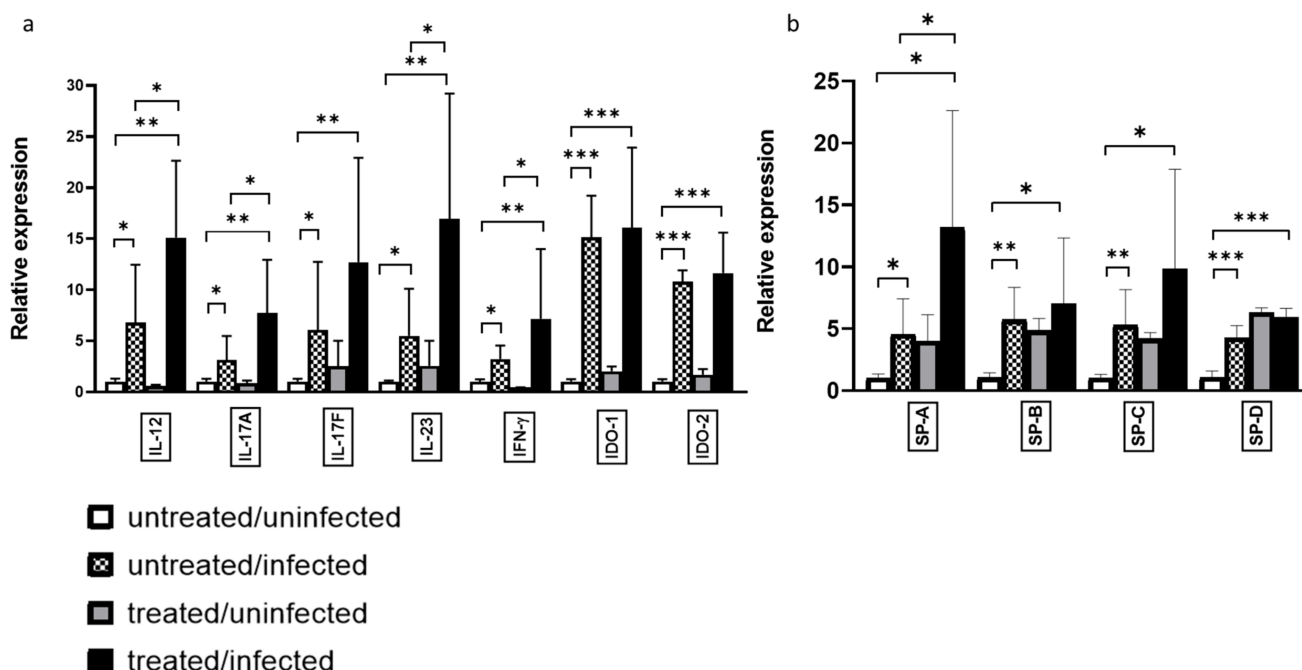


**Figure 2.** Relative expression of genes influenced by *C. pneumoniae* infection and Ax treatment. Mice were either infected with *C. pneumoniae* (or remained uninfected as a control), followed by treatment with Ax (5 mg/kg) (or remained untreated, for the control). RNA was extracted from the lungs, and gene expression was analyzed via RT-qPCR for (a) IL-12, IL-23, IL-17A, IL-17F, IFN-γ, IDO-1, and IDO-2 and (b) SP-A, SP-B, SP-C, and SP-D. Bars denote the mean and standard deviation of the expression levels for triplicate measurements (\*  $p < 0.05$ , \*\*  $p < 0.01$ , and \*\*\*  $p < 0.001$ ).

SPs play a crucial role in maintaining lung homeostasis; moreover, SP-D show an anti-*C. trachomatis* activity in genital mouse model [12,27–29]. Therefore, we determined the relative expression of SPs in the lungs of the mice. We found that all SPs were significantly upregulated in the untreated/infected mice compared to that of the uninfected/untreated group (SP-A, 4.55-fold; SP-B, 5.72-fold; SP-C, 5.28-fold; SP-D, 4.26-fold), suggesting that these anti-chlamydial mechanisms occur naturally in *C. pneumoniae*-infected mouse lungs. Notably, we observed a significant elevation in SP-A expression levels of mice in the treated/infected group compared to those of the untreated/infected group (2.89-fold) (Figure 2b).

After determining that the relative mRNA expression of *Ifng* was significantly higher in Ax-treated/infected mice than in untreated/infected mice, we investigated the protein expression levels of IFN- $\gamma$ . We measured the cytokine concentrations in lung supernatants and found that IFN- $\gamma$  levels were significantly higher in the *C. pneumoniae*-infected/Ax-treated group than in the untreated/infected group ( $p = 0.0041$ ) (Figure 3). We also measured the level of the pro-inflammatory cytokine IL-6; however, we did not observe significant differences between the expression levels of *C. pneumoniae*-infected and *C. pneumoniae*-infected/Ax-treated groups (Figure 3).

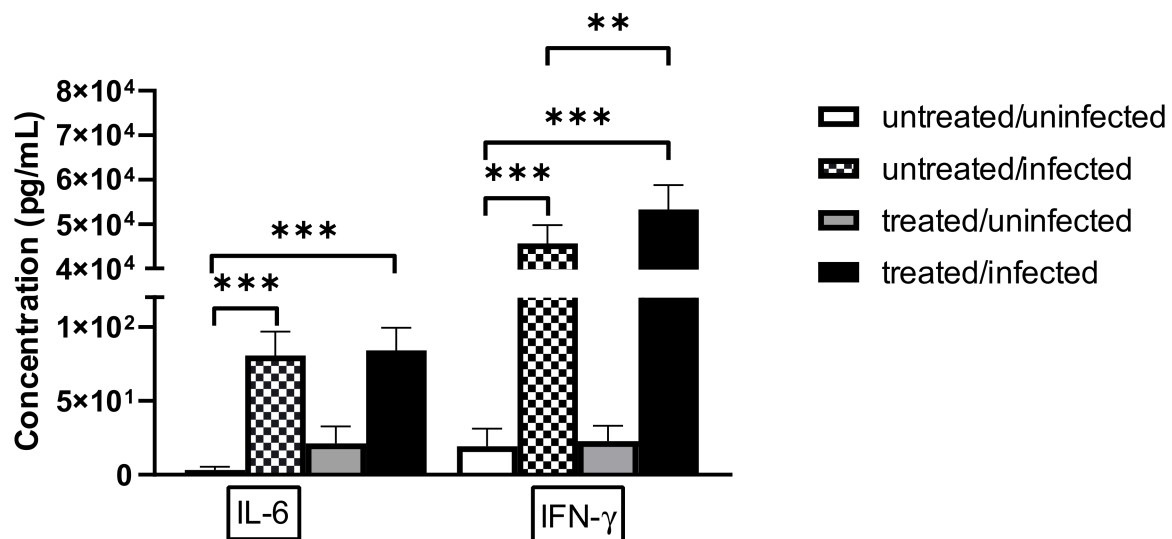


**Figure 3.** Concentrations of IL-6 and IFN- $\gamma$  in lung supernatants. Mice were infected intranasally with *C. pneumoniae* and treated with 5-mg/kg Ax for 6 days or left untreated and uninfected. On the seventh day post-infection, the mice were euthanized and the concentrations of IL-6 and IFN- $\gamma$  in the supernatants of the lungs were measured via ELISA. Each bar denotes the mean  $\pm$  standard deviation for 10 mice (\*\*  $p < 0.01$ , and \*\*\*  $p < 0.001$ ).

### 3.3. SP Treatment Increased the Attachment of *C. pneumoniae* to Macrophages and Decreased Bacterial Proliferation

After showing that Ax treatment increased the relative expression of SPs in the lungs of *C. pneumoniae*-infected mice, we investigated the effect of anti-chlamydial SP proteins on *C. pneumoniae* replication and attachment to macrophages in vitro. We found that the pre-treatment of EBs with SP-A or SP-D significantly reduced the number of *C. pneumoniae* inclusions (0.18-fold) ( $p = 0.021$ ) and (0.57-fold) ( $p = 0.034$ ), respectively, in infected cells. This anti-chlamydial effect was more prominent in SP-A treatment than in SP-D treatment (Figure 4). These results correspond to the findings of Oberley et al. [12,29], who showed that SP-A and SP-D can aggregate *C. pneumoniae*, thereby inhibiting the infection of cells.

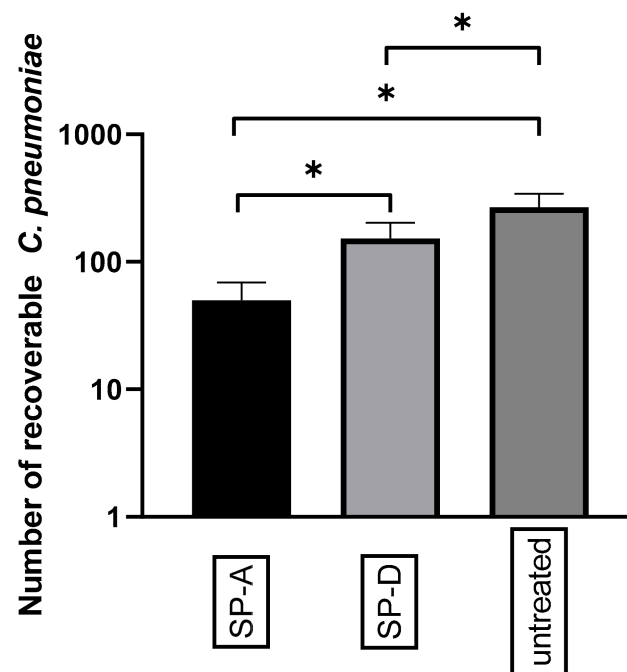


**Figure 4.** Anti-chlamydial effect of SP-A and SP-D. *C. pneumoniae* EBs were treated with either SP-A, SP-D, or left untreated. After 1 h of incubation, the samples were inoculated into McCoy cells and fixed 48 h post-infection. The number of *C. pneumoniae* inclusions was determined via indirect immunofluorescence staining. Each bar denotes the mean number of inclusions in three parallel cultures  $\pm$  standard deviation (\*  $p < 0.05$ ).

Oberley et al. demonstrated that SP-A-or SP-D-treated *C. pneumoniae* are recognized by THP-1 human monocytic cells with a higher efficiency than untreated bacteria [12]. Consequently, we investigated whether these findings were reproducible in J-774 murine macrophage cells. *C. pneumoniae* EBs were treated with SP-A or SP-D, and then, the samples were inoculated into J-774 cells. After 1 h of centrifugation, we stained the cells with *Chlamydia*-specific immunofluorescent antibodies, and it was found that the average pixel intensity of FITC was significantly elevated after treatment with both types of SPs compared to that seen in cells infected with untreated EBs. This indicated that a relatively larger number of *C. pneumoniae* cells were recognized by J-774 cells after SP treatment. This effect was more prominent in SP-A-treated *C. pneumoniae* than in SP-D-treated *C. pneumoniae* (SP-A 2.74-fold ( $p = 0.014$ )) and (SP-D 2.05-fold ( $p = 0.024$ )) (Figure 5) (Figure S1).

#### 3.4. Ax Treatment Did Not Induce Apoptosis via the Caspase-Dependent Pathway But Decreased ERK 1/2 Activation in *C. pneumoniae*-Infected Cells

It has been shown that *C. pneumoniae* can prevent the occurrence of host cell apoptosis; therefore, we investigated whether Ax treatment affected host cell death during *C. pneumoniae* infection. According to Galle et al., the assessment of apoptosis in *C. pneumoniae*-infected cells via annexin V staining is not accurate due to the *C. pneumoniae*-induced externalization of phosphatidylserine on the host cell membrane, which provides a binding site for annexin V and creates a false-positive apoptosis signal [30]. Therefore, we determined caspase 3/7 activity using flow cytometry. The analysis revealed that caspase 3/7 activity did not differ significantly between the treated/infected group and the untreated/infected group (Figure 6).

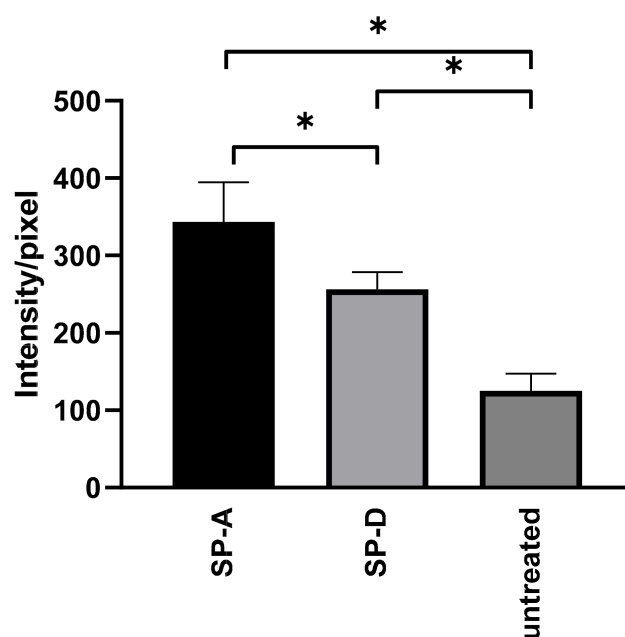


**Figure 5.** Effect of SP-A and SP-D treatment on *C. pneumoniae* attachment to J-774 cells. *C. pneumoniae* EBs were incubated with either SP-A or SP-D, or they were left untreated. After 1 h of incubation, the samples were inoculated into J-774 cells, and then, 1 h post-infection, the cells were fixed and stained via immunofluorescence. The average FITC intensity/pixel was measured. The results are expressed as the mean  $\pm$  standard deviation of the data from three independent experiments. Microscopic pictures are shown in supplement Figure S1, (\*  $p < 0.05$ ).

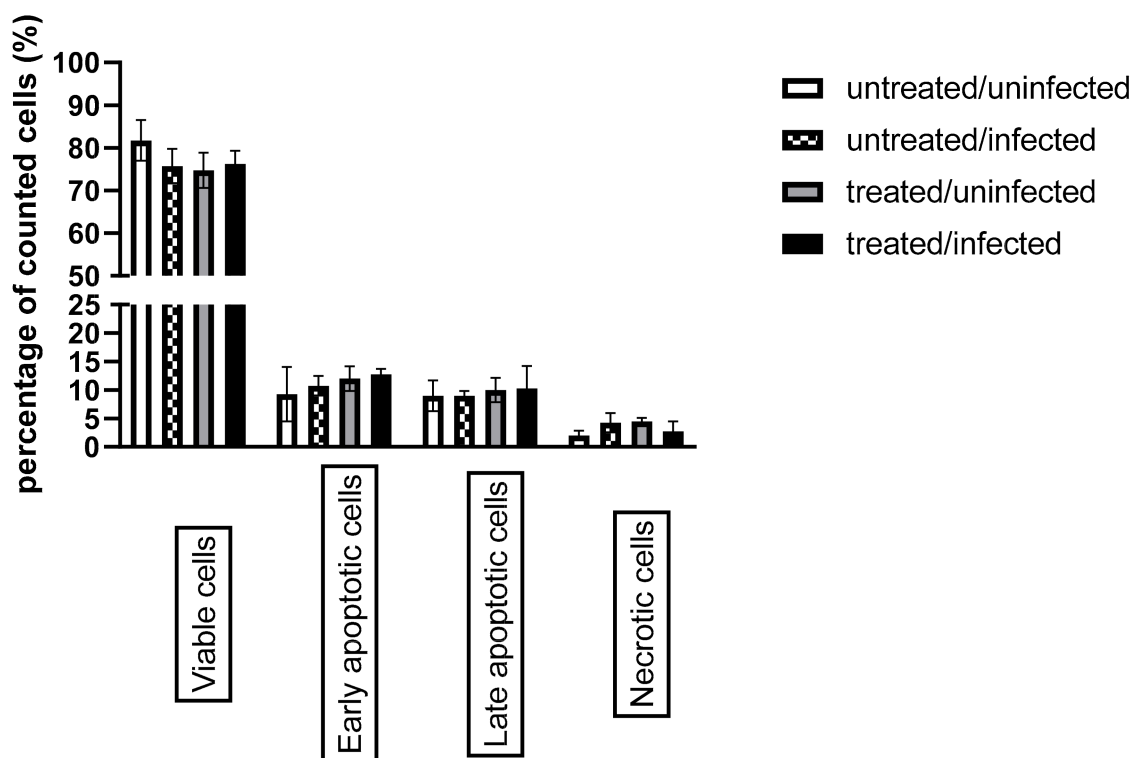


**Figure 6.** Evaluation of host cell apoptosis based on caspase 3/7 activity combined with propidium iodide staining. McCoy cells were infected with 0.01 MOI of *C. pneumoniae* and/or treated with 0.05-g/mL Ax or left untreated/uninfected. Flow cytometric analysis was performed 12 h post-infection to determine the status of apoptosis. The results are expressed as the mean  $\pm$  standard deviation of the data from three independent experiments. ( $p > 0.05$ ).

*C. pneumoniae* activates the ERK 1/2 pathway to acquire several essential molecules from host cells and avoid host cell apoptosis. Therefore, we investigated the effect of Ax treatment on the MAPK/ERK activity in *C. pneumoniae*-infected cells. Western blotting analysis showed that the ERK-1 (1.49-fold;  $p < 0.05$ ) and ERK-2 (2.04-fold;  $p < 0.05$ ) protein expression levels were significantly increased in untreated/infected cells compared to those in untreated/uninfected cells (Figure 7). We also observed that *C. pneumoniae* infection significantly increased the MSK-1 levels (2.25-fold) in untreated/infected cells compared to those in untreated/uninfected cells. MSK-1 is responsible for the activation of nuclear factor kappa-enhancer of B-cells and induction of early genes such as *c-fos*, *junB*, and *mkp-1* [31]. The Ax treatment of *C. pneumoniae*-infected cells significantly decreased the levels of c-RAF (0.42-fold), ERK 1 (0.16-fold), ERK 2 (0.15-fold), P90RSK1 (0.61-fold), P90RSK2 (0.67-fold), and MSK-1 (0.19-fold) ( $p < 0.05$ ) compared to those of the untreated/infected group (Figure 7).

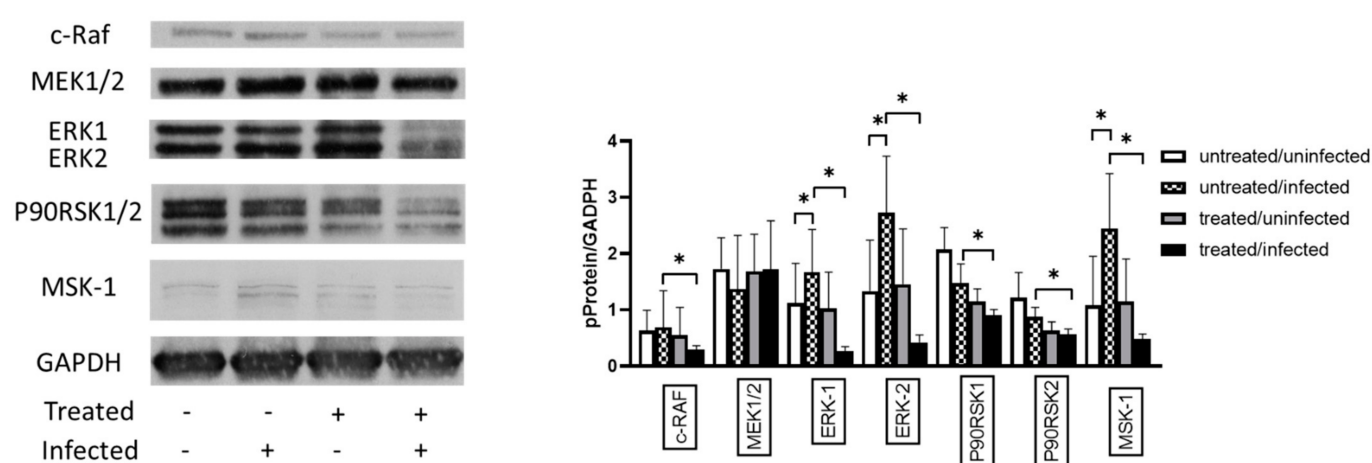


**Figure 7.** Analysis of the expression of proteins related to the MAPK/ERK pathway. McCoy cells were infected with 0.01 MOI *C. pneumoniae*, treated with 0.05-mg/mL Ax, infected with 0.01 MOI *C. pneumoniae* and treated with 0.05-mg/mL Ax, or left untreated. The cells were scraped at 12 h post-infection. Subsequently, proteins in the cell lysates were separated via SDS-PAGE and then blotted onto nitrocellulose membranes. Membranes were incubated with specific primary antibodies against phosphorylated forms of c-RAF, MEK1/2, P90RSK1/2, ERK1/2, MSK-1, and a housekeeping protein/loading control GAPDH. Horseradish-peroxidase-conjugated goat anti-rabbit IgG was used as secondary antibody. Chemiluminescence analysis was performed using the LumiGLO reagent, followed by the exposure of membranes to X-ray films. All films were scanned, and density of the protein bands was quantified using the Quantity One software. The ratio of phosphorylated protein/GAPDH was determined. The results are expressed as the mean  $\pm$  standard deviation of the data from three independent experiments. The shown Western blot is representative of parallel Western blots (\*  $p < 0.05$ ). MAPK, mitogen-activated protein kinase; ERK, extracellular signal-regulated kinase; c-RAF, RAF proto-oncogene serine/threonine-protein kinase; MEK1, dual specificity mitogen-activated protein kinase; MSK-1, mitogen- and stress-activated protein kinase 1; GAPDH, glyceraldehyde 3-phosphate dehydrogenase.

#### 4. Discussion

Ax, a metabolite of bromhexine, is considered a relatively safe over-the-counter drug. It is primarily recommended as a secretory agent for the treatment of various respiratory diseases that are associated with extensive mucus production. Ax treatment increases surfactant synthesis and facilitates their secretion from type II pneumocytes [32,33]. Furthermore, Ax exhibits voltage-dependent sodium channel inhibitory properties, which can be beneficial in cases of diseases associated with sore throat by incorporating Ax in lozenges [8,34]. Ax can also be used in the treatment of Gaucher disease and is considered a supplemental medication for treating Parkinson's disease, as it increases glucocerebrosidase activity [3,35]. Additionally, a recently published study suggested that when Ax is administered together with antibiotics, a relatively higher antibiotic concentration can

be obtained in the lungs due to its secretion-supporting function [36]. Several studies have shown that Ax exhibits antimicrobial characteristics. Ax treatment reverses the resistance of *Candida albicans* to fluconazole [37]. Moreover, it inhibits the mucoid conversion of *Pseudomonas aeruginosa*, facilitates the bactericidal activity of ciprofloxacin against biofilms, and exhibits synergy with vancomycin for the elimination of catheter-related *Staphylococcus epidermidis* biofilms both in vitro and in vivo [38]. Furthermore, Ax impedes the rhinovirus infection in primary cultures of human tracheal epithelial cells [39]. Ax also shows antibiofilm properties; the biofilm formed by *Pseudomonas aeruginosa* treated with Ax for 7 days is thinner and more fragmented than that formed by untreated cells [40]. In our previous study, we confirmed the dose-dependent anti-chlamydial activity of Ax in *C. pneumoniae* infection in vitro; however, the commonly applied human dose does not affect *C. pneumoniae* proliferation in mice [17].

It is known that Ax has a well-balanced and favorable risk-benefit profile [2]; therefore, we investigated the effect of a four-fold increase in Ax dose on *C. pneumoniae* infection. In our in vivo study, we found that 5-mg/kg Ax significantly decreased the number of viable *C. pneumoniae* IFUs in the lungs of mice. IL-17A is associated with a neutrophil influx in the lungs; mice infected with *C. pneumoniae* and treated with anti-IL-17A antibodies have a relatively higher *C. pneumoniae* burden [41,42]. IL-23 has been described to be essential for inducing the *C. pneumoniae*-specific Th17 response [43]. In our study, Ax treatment in *C. pneumoniae*-infected mice significantly increased the relative expression levels of IFN- $\gamma$ , IL-12, IL-17A, and IL-23 compared to those of the untreated/infected mice; additionally, the IFN- $\gamma$  levels were higher in the lungs of the Ax-treated *C. pneumoniae*-infected mice than in infected/untreated mice. These results suggest that Ax treatment may enhance inflammation in the lungs and promote the anti-chlamydial response, thus resulting in a reduction in bacterial burden.

Furthermore, additional factors may contribute to a decreased number of recoverable *C. pneumoniae* inclusions. SP-A and SP-D are known to play an immunological role in maintaining lung homeostasis. It has been shown that these proteins are able to aggregate *C. pneumoniae* and *C. trachomatis* and can facilitate the uptake of bacteria by human macrophages [12,29]. Our RT-qPCR results suggest elevated SP-A levels that might also contribute to the improved elimination of bacteria in Ax-treated mice. Our in vitro results are in agreement with this phenomenon, as we found that the pretreatment of *C. pneumoniae* with SP-A or SP-D decreased the number of *C. pneumoniae* inclusion in the McCoy cell line, probably due the aggregating effect of SP-A and SP-D, thus resulting in a smaller proportion of *C. pneumoniae* infected cells. According to our results, SP-A and SP-D increased *C. pneumoniae* attachment to mouse macrophage cells, similar to the findings in human macrophage cells [12].

It is known that *C. pneumoniae* can inhibit cell apoptosis, and our results are in agreement with these findings, as we could not detect elevated caspase 3/7 activity at 12 h pi [10,13,44]. Additionally, *C. pneumoniae* stimulates the ERK 1/2 pathway activity to prevent caspase-independent apoptosis. Similarly, we found that *C. pneumoniae* infection significantly enhanced the ERK 1/2 pathway activity compared to that in uninfected/untreated cells [10,11]. Notably, we observed a novel possible mechanism via which *C. pneumoniae* prevents host cell apoptosis: *C. pneumoniae* significantly elevates the levels of phosphorylated MSK-1, which can also promote BCL2-associated agonist of cell death (BAD) phosphorylation and lead to the repression of BAD-induced apoptosis [45,46]. When the cells were treated with Ax in *C. pneumoniae*-treated cells, MAPK/ERK activity was significantly reduced. This result suggests that the anti-chlamydial activity of Ax may be partially attributed to the reduced MAPK/ERK 1/2 activity. The MAPK/ERK 1/2 pathway also plays a crucial role in the nourishment of proliferating bacteria, and inhibition of this process is fatal to the pathogen; it has been shown that MAPK inhibitors can inhibit *C. pneumoniae* infection [11,47]. The level of the P90RSK1/2 protein was also found to be significantly decreased; this protein is crucial for the phosphorylation of several antiapoptotic proteins such as death-associated protein kinase 1 and BAD [48]. Additionally, the levels

of phosphorylated MSK-1 decrease significantly, which are known to result in apoptosis. These findings suggest that Ax treatment may induce apoptosis in *C. pneumoniae*-infected cells, thereby inhibiting bacterial proliferation.

The results of a phase 2 clinical trial showed that Ax is well-tolerated beyond its standard administration at 1.25 mg/kg [49]. Given the coronavirus disease 2019 (COVID-19) pandemic, several studies have shown that Ax can be used as a supplemental medication for treating COVID-19 [50–52]. Notably, MAPK/ERK activation plays a pivotal role in additional bacterial infections, including *Coxiella burnetii* infections, which are similar to *Chlamydia* infections. Therefore, we think it may be worth to investigate the role of Ax in *C. burnetii* infections.

## 5. Conclusions

Ax has been used as a medication since 1980 for treating respiratory infections; however, it was shown that Ax, at a normal dose used for humans, does not inhibit *C. pneumoniae* proliferation in mice. We found that *C. pneumoniae*-infected mice treated with four times higher doses of Ax than normal contained significantly fewer viable *C. pneumoniae* IFUs than those in untreated mice. The mRNA expression levels of IL-12, IL-23, IL-17F, IFN- $\gamma$ , and SP-A were significantly increased in infected mice treated with Ax compared to those in control mice. Moreover, we found that Ax treatment decreased the activity of the MAPK/ERK pathway, which may have induced apoptosis in infected cells. Based on our results, a higher dose of Ax exhibits an anti-chlamydial effect in mice, probable due to its modulating effects on the immunologic and metabolic pathways.

**Supplementary Materials:** The Supplementary Materials are available online at <https://www.mdpi.com/article/10.3390/microorganisms9040880/s1>.

**Author Contributions:** Formal analysis, T.C. and R.B.; Investigation, D.K. and R.G.; Supervision, K.B.; Writing—original draft, D.K.; and Writing—review & editing, D.P., D.P.V., and V.E. All authors have read and agreed to the published version of the manuscript.

**Funding:** The study was supported by GINOP-2.3.2-15-2016-00012, EFOP 3.6.3-VEKOP-16-2017-00009, Hungarian Ministry of Innovation and Technology UNKP-20-02, 20391 3/2018/FEKUSTRAT, and by Gedeon Richter's Talentum Foundation.

**Data Availability Statement:** Not applicable.

**Acknowledgments:** We thank Müllerné Deák Györgyi and Vigyikánné Váradi Anikó for their excellent technical support.

**Conflicts of Interest:** The authors declare no conflict of interest.

## References

1. Germouty, J.; Jirou-Najou, J.L. Clinical Efficacy of Ambroxol in the Treatment of Bronchial Stasis. Clinical Trial in 120 Patients at Two Different Doses. *Respiration* **1987**, *51* (Suppl. 1), 37–41. [CrossRef] [PubMed]
2. Cazan, D.; Klimek, L.; Sperl, A.; Plomer, M.; Kölsch, S. Safety of Ambroxol in the Treatment of Airway Diseases in Adult Patients. *Expert Opin. Drug Saf.* **2018**, *17*, 1211–1224. [CrossRef] [PubMed]
3. Balestrino, R.; Schapira, A.H.V. Glucocerebrosidase and Parkinson Disease: Molecular, Clinical, and Therapeutic Implications. *Neuroscientist* **2018**, *24*, 540–559. [CrossRef] [PubMed]
4. Gillissen, A.; Schärting, B.; Jaworska, M.; Bartling, A.; Rasche, K.; Schultze-Werninghaus, G. Oxidant Scavenger Function of Ambroxol in Vitro: A Comparison with N-Acetylcysteine. *Res. Exp. Med.* **1997**, *196*, 389–398. [CrossRef]
5. Aihara, M.; Dobashi, K.; Akiyama, M.; Naruse, I.; Nakazawa, T.; Mori, M. Effects of N-Acetylcysteine and Ambroxol on the Production of IL-12 and IL-10 in Human Alveolar Macrophages. *Respiration* **2000**, *67*, 662–671. [CrossRef]
6. He, W.; Xiao, W.; Zhang, X.; Sun, Y.; Chen, Y.; Chen, Q.; Fang, X.; Du, S.; Sha, X. Pulmonary-Affinity Paclitaxel Polymer Micelles in Response to Biological Functions of Ambroxol Enhance Therapeutic Effect on Lung Cancer. *Int. J. Nanomed.* **2020**, *15*, 779–793. [CrossRef]
7. Zhang, S.; Jiang, J.; Ren, Q.; Jia, Y.; Shen, J.; Shen, H.; Lin, X.; Lu, H.; Xie, Q. Ambroxol Inhalation Ameliorates LPS-Induced Airway Inflammation and Mucus Secretion through the Extracellular Signal-Regulated Kinase 1/2 Signaling Pathway. *Eur. J. Pharmacol.* **2016**, *775*, 138–148. [CrossRef]

8. de Mey, C.; Koelsch, S.; Richter, E.; Pohlmann, T.; Sousa, R. Efficacy and Safety of Ambroxol Lozenges in the Treatment of Acute Uncomplicated Sore Throat - a Pooled Analysis. *Drug Res.* **2016**, *66*, 384–392. [\[CrossRef\]](#)
9. Yang, B.; Yao, D.F.; Ohuchi, M.; Ide, M.; Yano, M.; Okumura, Y.; Kido, H. Ambroxol Suppresses Influenza-Virus Proliferation in the Mouse Airway by Increasing Antiviral Factor Levels. *Eur. Respir. J.* **2002**, *19*, 952–958. [\[CrossRef\]](#)
10. Kun, D.; Xiang-lin, C.; Ming, Z.; Qi, L. Chlamydia Inhibit Host Cell Apoptosis by Inducing Bag-1 via the MAPK/ERK Survival Pathway. *Apoptosis* **2013**, *18*, 1083–1092. [\[CrossRef\]](#)
11. Su, H.; McClarty, G.; Dong, F.; Hatch, G.M.; Pan, Z.K.; Zhong, G. Activation of Raf/MEK/ERK/CPLA2 Signaling Pathway Is Essential for Chlamydial Acquisition of Host Glycerophospholipids. *J. Biol. Chem.* **2004**, *279*, 9409–9416. [\[CrossRef\]](#)
12. Oberley, R.E.; Ault, K.A.; Neff, T.L.; Khubchandani, K.R.; Crouch, E.C.; Snyder, J.M. Surfactant Proteins A and D Enhance the Phagocytosis of Chlamydia into THP-1 Cells. *Am. J. Physiol. Lung Cell. Mol. Physiol.* **2004**, *287*, L296–L306. [\[CrossRef\]](#)
13. Sharma, M.; Rudel, T. Apoptosis Resistance in Chlamydia-Infected Cells: A Fate Worse than Death? *FEMS Immunol. Med. Microbiol.* **2009**, *55*, 154–161. [\[CrossRef\]](#)
14. Choroszy-Król, I.; Frej-Mądrzak, M.; Hober, M.; Sarowska, J.; Jama-Kmiecik, A. Infections Caused by Chlamydia Pneumoniae. *Adv. Clin. Exp. Med.* **2014**, *23*, 123–126. [\[CrossRef\]](#)
15. Petrovay, F.; Heltai, K.; Kis, Z.; Tresó, B.; Gonczol, E.; Burian, K.; Endresz, V.; Valyi-Nagy, I. Chronic Infections and Histamine, CRP and IL-6 Levels after Percutaneous Transluminal Coronary Angioplasty. *Inflamm. Res.* **2007**, *56*, 362–367. [\[CrossRef\]](#)
16. Burián, K.; Berencsi, K.; Endresz, V.; Gyulai, Z.; Valyi-Nagy, T.; Valyi-Nagy, I.; Bakay, M.; Geng, Y.; Virok, D.; Kari, L.; et al. Chlamydia Pneumoniae Exacerbates Aortic Inflammatory Foci Caused by Murine Cytomegalovirus Infection in Normocholesterolemic Mice. *Clin. Diagn. Lab. Immunol.* **2001**, *8*, 1263–1266. [\[CrossRef\]](#)
17. Kókai, D.; Mosolygó, T.; Virók, D.P.; Endrész, V.; Burián, K. N-Acetyl-Cysteine Increases the Replication of Chlamydia Pneumoniae and Prolongs the Clearance of the Pathogen from Mice. *J. Med. Microbiol.* **2018**, *67*, 702–708. [\[CrossRef\]](#)
18. Burián, K.; Hegyesi, H.; Buzás, E.; Endrész, V.; Kis, Z.; Falus, A.; Gönczöl, E. Chlamydia (Chlamydia) Pneumoniae Induces Histidine Decarboxylase Production in the Mouse Lung. *Immunol. Lett.* **2003**, *89*, 229–236. [\[CrossRef\]](#)
19. Balogh, E.P.; Faludi, I.; Virók, D.P.; Endrész, V.; Burián, K. Chlamydia Pneumoniae Induces Production of the Defensin-like MIG/CXCL9, Which Has in Vitro Antichlamydial Activity. *Int. J. Med. Microbiol.* **2011**, *301*, 252–259. [\[CrossRef\]](#)
20. Caldwell, H.D.; Kromhout, J.; Schachter, J. Purification and Partial Characterization of the Major Outer Membrane Protein of Chlamydia Trachomatis. *Infect. Immun.* **1981**, *31*, 1161–1176. [\[CrossRef\]](#)
21. Mosolygó, T.; Szabó, Á.M.; Balogh, E.P.; Faludi, I.; Virók, D.P.; Endrész, V.; Samu, A.; Krenács, T.; Burián, K. Protection Promoted by PGP3 or PGP4 against Chlamydia Muridarum Is Mediated by CD4+ Cells in C57BL/6N Mice. *Vaccine* **2014**, *32*, 5228–5233. [\[CrossRef\]](#) [\[PubMed\]](#)
22. Hellemans, J.; Mortier, G.; De Paepe, A.; Speleman, F.; Vandesompele, J. QBase Relative Quantification Framework and Software for Management and Automated Analysis of Real-Time Quantitative PCR Data. *Genome Biol.* **2007**, *8*, R19. [\[CrossRef\]](#) [\[PubMed\]](#)
23. Gáspár, R.; Pipicz, M.; Hawchar, F.; Kovács, D.; Djirackor, L.; Görbe, A.; Varga, Z.V.; Kiricsi, M.; Petrovski, G.; Gácsér, A.; et al. The Cytoprotective Effect of Biglycan Core Protein Involves Toll-like Receptor 4 Signaling in Cardiomyocytes. *J. Mol. Cell. Cardiol.* **2016**, *99*, 138–150. [\[CrossRef\]](#) [\[PubMed\]](#)
24. Szabó, M.R.; Gáspár, R.; Pipicz, M.; Zsindely, N.; Diószegi, P.; Sárközy, M.; Bodai, L.; Csont, T. Hypercholesterolemia Interferes with Induction of MiR-125b-1-3p in Preconditioned Hearts. *Int. J. Mol. Sci.* **2020**, *21*, 3744. [\[CrossRef\]](#)
25. Virok, D.P.; Raffai, T.; Kókai, D.; Paróczai, D.; Bogdanov, A.; Veres, G.; Vécsei, L.; Poliska, S.; Tiszlavicz, L.; Somogyvári, F.; et al. Indoleamine 2,3-Dioxygenase Activity in Chlamydia Muridarum and Chlamydia Pneumoniae Infected Mouse Lung Tissues. *Front. Cell. Infect. Microbiol.* **2019**, *9*, 192. [\[CrossRef\]](#)
26. Roshick, C.; Wood, H.; Caldwell, H.D.; McClarty, G. Comparison of Gamma Interferon-Mediated Antichlamydial Defense Mechanisms in Human and Mouse Cells. *Infect. Immun.* **2006**, *74*, 225–238. [\[CrossRef\]](#)
27. Wang, Z.; Xu, M.; Wang, Y.; Wang, T.; Wu, N.; Zheng, W.; Duan, H. Air Particulate Matter Pollution and Circulating Surfactant Protein: A Systemic Review and Meta-Analysis. *Chemosphere* **2021**, *272*, 129564. [\[CrossRef\]](#)
28. Johansson, J.; Curstedt, T. Synthetic Surfactants with SP-B and SP-C Analogues to Enable Worldwide Treatment of Neonatal Respiratory Distress Syndrome and Other Lung Diseases. *J. Intern. Med.* **2019**, *285*, 165–186. [\[CrossRef\]](#)
29. Oberley, R.E.; Goss, K.L.; Ault, K.A.; Crouch, E.C.; Snyder, J.M. Surfactant Protein D Is Present in the Human Female Reproductive Tract and Inhibits Chlamydia Trachomatis Infection. *Mol. Hum. Reprod.* **2004**, *10*, 861–870. [\[CrossRef\]](#)
30. Galle, J.N.; Fechtner, T.; Eierhoff, T.; Römer, W.; Hegemann, J.H. A Chlamydia Pneumoniae Adhesin Induces Phosphatidylserine Exposure on Host Cells. *Nat. Commun.* **2019**, *10*, 4644. [\[CrossRef\]](#)
31. McCOY, C.E.; Campbell, D.G.; Deak, M.; Bloomberg, G.B.; Arthur, J.S.C. MSK1 Activity Is Controlled by Multiple Phosphorylation Sites. *Biochem. J.* **2005**, *387*, 507–517. [\[CrossRef\]](#)
32. Seifart, C.; Clostermann, U.; Seifart, U.; Müller, B.; Vogelmeier, C.; von Wichert, P.; Fehrenbach, H. Cell-Specific Modulation of Surfactant Proteins by Ambroxol Treatment. *Toxicol. Appl. Pharmacol.* **2005**, *203*, 27–35. [\[CrossRef\]](#)
33. Fois, G.; Hobi, N.; Felder, E.; Ziegler, A.; Miklavc, P.; Walther, P.; Radermacher, P.; Haller, T.; Dietl, P. A New Role for an Old Drug: Ambroxol Triggers Lysosomal Exocytosis via PH-Dependent Ca<sup>2+</sup> Release from Acidic Ca<sup>2+</sup> Stores. *Cell Calcium* **2015**, *58*, 628–637. [\[CrossRef\]](#)
34. Weiser, T. Comparison of the Effects of Four Na<sup>+</sup> Channel Analgesics on TTX-Resistant Na<sup>+</sup> Currents in Rat Sensory Neurons and Recombinant Nav1.2 Channels. *Neurosci. Lett.* **2006**, *395*, 179–184. [\[CrossRef\]](#)

35. McNeill, A.; Magalhaes, J.; Shen, C.; Chau, K.-Y.; Hughes, D.; Mehta, A.; Foltynie, T.; Cooper, J.M.; Abramov, A.Y.; Gegg, M.; et al. Ambroxol Improves Lysosomal Biochemistry in Glucocerebrosidase Mutation-Linked Parkinson Disease Cells. *Brain* **2014**, *137*, 1481–1495. [CrossRef]
36. Deretic, V.; Timmins, G.S. Enhancement of Lung Levels of Antibiotics by Ambroxol and Bromhexine. *Expert Opin. Drug Metab. Toxicol.* **2019**, *15*, 213–218. [CrossRef]
37. Li, X.; Zhao, Y.; Huang, X.; Yu, C.; Yang, Y.; Sun, S. Ambroxol Hydrochloride Combined with Fluconazole Reverses the Resistance of *Candida Albicans* to Fluconazole. *Front. Cell. Infect. Microbiol.* **2017**, *7*, 124. [CrossRef]
38. Zhang, Y.; Fu, Y.; Yu, J.; Ai, Q.; Li, J.; Peng, N.; Song, S.; He, Y.; Wang, Z. Synergy of Ambroxol with Vancomycin in Elimination of Catheter-Related *Staphylococcus Epidermidis* Biofilm in Vitro and in Vivo. *J. Infect. Chemother.* **2015**, *21*, 808–815. [CrossRef]
39. Yamaya, M.; Nishimura, H.; Nadine, L.K.; Ota, C.; Kubo, H.; Nagatomi, R. Ambroxol Inhibits Rhinovirus Infection in Primary Cultures of Human Tracheal Epithelial Cells. *Arch. Pharm. Res.* **2014**, *37*, 520–529. [CrossRef]
40. Cataldi, M.; Sblendorio, V.; Leo, A.; Piazza, O. Biofilm-Dependent Airway Infections: A Role for Ambroxol? *Pulm. Pharmacol. Ther.* **2014**, *28*, 98–108. [CrossRef]
41. Mosolygó, T.; Korcsik, J.; Balogh, E.P.; Faludi, I.; Virók, D.P.; Endrész, V.; Burián, K. *Chlamydia Pneumoniae* Re-Infection Triggers the Production of IL-17A and IL-17E, Important Regulators of Airway Inflammation. *Inflamm. Res.* **2013**, *62*, 451–460. [CrossRef] [PubMed]
42. Neutrophils, Interleukin-17A and Lung Disease | European Respiratory Society. Available online: [https://erj.ersjournals.com/content/25/1/159.abstract?ijkey=26df422c417132c793da0a7c0d7a6f922caad19d&keytype=tf\\_ipsecsha](https://erj.ersjournals.com/content/25/1/159.abstract?ijkey=26df422c417132c793da0a7c0d7a6f922caad19d&keytype=tf_ipsecsha) (accessed on 31 July 2020).
43. Frazer, L.C.; Scurlock, A.M.; Zurenski, M.A.; Riley, M.M.; Mintus, M.; Pociask, D.A.; Sullivan, J.E.; Andrews, C.W.; Darville, T. IL-23 Induces IL-22 and IL-17 Production in Response to *Chlamydia Muridarum* Genital Tract Infection, but the Absence of These Cytokines Does Not Influence Disease Pathogenesis. *Am. J. Reprod. Immunol.* **2013**, *70*. [CrossRef] [PubMed]
44. Matsuo, J.; Haga, S.; Hashimoto, K.; Okubo, T.; Ozawa, T.; Ozaki, M.; Yamaguchi, H. Activation of Caspase-3 during *Chlamydia Trachomatis*-Induced Apoptosis at a Late Stage. *Can. J. Microbiol.* **2019**, *65*, 135–143. [CrossRef] [PubMed]
45. She, Q.-B.; Ma, W.-Y.; Zhong, S.; Dong, Z. Activation of JNK1, RSK2, and MSK1 Is Involved in Serine 112 Phosphorylation of Bad by Ultraviolet B Radiation. *J. Biol. Chem.* **2002**, *277*, 24039–24048. [CrossRef] [PubMed]
46. Cook, S.J.; Stuart, K.; Gilley, R.; Sale, M.J. Control of Cell Death and Mitochondrial Fission by ERK1/2 MAP Kinase Signalling. *FEBS J.* **2017**, *284*, 4177–4195. [CrossRef] [PubMed]
47. Kortesoja, M.; Trofin, R.E.; Hanski, L. A Platform for Studying the Transfer of *Chlamydia Pneumoniae* Infection between Respiratory Epithelium and Phagocytes. *J. Microbiol. Methods* **2020**, *171*, 105857. [CrossRef]
48. Lara, R.; Seckl, M.J.; Pardo, O.E. The P90 RSK Family Members: Common Functions and Isoform Specificity. *Cancer Res.* **2013**, *73*, 5301–5308. [CrossRef]
49. Mullin, S.; Smith, L.; Lee, K.; D'Souza, G.; Woodgate, P.; Elflein, J.; Hällqvist, J.; Toffoli, M.; Streeter, A.; Hosking, J.; et al. Ambroxol for the Treatment of Patients With Parkinson Disease With and Without Glucocerebrosidase Gene Mutations: A Nonrandomized, Noncontrolled Trial. *JAMA Neurol.* **2020**, *77*, 427–434. [CrossRef]
50. Olaleye, O.A.; Kaur, M.; Onyenaka, C.C. Ambroxol Hydrochloride Inhibits the Interaction between Severe Acute Respiratory Syndrome Coronavirus 2 Spike Protein's Receptor Binding Domain and Recombinant Human ACE2. *bioRxiv* **2020**. [CrossRef]
51. Alkotaji, M. Azithromycin and Ambroxol as Potential Pharmacotherapy for SARS-CoV-2. *Int. J. Antimicrob. Agents* **2020**, *56*, 106192. [CrossRef]
52. Bradfute, S.B.; Ye, C.; Clarke, E.C.; Kumar, S.; Timmins, G.S.; Deretic, V. Ambroxol and Ciprofloxacin Show Activity Against SARS-CoV2 in Vero E6 Cells at Clinically-Relevant Concentrations. *bioRxiv* **2020**. [CrossRef]